

MASTER THESIS

Optimizing Uniform Ligand Density on DNA Origami for Th1 Activation

written at
the University of Applied Sciences
IMC FH Krems

in the degree program
Medical and Pharmaceutical Biotechnology, MA VZ

under the supervision of
Priv.Doz. Dr. Reinhard Klein

by
Stephanie Walcher

12/1/0571/040

Statutory Declaration

Stephanie Walcher
Liebknechtgasse 7/34/3 1160 Vienna, Austria

“ I declare in lieu of an oath that I have written this master paper myself and that I have not used any sources or resources other than stated for its preparation. I further declare that I have clearly indicated all direct and indirect quotations. This master paper has not been submitted elsewhere for examination purposes.”

Vienna, April 13th 2017

(Place, Date)

Stephanie Walcher

(Signature Author)

Foreword

“Breakthrough discoveries cannot change the world if they do not leave the lab.”

- Wyss Institute for Biologically Inspired Engineering

This thesis has been written with respect to an internship of about eight months in the course of the Master degree program *Medical and Pharmaceutical Biotechnology* at the IMC University of Applied Sciences in Krems, Austria. The aim was to contribute to the work of Prof. Dr. William Shih’s group at the Wyss Institute for Biologically Inspired Engineering in Boston, Massachusetts, gain experience in the relevant field of research, as well as produce an autonomous scientific Master thesis in accordance with the state-of-the-art academic standards and the requirements of professional practice set by the university.

I was assigned a project which comprised genetic engineering and transformation of a protein sequence in a plasmid, followed by protein expression in *E.coli*, solubilization and refolding if required, and finally protein purification.

All oligo nucleotide properties were derived from the oligo analyser tool on the *IDT* web page. Sample sequencing was performed externally by *Genewiz*. All sequences are presented in the Appendix.

Acknowledgements

I am earnestly thankful for having had the opportunity to contribute to Dr. William Shih's work at the Wyss Institute for Biologically Inspired Engineering in Boston, Massachusetts. I have learnt a lot about the scientific approach to obtaining the right answers, and even more importantly, asking pertinent questions. Apart from that I am very grateful for all the inspiring conferences, workshops, and symposia I was able to attend. Last but not least I truly enjoyed the laboratory and department retreats and celebrations I could take part in. I do feel the invaluable experience I have gained in Boston helped me become the scientist and the person I am today.

I am enormously grateful to the Austrian Marshall Plan Foundation for the financial support, without which the wonderful experiences and inspiring training at the Wyss Institute for Biologically Inspired Engineering would not have been possible.

Of those who have helped me, my especial gratitude is due to my supervisor, Prof. Dr. William Shih, for his support in my project. Also I want to thank my internal supervisor, Dr. Reinhard Klein.

I greatly appreciate my family, especially my parents, for their motivation and their financial support during my entire studies. I am grateful to my professors, especially Dr. Entler, who organizes the ARTS program. Last but not least, I want to thank my colleagues, all current and former group members, for their support and scientific input, as well as for providing a pleasant working atmosphere. Especially I want to thank my mentor, Leo Chou, who continuously gave me feedback and helpful advice on the project. In the same way I appreciate my fellow students and friends at the IMC Krems for the enjoyable company during my entire studies.

Stephanie Walcher

Abstract

Modern-day efforts to eradicate tumor tissue have moved well beyond traditional methods, such as chemotherapy. A subset of therapeutic cancer vaccines aims to awaken the stagnant immune system in the tumor micro environment by precisely targeted activation of antigen presenting cells (APCs) and establishment of a robust T-lymphocyte (TC) response. Biasing TC differentiation towards a Th1-immune response is the key to reliable cross-priming and activation of lethal cytotoxic T-lymphocytes (CTLs). This project is part of a larger scheme that aims to target the surface receptor *DEC-205* with decorated DNA origami nano particles without inducing cross-linking of the receptors, which was shown to favor an unwanted Th2 immune response. *DEC-205* is a readily endocytosed surface receptor on dendritic cells (DCs), which are among the most powerful APCs. Any antigen incorporated into the DNA origami structure has a high potential to be cross-presented to naïve CD8+ TCs with the result of activating the cells and initiating a body-own immune response.

The scope of this thesis focuses on the expression of the targeting antibody affinity ligand *anti-DEC-205* with a purification tag and a SNAP tag. The project opens with the preparation of plasmids by Gibson Cloning, followed by expression experiments in *E.coli* and finally finishes with protein purification and analysis. Final chapters elaborate on future perspectives as well as alternative approaches.

Keywords: DNA origami, therapeutic cancer vaccine, DEC-205, PCR, Gibson Cloning, E.coli expression, His tag chromatography, SDS PAGE

Contents

1	Introduction	1
1.1	Scope of Work	1
1.2	Methodical Approach	2
1.3	Structure of Thesis	2
2	Background	3
2.1	Basic Immune Response	3
2.1.1	Th1 and Th2 Immune Response	5
2.2	Immunotherapy on the Rise	6
2.2.1	Immunotherapeutic Approaches	7
2.2.2	Endogenous and Exogenous Vaccines	10
2.3	A Closer Look at the Dendritic Cell	12
2.3.1	DEC-205	13
2.4	The Role of DNA Origami	18
2.4.1	How Structures Fold	18
2.4.2	Achievements in the Field	21
2.5	Procedural Background Notes	22
2.5.1	The Candlestick	22
2.5.2	Gibson Cloning	23
3	Methods	25
3.1	Cell Lines	25
3.2	Molecular Cloning	26
3.2.1	Transformation and Quality Controls	29
3.3	Protein Expression and Processing	31
3.3.1	Bacterial Cell Culture	31
3.3.2	Sample Lysis and Analysis	32
4	Results	39
4.1	Molecular Cloning in pUC57	39
4.1.1	Cloning pUC57 in BL21(DE3)	39

4.2	Protein Expression in pUC57	41
4.3	Molecular Cloning in pET30a	44
4.4	Protein Expression in pET30a	45
4.4.1	Time Course Experiments	47
4.4.2	Selected Sample Analysis: Lysis	49
4.4.3	Trouble Shooting: Glycerol Stocks	50
4.4.4	Protein Expression and Solubilization	52
4.5	SHuffleT7 Express Protein Expression	54
4.5.1	VH-2.2 and VH-3.1	55
4.5.2	VH-1.1	56
4.6	Troubleshooting: Genomic Code	57
4.6.1	Alternative Approach to Genome Verification	59
4.6.2	Verification by Restriction Digest	60
4.6.3	Sequencing of VH-1.1	65
4.7	Summary	69
5	Discussion	73
5.1	Expression in pUC57 in BL21(DE3)	73
5.2	Expression in pET30a in BL21(DE3)	74
5.2.1	Expression Parameters	75
5.2.2	SHuffle T7 Express Cell Line	76
5.3	Suggestions for Alternative Approaches	76
5.3.1	Expressed Protein Ligation	77
5.3.2	RNA-Aptamer	78
5.4	Further Applications	78
5.4.1	Th1-Bias	78
5.4.2	Logic-Gated Cell Signaling	79
5.5	Conclusion	79
5.6	Outlook	80
	List of Figures	81
	List of Tables	83
	A Acronyms	85
	Bibliography	89
B	Sequences	97
B.1	Sequences of Insert Templates for Gibson Cloning	97
B.2	Primers	99
B.2.1	Gibson Cloning	99

B.2.2	PCR and colony PCR	100
B.2.3	Sequencing	100

Introduction

Traditional vaccines (e.g., preventative vaccines for microbial pathogens) prime the immune system by administering protein antigens and adjuvants that activate APCs. Activated APCs initiate a humoral (Th2) response, as well as the production of antibodies directed against the pathogen by B-lymphocytes, some of which are retained as "immunological memory". This approach allows the immune system to respond faster and more efficiently upon the next infection.

In the case of established tumors, however, APCs only poorly activate and do not initiate a potent and long-lived immune response. Therapeutic vaccines, as opposed to preventive vaccines, accomplish a much more effective response by biasing the immune system towards a cellular (Th1) response, which is directed against intracellular pathogens. DCs are among the most potent APCs that can regulate the magnitude and type of TC response that develops. Hence, there is great interest in targeting DCs in cancer vaccination therapy (e.g., Ref. [1], Ref. [34]).

An emerging idea has been to precisely target and activate DC by designing nanoparticles that act similar to intact pathogens. The particles may contain an antigen that will subsequently be presented to a naïve TCs by the activated DCs, thereby evoking a T-cell receptor (TCR)-signal and a co-stimulatory signal to drive the activated effector TC into differentiation and proliferation. A rapidly growing field of research is devoted to elucidating the exact design parameters of the nano-particles that control the quality of the the immune response or even regulate it directly (e.g., Ref. [38], [51]).

1.1 Scope of Work

The scope of this thesis is to design and produce the affinity ligand on a nano-particle that can bias the immune response towards a Th1-response by interaction with naïve

DCs. This work will contribute to the presentation of a strategy toward an improved cancer vaccine based on engineered nano-particles, the main aim of which is to bias the immune system towards a Th1-response, rather than a Th2 response, and target tumor tissue.

1.2 Methodical Approach

First, a bacterial cell line is engineered to express upon induction with Isopropyl B-D-1-thiogalactopyranoside (IPTG) a fusion protein consisting of (1) the single chain variable fragment (ScFv) that binds to DEC205, a type I cell surface receptor expressed primarily by DCs, coupled to (2) a purification tag (polyhistidine-tag) and (3) a SNAP-tag. The cloning technique applied in this step is Gibson Cloning, followed by transformation into *E.coli* competent cells. Expression of the fusion protein in the soluble fraction is strongly encouraged because it permits the omission of solubilization steps, which greatly increases the yield and ease of production and purification. After successful protein expression, solubilization and refolding (if required), and purification by His-tag chromatography the fragment is fused to a previously folded cylindrical DNA origami structure.

1.3 Structure of Thesis

Chapter 2 will inform the reader on relevant background information on current cancer vaccine strategies, the two main associated immune responses, and the significance of DNA origami.

Chapter 3 will focus on the detailed methodological approach to genetic engineering, protein expression, and protein purification, including genetic engineering in two common plasmids (pC57 and pET30a), protein expression in two competent *E.coli* cell lines, BL21(DE3) and SHuffleT7 Express, and protein purification by His tag chromatography.

Chapter 4 will give a comprehensive summary of the results and chapter 5 will provide objective interpretations and conclusions of the given data as well as offer suggestions for future perspectives and alternative approaches in the project.

CHAPTER 2

Background

Cytotoxic approaches, such as chemotherapy or radiation therapy, have traditionally been employed by oncologists to induce apoptosis in cancer cells and thereby reduce tumor volume, which is the major criterion in determining effectiveness of cancer therapies specified by the World Health Organization (WHO). However, this type of treatment does not necessarily guarantee improvement in survival: lethal drug-resistant cells may emerge, aside from the fact that cytotoxic therapies are incapable of selectively targeting cancer tissue while sparing healthy tissue.

This chapter describes the basic steps of an immune response starting with pathogen recognition and ending with a directed TC response (section 2.1), followed by an introduction into current immunotherapy (section 2.2) and the significance of specific targeting of the DC and its receptor DEC-205 (section 2.3). It finishes with a brief guide to DNA origami (section 2.4), an extraordinary tool that may revolutionize modern-day cancer therapy. At the very end of this chapter brief notes on some procedures in the context of this thesis can be found.

2.1 Basic Immune Response

Before going into details about how the immune system is evaded by tumor tissue and how various therapies aim to support the immune system, it is important to understand the basics of an immune response. Here it will be categorized into three major steps (refer to Figure 2.1).

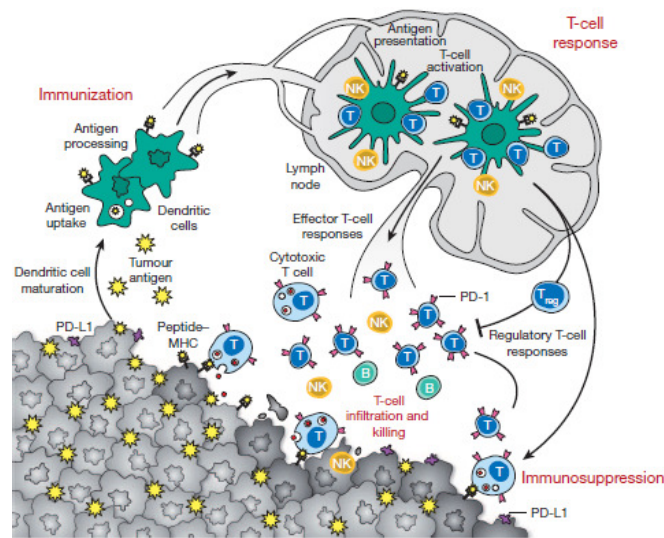


Figure 2.1: This figure illustrates the three major steps in creating an immune response: Sampling of the target site by antigen presenting cells (APCs), especially dendritic cells (DCs); processing and presentation to T-lymphocytes (TCs) at the lymph node; and infiltration of tumor site by activated TCs. The maturation (danger) stimulus in conjunction with co-stimulatory TC surface receptors and their ligands on the DC dictates the class of TCs and absence of a maturation signal on the DC leads to induction of tolerance by TC deletion, anergy, or regulatory TC production. Tumors have the ability to suppress an immune response in various ways, including, but not limited to upregulation of immunosuppressive programmed death-ligand 1 (PD-L1) or -L2, downregulation of major histocompatibility complex (MHC) class I and II, and release of chemical immunosuppressive molecules (such as Prostaglandin E2, arginase, and IDO) and vascular endothelial growth factor (VEGF), which inhibits TC diapedesis from the vasculature. Taken from Ref. [53]

The first cells on site, save tissue cells, are DCs, which are among the most powerful APCs because they feature both MHC class I and MHC class II surface molecules and can present the antigen in its native form. DCs collect samples of the antigen on site, process them, and present them on their surface MHC molecules upon activation, rather than progressing into tolerance. In case of therapeutic vaccines, for example, these antigens may be supplied exogenously in the form of proteins that are typical of cancer or differentiation antigens associated with the cancer’s tissue of origin. Activation (‘danger’) signals may also be provided therapeutically by agonist antibodies against activating receptors.

DCs then travel to the lymphoid organs where they activate TCs by the so-called *immunological handshake*: the MHC complex on the DC, including the presented antigen, binds to the TCR and its co-receptors and the danger-signal expressed on the DC is recognized by another surface receptor on the TC. Should the DC lack the danger signal and present the antigen under steady state conditions, it will instead induce tolerance

by regulatory TC production, which would disagree with an anti-tumor response. Activated DCs may also trigger natural killer (NK) cells, which have cytotoxic abilities that may also contribute to an anti-tumor response.

Activated TCs may progress down two major paths depending on the nature of the antigens and the cytokine environment: Th1 or Th2 cells (refer to section 2.1.1). This decision is detrimental for the following immune response and will further amplify itself while cross-inhibiting the opposing path. For this reason, the lymph node is recognized as another powerful site of therapeutic intervention offering the prospect to sway the immune response into one direction or the other.

Lastly, activated TCs must travel to and enter the tumor site to perform their functions and eliminate the mutated tissue. This critical step is often suppressed by cancer and in fact has been identified as one of the major challenges in immunotherapy. Cancer-associated fibroblasts can recruit immunosuppressive cells and also directly suppress the activity of effector TCs by secretion of tumor growth factor beta (TGF- β). In some cases the tumor cells completely escape detection by the immune system: down-regulation of surface ligands such as MHC class I, which is expressed on all tissue cells and provides the basis of antigen presentation, or upregulation of surface ligands that mediate TC anergy and exhaustion, such as programmed death-ligand 1 (PD-L1), prevent the onset of any antigen-driven immune response. Further, regulatory TCs, which are promoted by secreted adenosine and the accumulation of which in tumors is directly correlated with poor diagnostic outcome (refer to e.g., Ref. [19]) suppress TC activation and expansion. interleukin-10 (IL-10) secretion induced by vascular endothelial growth factor (VEGF) and down-regulated interferon gamma (IFN- γ) secretion from TCs leads to further immunosuppression (Ref. [71]).

2.1.1 Th1 and Th2 Immune Response

TCs can be broadly classified as either so-called *helper TCs*, which express the surface co-receptor CD4 and respond to peptide presentation on MHC class II, and *cytotoxic TCs*, which are characterized by CD8 expression and respond to peptide presentation on MHC class I.

MHC class I presents mostly intracellular peptide fragments, so it is clear that the presenting cell is also the infected cell. MHC class II is present on APCs and presents mostly extracellularly derived antigens. Here the presenting cell is not automatically the infected cell.

However, it has been recently shown that cross-priming allows even intracellular proteins to be presented in the context of MHC class II. *Cross-priming* of naïve CD8+ TCs is the result of antigen *cross-presentation* on APCs. So far cross-presentation on DCs has been characterized in the most depth. In the process of cross-presentation peptides are taken up from the environment around the cell, processed, directed to the endosomal pathway, and presented as antigens on both MHC class I and class II with-

out infecting the DC first. This is unusual because peptides presented by MHC class I are normally derived from within a cell. DCs then prime CTLs, which have the ability to kill virus-infected or otherwise compromised body-own cells (demonstrated in, e.g., Ref [72]). Therefore, cross-presentation can greatly amplify the number of activated CD8+ TCs and at the same time, via classical extracellularly derived antigen presentation on MHC class II, activate CD4+ helper TCs. Cross-presentation and cross-priming are a major theme in many cancer vaccines because of their contributions to creating an endogenous immune response (e.g., Ref. [43]).

While cytotoxic TCs (activated CD8+ TCs) have the ability to directly kill body-own cells (hence tumor cells), helper TCs amplify an immune response by recruiting and activating other *effector cells*. Recently, it has been proposed that Th1 cells also have the ability to eliminate tumor cells by releasing cytokines that bind death receptors on the tumor cell surface (Ref. [43]).

There is ongoing debate on how helper-TCs differentiate into Th1 or Th2 cells. Two major theories exist. One theory holds that the TCs differentiate according to the cytokine stimulation, while the other suggests they randomly differentiate but are selected due to the cytokine environment. In either case the cytokine environment at the site of antigen deposition or in the local lymph node plays an important role, and APCs, such as DCs, largely impact the cytokine population.

Th2 immune responses are broadly directed against extracellular pathogens, which are fought by secreting selected antibodies. Hence, the Th2 response is often referred to as *humoral* immune response. In cancer immunotherapy a Th2 response is not desired because it cross-inhibits the Th1 response. As mentioned previously, the Th1 response is especially effective against intracellular pathogens and, therefore, tumor cells. Further, Th1-cells are especially effective in activating the lethal CTLs.

It is illogical for the immune system to promote both Th1 and Th2 responses at the same time, so the two responses are programmed to cross-inhibit each other. Only one of them is amplified at a time while the other is suppressed.

An easy way to determine whether the Th1 or the Th2 response is active is to measure the cytokine environment in a given sample. Th1 cells will thrive on IFN- γ , tumor necrosis factor alpha (TNF- α), and IL-2, whereas Th2 cells secrete IL-4, IL-5, IL-6, IL-10, and IL-13. At the point of differentiation Th1 cells are mainly responsive to IL-12 while Th2 cells develop in the presence of IL-4 and the absence of IL-12.

2.2 Immunotherapy on the Rise

At the start, various complementary immunosuppressive barriers erected by the cancer made it seemingly impossible to pin down and eradicate cancer cells completely. Tumor antigens are often closely related or even identical to self-antigens, which makes it hard to separate a therapeutic response from a deadly auto-immune response. Furthermore,

as previously mentioned, relevant TCs may be depleted or exhausted and the tumor micro-environment is inherently immunosuppressive.

However, increasing understanding of the complex mechanisms involved in the immune response has slowly begun to set the stage for immunotherapy. In recent years multiple academic institutions and companies have contributed to its increasing success and a number of strategies have been devised that tackle tumor tissue from different angles.

2.2.1 Immunotherapeutic Approaches

Immunotherapy comes in a variety of flavors. For instance, adoptive cell transfer is a rather experimental approach where TCs that managed to enter the tumor site are isolated from a patient, stimulated ex-vivo using cytokines, and then re-introduced into the same patient's blood stream. Even though this type of immunotherapy has been successful to the point of completely eradicating the disease for years in some patients (e.g., refer to Ref. [24, 61]), it is still deemed inherently risky and tends to be avoided by biotech-pharmaceutical companies given the safety issues around selecting a target, manufacturing complexities, and associated costs.

Another approach is based on a non-cell system that is designed to cause the destruction of tumor tissue: a number of therapeutic antibody–drug conjugates - such as *ado-trastuzumab emtansine* for the treatment of some types of breast cancer, or *rentuximab vedotin* and *ibrutumomab tiuxetan* for some types of lymphoma (Ref. [37]). Therapeutic antibodies can also be supplied alone. One prominent example is *rituximab*, which induces antibody-dependent cell-mediated cytotoxicity and complement-dependent cytotoxicity. Medications of both types have been approved by the U.S. Food and Drug Administration (FDA).

A different set of antibodies does not target tumor cells directly, but instead they target lymphocyte receptors or their ligands and enhance endogenous anti-tumor activity. Possibly the most promising recent development in cancer immunotherapy are so-called checkpoint modulators, which act on immune checkpoints that under normal physiological conditions fulfil the important role of maintaining self-tolerance and preventing auto-immunity. Checkpoint modulators have had impressive therapeutic success in some types of cancers (e.g., Ref. [13, 35, 58]).

Tumor micro-environments can dysregulate various immune-checkpoint proteins and thereby block immune cells that would normally be able to recognize and kill the mutated tissue. It is the goal of checkpoint modulators to unleash the breaks on the paralysed immune response.

Two drugs, which act on pathways involving cytotoxic T-lymphocyte-associated antigen 4 (CTLA-4) or PD-L1- both inhibitory immune-checkpoint receptors, are currently either approved as orphan drug (monoclonal antibody to CTLA-4 *Ipilimumab*, March 2011, FDA approved for melanoma) or are being investigated in phase III clinical trials (*MDX-1106* in patients with melanoma, renal, and lung cancers).

CTLA-4 is expressed on the surface of TCs upon activation and binds to members of the B7 family, which are expressed on the surface of APCs as *danger signals*. Binding of CTLA-4 to a danger signal inhibits further activation and expansion of TCs (2.2). Even though this mechanism may seem counter-intuitive when it comes to eradicating tumor tissue, it is a crucial function to prevent chronic autoimmune inflammation, as was illustrated in mice by Tivol et al. about ten years ago (Ref. [75]).

PD-L1 is primarily expressed on the surface of activated TCs and has a similar inhibitory function. PD-L1 binds to ligands on potential targets, such as tumor cells. Binding leaves the TC exhausted (meaning unresponsive) and thereby limits its ability to fight tumor cells that express these ligands in large amounts on their surface, e.g., melanoma, ovarian, renal, or hepatocellular cancer (Ref. [63]). Antibodies that block PD-1 show promising results in clinical trials, plus they seem to have a safer toxicity profile than *ipilimumab*.

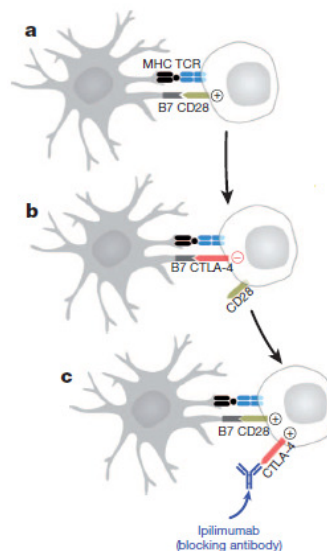


Figure 2.2: *a: Interlinkage of the antigen presenting major histocompatibility complex (MHC) molecule with the T-cell receptor (TCR) as well as the danger signal B7 on the antigen presenting cell (APC) with the co-receptor CD28 on the T-lymphocyte (TC) results in activation; b: Increasing expression of cytotoxic T-lymphocyte-associated antigen 4 (CTLA-4) competes for interaction with B7 and results in an anti-tumor response; c: Ipilimumab binds and blocks CTLA-4 to promote pro-inflammatory signalling. Adjusted from Ref. [53]*

Current research is being focused on finding out why certain checkpoint inhibitors are effective in some patients but not in others, and on expanding the range of applicability of checkpoint inhibitors to other types of cancer. It is likely that targeting one

single receptor is insufficient for sustained tumor protection and combinational checkpoint blockage needs to be applied. Even traditional chemotherapeutic drugs are applied in combination, so it comes only naturally that immunotherapeutic drugs are also combined to diversify the immune response and target resistances. Since immunotherapeutic agents have well-defined targets, it is possible to combine them rationally, as long as this makes sense biologically. This idea is exemplified in section 2.2.1.

Combinational Therapies

Progress has been made in melanoma patients with a mutation that has an influence on cancer metabolism. The mutation activates *BRAF*: Roche has developed an inhibitor that shows promising results in 50% of the patients before another mutation leads to overexpression of an alternative pathway. Even though it is feasible to also block this pathway, it is very likely that the tumor will undergo subsequent mutations and thereby continuously escape the treatment strategies (Ref. [14]).

The above example shows the weaknesses of purely metabolic treatments. Roche has also been working on different strategies that are based on TC immunity. Recently a promising phase II study combining Roche's *vemurafenib* with *ipilimumab* was conducted. The two antibodies support each other by first setting free information on the tumor and then promoting its presentation to enable a targeted response. It has been found out that tumor cells can die in various fashions, where some forms of apoptosis in fact amplify the tumor-directed immune response (Ref. [56]). Consequently, drugs that lead to this type of cell death will be more potent candidates for combinational therapies than others. *Ipilimumab* is expected to enhance TC priming by presentation of endogenous tumor antigens released as a result of tumor cell death induced by *vemurafenib* (Ref. [2]). Median overall survival was increased and the safety profile of the treatment is considered manageable. Combining metabolic treatments, such as *BRAF* discussed in the first example, with antibodies is being planned.

Finally, two or more immunotherapeutic drugs could be combined with each other, as long as the combination makes sense biologically. Two inhibitory antibodies that target CTLA-4 or PD-L1 and were briefly discussed above make a great combination for releasing the breaks on checkpoint blockage at two different stages in the TC response. If combined, the two antibodies may likely have a larger impact. CTLA-4 blocking antibody encourages activation and proliferation of TCs while a PD-1 blocking antibody will bind upregulated PD-L1 on tumor cells. Thus the combination drug works on both the activation stage, which improves both *de novo* responses and pre-existing responses, as well as on the effector stage.

However, the possibility that the tumor micro-environment may change and that the TC and DC developments may be altered due to the combination therapy needs to be considered. Furthermore, all drug combinations are expected to be dose- and/or schedule dependent and great care must be exercised when designing clinical protocols.

As a final note, the number of receptors that could potentially serve as targets for agonising antibodies, such as PD-L1, increases rapidly, but caution needs to be exercised when amplifying the tools in the immune system's powerful repertoire. In fact, it proves to be the case that toxicity by itself will not determine a positive therapeutic outcome: in a standard trial many patients will experience inflammatory pathology in the form of so-called *cytokine storms* but not all of them reap benefits of an anti-cancer immune response (Ref. [12]).

2.2.2 Endogenous and Exogenous Vaccines

There is some debate in the scientific community whether endogenous or exogenous approaches are better suited for the supply of antigens that will subsequently define a target for the immune response.

Endogenous vaccines mobilize antigens from the patient's own tumor *in situ*. The aim is to induce cell death in an environment that favors tumor-derived antigens uptake and processing by DCs. While the response allows for presentation of multiple hundreds of mutations expressed by the cancer cells, it is also inherently less controllable than exogenous vaccines.

Exogenous vaccines are packed into antibody delivery vehicles which are targeted to DCs, encoded in viral vectors, or administered as peptides or proteins in a suitable adjuvant, such as modified liposomes (Ref. [79], surface modified nanoparticles see Ref. [7]), or possibly, as will be discussed later in this thesis, three dimensional scaffolds such as DNA origami shapes.

Exogenous vaccines have previously been highly effective in establishing protective immunity against infectious agents, but have been hampered by complications in finding optimal adjuvants. An ideal adjuvant allows for maximum uptake and processing by DCs, and additionally supports administration of co-stimulatory signals that facilitate TC activation and overcome immunosuppression. In addition, selection of an antigens to be delivered is not trivial: a poor choice may result in a low number of TCs that have high affinity TCRs because the tolerance barrier is too high.

Antigens and Adjuvants

To induce immunity rather than tolerance, it is imperative to remember to also co-deliver an activation (danger) signal together with the antigen. It was mentioned above in section 2.1 that lack of the danger signal on APCs leads to tolerance and cancellation of an aggressive immune response. Adjuvants are supposed to fulfill the role of the danger signal and boost the immune response.

Delivering the adjuvant together with the antigen has another significant advantage: Only cells that have actually "seen" the antigen are activated, which is crucial for efficient CD8+ TC priming. APCs that randomly take up the antigen, but fail to also display

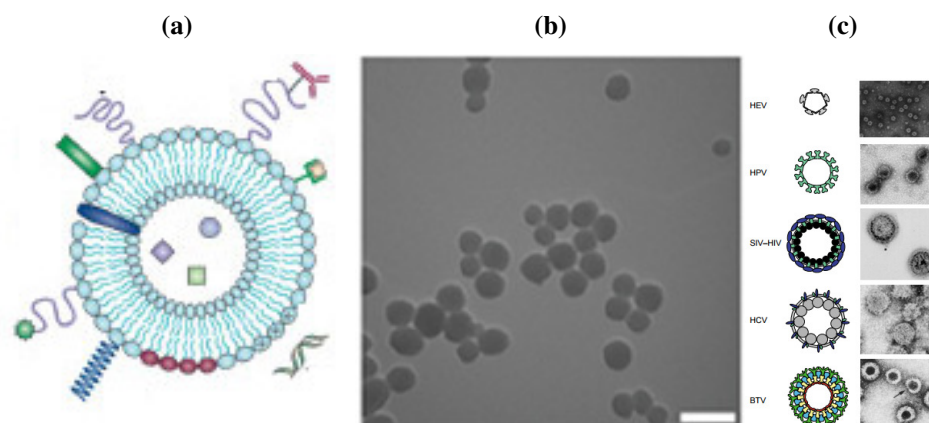


Figure 2.3: (a) Liposome decorated with e.g.:protective polymer, targeting ligand, DNA, stimuli-sensitive polymer. Ref. [76]; (b) Silica beads, non-decorated. 81 ± 12.3 nm. TEM images. Ref. [67]; (c) Virus-like particles, cartoon and electron microscope image, 100nm diameter Ref. [55].

the accompanying danger signal, may lead to induction of tolerance to that particular antigen. In effect the therapy pulls the immune system into two opposing directions: fight the antigen (because it is *dangerous*) versus tolerate the antigen (because it is body-own).

As opposed to studies that aim for a humoral (Th2) response (e.g., Ref. [41]), studies that aim for a cellular (Th1) response tend to effectively link the antigen and adjuvant together, where linkage is not limited to chemical cross-linkage but also covers packaging antigens and adjuvants into vehicles (polymer particles, liposomes, viruslike particles, or three-dimensional scaffolds, see Ref. [18, 80], refer to Figure 2.3). Polymers are more stable than liposomes and they constitute nonimmunogenic vehicles. Virus-like particles are intrinsic immunostimulators, which makes polymers safer and more flexible. If biodegradable, polymers can even be programmed to release their material over days to weeks.

Three dimensional scaffolds, and especially DNA origami, can even be programmed in such a way that they display a particular outer shape and pattern of receptors in spacial correlation to each other, which opens many doors to precise targeting and delivery. Further design parameters such as cargo, surface molecule display, exact shape or size, are very important questions that are yet to be clearly answered. Generally, it has been shown that nanoparticles below 300–500 nm in diameter are internalized more rapidly into DCs than particles that are larger than 1–2 μm in diameter (Ref. [27]). The small size also allows for lymphatic drainage rather than relying on transport by peripheral DCs.

As a consequence, targeting DCs allows for a lower vaccine dose for activation, the

same specific cell that receives the antigen also receives the adjuvant, and multiple specific subsets of DCs could be targeted, which is convenient for inducing a certain TC response but absolutely necessary for inducing optimal TC immunity (Ref. [57]). Supplying antigen and adjuvant in the same targeted compartment has also been shown to improve cellular uptake and enhanced cross-presentation (e.g., Ref. [7]). The latter point will be discussed more in depth in section 2.3 as it is one of the major pillars of this project.

Last but not least, targeted co-administration decreases the risk of adverse side effects such as autoimmunity, tolerance, or aforementioned systemic cytokine release by overstimulated tissue cells often termed "*cytokine storms*". It should be stressed that if the delivered antigens are presented without the necessary activation signal, tolerance is the result. Similarly, if the adjuvant boots APCs with no selected antigen danger may arise. APCs that receive activation stimuli by, e.g., toll-like receptor (TLR) agonists may induce or amplify (dormant) autoimmunity against presented self-antigen (Ref. [54]). This issue makes controlled administration vital. In the future it may even be possible to tailor a specific immune response such as Th1, Th2, Th17 etc. by well-designed targeting.

2.3 A Closer Look at the Dendritic Cell

As mentioned above, DCs are powerful APCs and a vital part of the immune response chain. They constantly sample their environment and then travel to the lymph node and present the antigens to naïve TCs.

The key to recognizing infectious agents or their products lies in a wide range of receptors on the DC surface: TLRs, C-type lectin receptors (CLRs), retinoic-acid-inducible gene I-like receptors, nucleotide-binding oligomerisation domain-like receptors, and cytoplasmic DNA sensors (e.g., Ref. [46]), some of which detect motifs typical for bacteria or viruses, such as non-methylated cytosine-guanosine (CpG).

TLRs are popular targets of vaccines, because they mediate adjuvanticity, meaning that they activate APCs. The receptors detect intracellular or extracellular pathogens depending on their cellular location. Intracellular TLRs, for example, are recognized as good targets for synthetic vaccine adjuvants such as dsRNA mimetic polyinosinic: polycytidylic acid as TLR3 agonists.

While TLRs are mostly used as targets for cell activation, CLRs facilitate receptor-mediated endocytosis by binding carbohydrate ligands (Ref. [44]). Due to their potential therapeutic value these receptors have been extensively studied and synthetic agonists have been developed (e.g., Ref. [9, 45]). The following section will present one CLR in more detail.

2.3.1 DEC-205

DEC-205 is a largely characterized CLR predominantly expressed on DCs. The 205 kDa molecule that has a cysteine rich domain, a fibronectin type II domain, and ten C-type lectin-like domains, as well as an internalization sequence in its cytoplasmic tail (Ref. [39]). DEC-205 has an acidic amino acid sequence that targets ligands to late endosomes, which is where MHC-II recruits antigens for presentation (Ref. [52]).

Even though the receptor's exact function is still unclear and a singular natural ligand has not been determined, DEC-205 has been shown to have unspecific endocytic capacity, which is an invaluable advantage in vaccine delivery. DEC-205 also facilitates antigen presentation after endocytosis when targeted with antigen-bearing monoclonal antibodies (Ref. [10]). This process is referred to as *cross-presentation* and was mentioned in earlier sections of this chapter (refer to section 2.1.1). After the discovery of the targeting properties of antibodies that recognize DEC-205 (in Ref. [52], among others) the receptor as well as other CLRs on DCs were intensely studied by various groups for their antigen uptake and (cross-) presentation abilities (Ref. [52, 32, 64]).

In mice, it has been found that the receptor Clec9a is almost exclusively expressed by the CD8- α + subset of DCs. This subset is particularly useful for the cross-presentation of antigens and the priming of CD8+ TCs. Hence, the receptor Clec9a is especially interesting when the goal is to induce cellular immunity in mice, which requires strong Th1-response (see section 2.1.1).

Recently, a human equivalent of the mouse CD8- α + cells has been found: the BDCA3+ (CD141+) DC subset was determined by phenotypic characteristics, the expression of particular transcription factors (Ref. [29, 65]), and the fact that they cross-present antigens to CD8+ TCs and have a superior ability to induce a Th1 response (Ref. [6, 17, 40]). Due to its susceptibility to precise targeting and the resulting antigen presentation, this subset of DCs has been exploited for immunostimulation ever since. Conversely, a recent study reported that the tissue-resident BDCA3+ (CD141+) DCs in the dermis of human skin produce IL-10 and stimulate regulatory TC production constitutively, which was significantly upregulated after CD40 cross-linking. Both IL-10 production and regulatory TC accumulation are associated with immunosuppression (Ref. [16]).

In a recent study by A. Bandyopadhyay *et. al.* the CLR DEC-205 was targeted with monoclonal antibody (mAb)-decorated biodegradable nanoparticles (Ref. [7]). The mAbs were spread on the nanoparticle surface at different densities to assess density-dependent cytokine production (refer to Figure 2.4). Table 2.1 summarizes the effects of relevant cytokines. This was the first study to collect information about ligand density dependence of the immune response and has a large influence on the project discussed in this thesis.

It has been shown previously that antibody-mediated antigen targeting via the DEC-205 receptor can improve the efficiency of immunotherapy by TC immunity: an antigen inte-

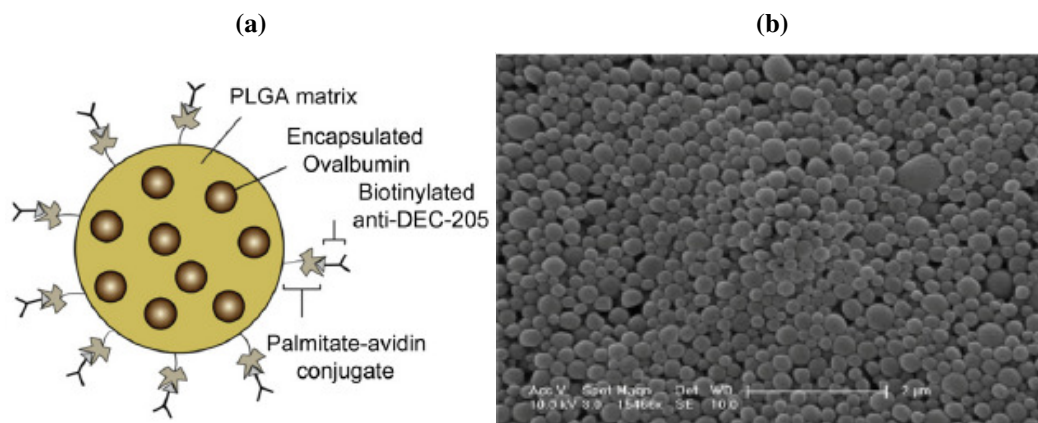


Figure 2.4: (a) A schematic view of the nanoparticle designed by Bandyopadhyay *et. al.* to study ligand-density dependence of a cytokine response (not to scale). PLGA = poly lactic-co-glycolic acid, a copolymer that is biodegradable and biocompatible and, therefore, often found in therapeutic devices. Taken from Ref. [7]; (b) Scanning electron microscopy image of surface modified nanoparticles. Taken from Ref. [7].

grated into a chimeric mAb was successfully presented by DCs on their MHC class I and class II molecules and both CD4⁺ and CD8⁺ TC responses were significantly enhanced. When combined with an agonist (subcutaneous injection of anti-CD40) the anti-DEC-205-antigen complex systematically targeted DCs and was presented on MHC class I for periods of up to two weeks even in low doses (Ref.[11]).

In the study by Bandyopadhyay *et. al.* biotinylated anti-DEC-205 was linked to avidin-surface modified poly lactide-co-glycolic acid (PLGA)-nanoparticles by incubation at various concentrations (demonstrated in Ref. [25]) and the nanoparticles were loaded with the antigens ovalbumin (refer to Figure 2.4). Then, the nanoparticles were tested in vitro and in vivo.

It was found that nanoparticles induced IL-10 production in DCs, with levels correlating with the concentration of anti-DEC-205 mAb on the nanoparticle surface (refer to Fig.2.5). IL-12 production by the DCs remained constant, regardless of the surface density of the affinity ligand. IL-10 inhibits a variety of cytokines, such as IL-2, a general T-helper cell growth factor, and IFN- γ , which supports mostly innate immunity (natural killer cells, CTLs, Th1-CD4⁺ cells) by stimulating IL-12 production by and inhibiting the Th2-enhancing IL-4.

TCs primed with these DCs produced IFN- γ at constant levels as well IL-10 and IL-5. Notably, only the production of IL-10 and IL-5 was influenced by the surface density of anti-DEC-205 mAb but not IFN- γ production. Nanoparticle uptake into DC was measured by Coumarin 6-staining and did not correlate with the surface density of ligands. In mice, levels of IFN- γ were increased when exposed to targeted nanoparticles and

Overall Effect	Cytokine	Secreted by	Features
multiple pleiotropic, downregulates Th1, upregulates B-cell survival and proliferation	IL-10	DCs, activated Th-1 cells	promotes IL-4 secretion, inhibits IL-12 (by DC, IL-12 and IL-2 (by Th-cells), preserves chosen Th-response
Th2	IL-4	Th cells, Th-2 cells	promotes Th-2 cytokines including itself and TGF-B which inhibits Th1 response
Th2	IL-5	Th2-cells, mast cells, eosinophils	stimulates B-cell growth and increases antibody secretion
general TC growth factor	IL-2	naïve Th-cells, Th1, CTLs	stimulates IFN- γ production in Th-cells, promoting Th1 response
feedback loop to Th1 and suppression of Th2	IL-12	DCs, macrophages	inhibits IL-4, thereby preserving Th1 response
induces Th1 response + positive feedback while suppressing Th2 response	IFN- γ	Natural killer cells, Th1 cells, CTLs	activates innate immunity, stimulates MHC class I + II upregulation

Table 2.1: Summary of relevant cytokines

IL-10 as well as IL-5 production was induced (refer to Figure 2.6). In agreement with the group's in vitro results, only the production of IL-10 and IL-5 correlated with the surface density of anti-DEC-205 surface decoration but not the production of IFN- γ .

In a secondary experiment the amount of circulating antigen-specific antibodies in mice receiving nanoparticles was measured. In this experiment the antibody titer correlated with the surface density of anti-DEC-205 on nanoparticles (not shown). This means that a high density of nanoparticle decorations results in a high antibody titer, which is a hallmark of the Th2 immune response.

Taken together, the group's results suggest that a higher density of anti-DEC-205 decoration on nanoparticles favors a humoral (Th2) response.

The Bandyopadhyay group relates their results to a conclusion formed in a study by Chieppa *et. al.* (Ref. [15]), according to which cross-linkage of mannose receptors on the surface of DCs leads to an anti-inflammatory response. Bandyopadhyay *et. al.* confirmed the theory by experimenting with complexes of biotinylated anti-DEC-205 mAb with avidin. Monocyte-derived DCs with cross-linked mannose receptors were

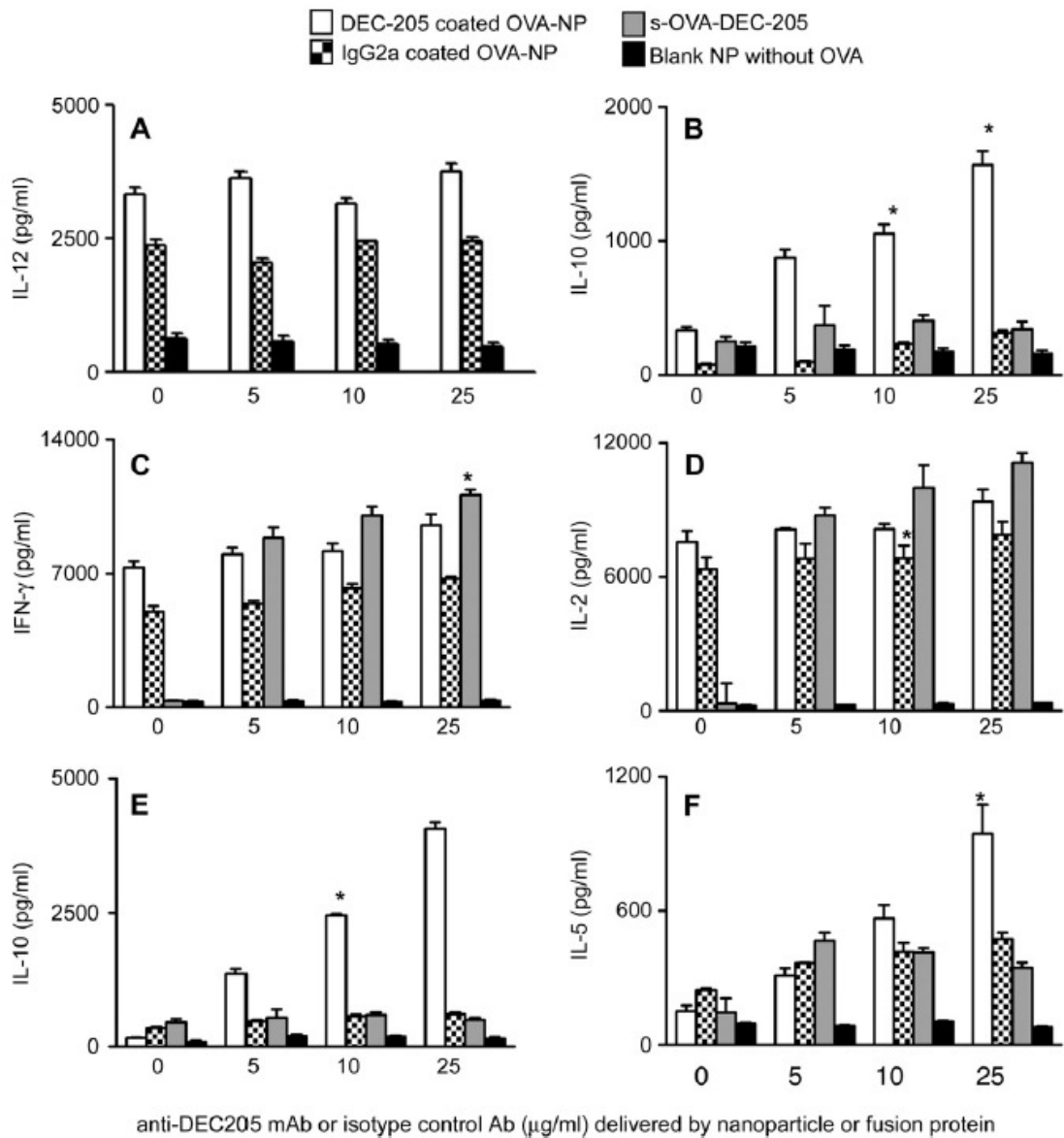


Figure 2.5: Targeted nanoparticles induce cytokine production in dendritic cells (DCs) (panels A and B) and T-lymphocytes (TCs) (panels C-F). Cytokines were measured using cytokine-specific ELISA. Values along the x-axis represent amount of anti-DEC-205 or control monoclonal antibody (mAb) IgG2a. Nanoparticles were loaded with ovalbumin or left empty. While IL-12 and interferon gamma (IFN- γ) production by TCs remains similar, increased IL-10 compared to non-targeted nanoparticles without antigens can be observed with anti-DEC-205 decorated nanoparticles. The greatest amount of IL-5 was produced by targeted nanoparticles. Taken from Ref. [7]

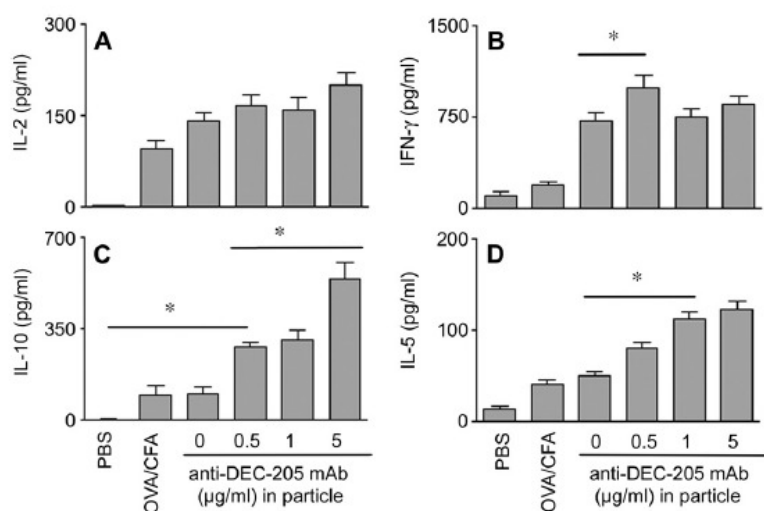


Figure 2.6: Secondary immunization of mice. Cytokine productions are consistent with in vitro results: IFN- γ and IL-2 secretions are constant while IL-10 and IL-5 secretions increase with increasing affinity ligand density. Taken from Ref. [7].

only able to produce IL-10, among other tolerance-inducing cytokines and chemokines, but not pro-inflammatory IL-12.

Bandyopadhyay *et al.* on the other hand showed that DCs targeted with (ovalbumin) nanoparticles encouraged IL-10 production without reducing IL-12 production, which prompted production of IFN- γ , IL-10, and IL-5 in primed TCs and promotes a Th2 response. When the cytokine response is combined with other effects of densely anti-DEC-205-decorated nanoparticles, including the upregulation of the scavenger (pattern recognition) receptor CD36 on DCs the response is amplified (Ref. [7], data not shown here).

CD36 is involved in innate immune responses and is often found to be upregulated in endothelial cells, macrophages and DCs responding to apoptotic cells or microbes. Upregulation of CD36 has been shown to increase IL-10 secretion (Ref. [26]). The upregulation of CD36 on DCs and the accompanying cytokine program are believed to be linked to densely decorated nanoparticles mimicking apoptotic cells (Ref. [7]).

In conclusion, the study by Bandyopadhyay *et al.* contributed important findings for the design of nanoparticle-vaccines. A high density of anti-DEC-205 favors a Th2 immune response, presumably due to cross-linkage of the receptor DEC-205 on DCs. Upregulation of the scavenger receptor CD36 is likely associated with the cytokine profile supporting a Th2 response. A Th2 response cross-inhibits a Th1 response. **In order to promote a Th1 immune response directed against cancer it is therefore vital to minimize cross-linkage of DEC205 while still allowing for specific targeting of DCs.**

2.4 The Role of DNA Origami

DNA origami provides an ingenious tool to precisely specify and manipulate DNA objects on a nanometer scale. No other technique permits exact control over shape or spacing of decoration on nano-objects the way DNA origami does. In the past years various groups have presented some astounding demonstrations of this tool, ranging from 2D smiley faces to cylinders and domes to a box with flexible hinges on its lid (Ref. [22]). Today, positioning accuracy has been increased to about 0.04 nm. The focus of current research is to find concrete practical applications that exploit all or some of the unique features of DNA origami to justify the high cost of building material.

2.4.1 How Structures Fold

In 1982, the scientific community started thinking of DNA as a construction material rather than an information carrier for the first time (Ref. [66]). Seeman *et al.* produced so-called *DNA tiles*, which can be "glued together" like tiny building blocks on the basis of inherent Watson-Crick self-recognition of DNA. Even though this technique had its limits in the error-prone and lengthy synthetic process as well as in its lack of structural complexity, the general principles proved to be robust. Thus, the field of *DNA nanotechnology* emerged.

In 2006, a major breakthrough transformed DNA nanotechnology: a new technique that is not based on the assembly of tiles was refined by the Rothemund lab (Ref. [62]). Even though in 2003 and 2004 Yin *et al.* (Ref. [78]) and Shih *et al.* (Ref. [70]) presented the first examples of the *scaffold* technique by folding a single DNA strand of about 1600 nucleotides length into an octahedron (~22 nm in diameter), Rothemund *et al.* had the most impressive impact because their DNA objects did not rely on designing or editing the scaffold strand.

The main idea of *scaffold based DNA origami* includes a long single-stranded *scaffold strand*, usually derived from the 7.25 kilobase long circular M13 phage genome, and a multitude of short *staple strands* designed as complementary sequences. The scaffold strand can be pinched into virtually any shape when the staple strands anneal to the scaffold by Watson-Crick base pairing. Thus, a 2D planar shape is constructed entirely by self-assembly. The exact designing process is much more complicated than this basic description implies, but one general rule applies:

Every helix is linked to two neighboring helices by periodic cross-overs every 1.5 helix turns, that is every 16bp for B-type DNA. Thus, there is a cross-over every 180°, which neatly arranges helices into a planar sheet. 2.7 elaborates on the design principles of planar DNA origami.

Since the scaffold approach does not rely on multiple scaffold elements binding to each other it is independent of relative stoichiometric ratios. Due to the entropic advantage of having one single long scaffold strand rather than assembling tiles sequentially

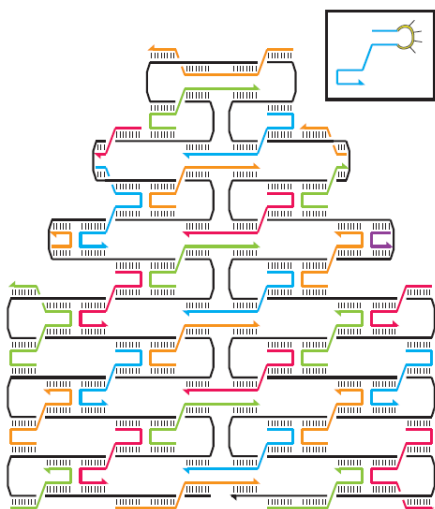


Figure 2.7: To design a DNA origami object, first the object is viewed as helix bundles stacked on top of each other and linked by periodic Holliday junctions. A scaffold strand winds through the helices back and forth in a raster pattern, incorporating one of the two helix strands at a time. Staple strands are added. They are complementary short sequences that span helices and "pinch" the scaffold into the desired shape. At helix-cross overs the staples reverse direction. Anti-parallel cross-overs proved to be especially robust. This figure is slightly misleading, because in fact the design leaves no single base unpaired. Taken from Ref. [62].

the technique is also faster than tile assembly and synthesis protocols are less time-consuming, let alone much easier to follow.

The same general principle that was refined by Rothemund *et. al.* can also be applied to create hollow or closed 3D structures: the trick is to stack and angle multiple 2D layers by introducing more cross-overs. One of the first examples for this approach was the DNA-box in the top row of figure 2.8. The box features a lid on top that can be opened if the correct "key" is inserted. Elongated staple strands with toehold extensions decorate the lid on one side and a flexible hinge is placed on the opposite side. The toehold extensions can be displaced by single strand displacement of the correct complementary "key" strand. This structure was the first to change topology upon an external stimulus (Ref. [4]).

A challenge was that the single layer structures were often unstable and could offer only weak resistance to mechanical stress. Shih *et. al.* demonstrated cleverly that densely packed layers of antiparallel helices can be linked by cross-overs in such a way that their *register* (i.e. relative displacement with respect to the axis of the helix) defines the way adjacent helices are interconnected (Ref. [23]). Every helix is connected to three adjacent helices by cross-overs that are at a relative angle of 120° and are spaced every 7 base pairs along the helical axis. The 3D structure's cross-section is, therefore, hexagonal and resembles a honeycomb lattice (see 2.8 third row). Hence, with this broadly applicable method the geometry of basic building blocks can be elegantly defined.

3D-structures self-assemble in a one-pot-reaction using thermal annealing cycles that take three days up to one week, depending on the complexity of the structure. Examples are the monolith or a square nut that can be seen in Figure 2.8 in the third row.

The DNA nanotechnology platform also demonstrated that they could modify the lattice

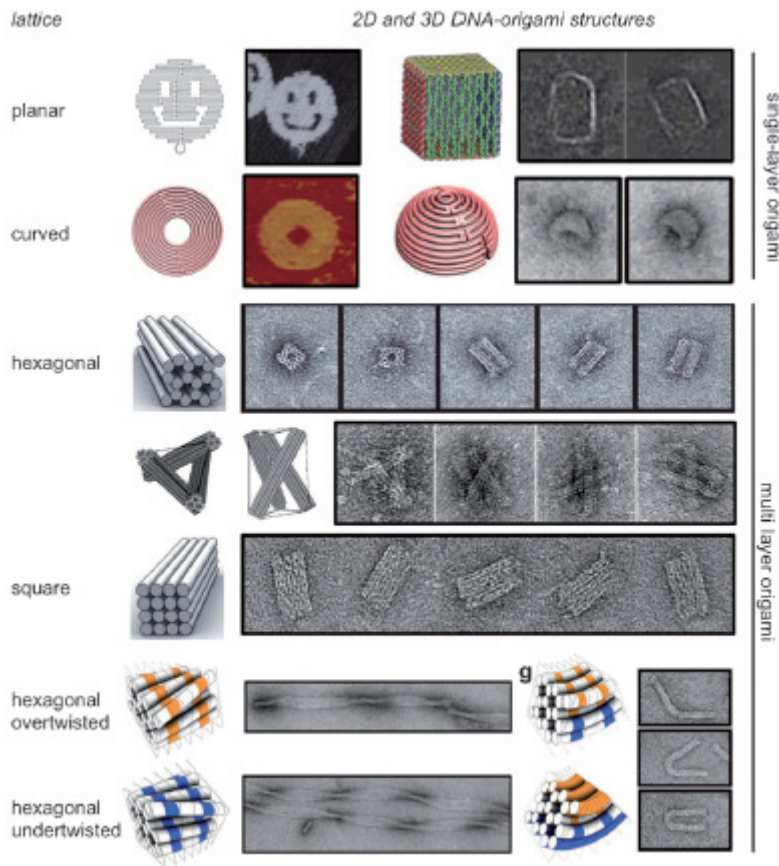


Figure 2.8: Single layer and multi-layer examples of DNA origami structures, Reprinted from Ref. [4, 21, 23, 62].

from a honeycomb to a square design, thus creating flat surfaces, smaller cavities, and denser structures (Ref. [42], third row from the bottom in Figure 2.8).

Finally, Dietz *et. al.* illustrated that supertwisted helical axes can be created by insertion or deletion of base pairs of the regular 7 base pair-spaces between cross-overs. Thus, globally twisted or curved structures can be created (last two rows in Figure 2.8). Another approach to 3D DNA origami design pursued by Liedl *et. al.* (Ref. [49]) was fittingly termed "*Tensegrity*", which is a combination of the words "tendon" and "integrity". The principle is inspired by macroscopic architecture, where rigid sticks (termed "struts") are often linked by flexible linkers ("tendons"). While the struts push outwards the linkers pull inwards, thus balancing the force and creating a rigid object. In DNA origami the struts are replaced by helix bundles and the linkers are single stranded DNA segments, which function as entropic spring tendons (refer to Figure 2.8 forth row from the top). Hence, a mechanically responsive DNA object similar to the box with a lid described above may be created.

Even though the extension of Rothmund's theory seems natural, it should be mentioned that 3D objects are nowhere near as straightforward as 2D objects and their design in-

volves many more parameters than the arrangement of cross-overs. Fortunately, software tools such as *caDNAno* have been developed to assist the process. Even though one cannot completely rely on the software to design objects of any shape or size, the software tools do greatly speed up the process and eliminate human errors in the entirely manual design process.

2.4.2 Achievements in the Field

Perhaps one of the most compelling achievement in recent years was published by Douglas *et. al.* in 2012. Douglas *et. al.* created a structure that has robot-like characteristics and can sense, compute and actuate.

If the DNA structure senses defined cell surface inputs, it changes confirmation ("*opens*") to expose previously hidden surfaces and deliver a payload to the cells. The hexagonal, barrel-shaped device of the dimensions 35 nm × 35 nm × 45 nm can be loaded with a wide range of materials, such as antibody Fab fragments or gold particles, which can be organized in precise DNA origami-trademark fashion (see Ref. [22]).

A logic *AND* gate encoded by staples modified with DNA aptamers (i.e. oligonucleotide molecules that bind to a specific target molecule) controls the opening of the lid and the subsequent conformational change that leads to delivery of contents. Aptamer locks work in binary fashion, that is either they bind ("1") or they do not bind ("0"). Only when all encoded locks bind the lid will open, thus representing an *AND*-function (refer to Figure 2.9). The device was recently studied *in vivo* in a cockroach model, where the nano robotic devices resolved various logical gates (*AND*, *OR*, *XOR*, *NAND*, *NOT*, *CNOT* and a half adder) (Ref. [3]).

Douglas *et. al.*'s nano robotic device illustrates one of the unmatched strengths of DNA nanostructures. They can be engineered to allow unique access at precisely specified positions: selected staple sequences protrude out of the origami plane to expose single stranded "handles". Proteins, fluorophores, or nanoparticles, such as aptamers, can be functionalized with complementary single stranded DNA "anti handles" that bind to the protruding staple sequence, thus effectively linking the two components by a so-called *handle-anti handle* hybridization. Aside from engineering lock systems, this concept is far more often used to fuse molecules in close proximity to a DNA tile and study nano scale interactions.

For example, Fu *et. al.* assayed and enhanced enzymatic activity in protein cascades (Ref. [28]) and Shaw *et. al.* studied distance-dependent effects in receptor–ligand interactions on cell membranes. Ephrin-A5 ligands were connected to DNA origami at different distances and then exposed to a breast cancer cell line, with the result that closely spaced ligands phosphorylate and activated EphA2 receptors more effectively than widely spaced ligands (Ref. [69]).

Similarly, DNA nanostructures can also be used to study motor protein assemblies, such as motors walking on microtubule filaments. Kinesin-1 and dynein were coupled to the

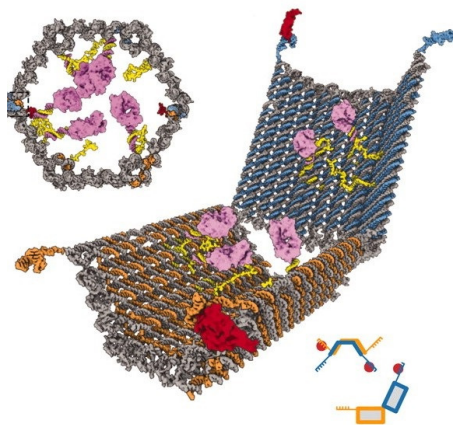


Figure 2.9: Front view of a DNA origami device designed by Douglas *et. al.* that carries a variety of precisely positioned materials, such as gold nanoparticles and antibody Fab fragments, and can resolve a logical gate upon which it will change confirmation and deliver the payload. Two DNA-aptamer locks fasten the front of the device on the left (dotted lines in the left cross sectional image) and right. Reprinted from Ref. [22].

same DNA nano structure-cargo and then proceeded to engage in a tug of war. The process continued until one of the two molecules was released by photocleavable linkers (Ref. [20]).

In the field of fluorescence and super resolution imaging DNA nano structures offer great potential. Förster resonance energy transfer (FRET) data obtained from placing donor and acceptor dyes at specific distances on DNA origami structures allowed the direct correlation of the theoretical distance dependence of energy transfer (Ref. [73]). Finally, exploiting the unique features of DNA origami a new super resolution technique has been developed. So-called DNA points accumulation imaging in nanoscale topography (PAINT) relies on stochastic switching between fluorescence on- and off-states, which is facilitated by repetitive, transient binding of short, fluorescently labeled *imager strands* to complementary *docking strands*. Every time an imager strand binds, its fluorescence emission is detected and marked for super resolution reconstruction. PAINT is an improvement over other tools like stochastic optical reconstruction microscopy (STORM) or photo-activated localization microscopy (PALM) in some aspects because it allows decoupling of "blinking" (seemingly random switching between "on" and "off" states) of fluorophores from their complex photophysical properties for single-molecule localization.

2.5 Procedural Background Notes

2.5.1 The Candlestick

The origami structure that will likely be used in this project is a 60nm high x 30nm wide cylindrical barrel made from the ~7 kb long single stranded M13 phage genome. It was designed in-house by a member of the Shih lab.

2.5.2 Gibson Cloning

Molecular cloning was performed for the assembly of two different constructs. Each time the *Gibson Cloning* technique was applied.

Gibson Cloning is a simple, rapid cloning method that is particularly useful for the assembly of multiple DNA fragments regardless of their length or end-compatibility. The incubation time is as little as 15 min to one hour, so the entire process can be run in a day. This isothermal reaction is set up in a single tube and the end result is a double-stranded fully sealed DNA molecule that can be directly used for bacterial transformation, as was done in this project.

Fragments need to have overlapping regions at the desired joining sections. These can be added by polymerase chain reaction (PCR) by designing primers that feature "overlaps", i.e. nucleotides identical to the adjacent joining fragment. It is recommended that one uses a high-fidelity DNA polymerase in this step.

After amplification of the overlapping fragments to be assembled by PCR the reaction is incubated in a master mix consisting of three enzymes: an exonuclease, a proprietary DNA polymerase, and a DNA ligase, which work in the following way (refer to Figure 2.10):

- First, the exonuclease chews off nucleotides of the double stranded fragments in 5'-3' direction. The fragments base pair to create the desired construct.
- Next, DNA polymerase fills the gaps in the sequence.
- Finally, DNA ligase seals the remaining nicks in the double stranded DNA.

Before construct assembly it is recommendable to digest the original template by addition of Dpn1. The restriction endonuclease cleaves exclusively methylated recognition sites (GA-TC), but does not cleave the PCR product, which is not methylated. This step greatly enhances transformation efficiency by reducing template background.

Even though in this project only two fragments were joined, as many as six fragments can be successfully joined by Gibson Cloning.

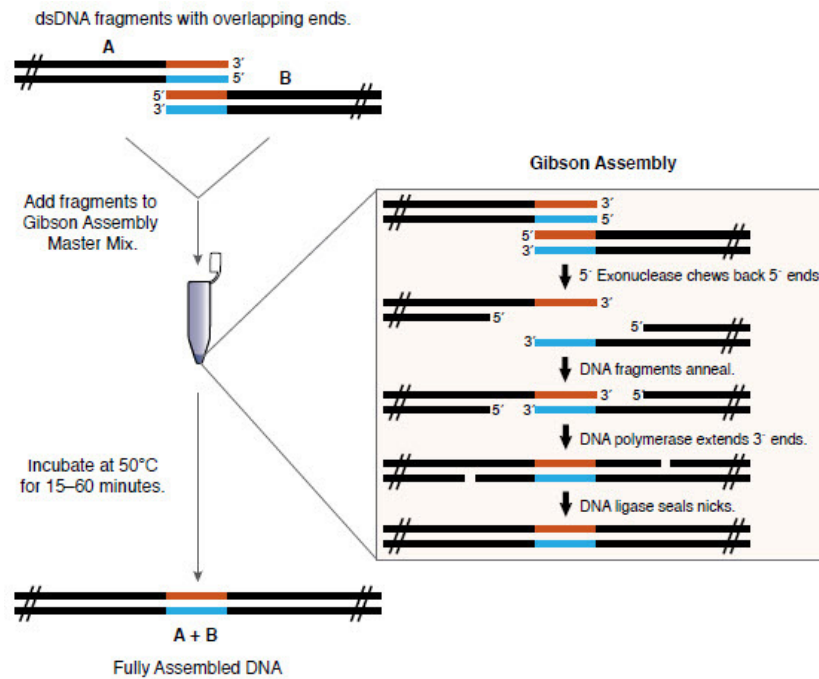


Figure 2.10: Procedural steps involved in the Gibson Assembly cloning method. Two double stranded fragments are to be joined, A and B. Both fragments feature overlapping regions. The fragments are incubated with a master mix containing an exonuclease, that chews back the 5' ends; a DNA polymerase, that extends the 3' ends of the joined fragments; and a DNA ligase that fills the nicks in the double stranded construct. The reaction takes max. 1 hour at 50 °C and the product can be directly used for transformation. Reprinted from [8].

CHAPTER 3

Methods

This chapter describes the methods and materials used in the context of this Master thesis. The chapter is divided into the following three main sections: Cell Lines (section 3.1), Molecular Cloning (section 3.2), and Protein Expression and Processing (section 3.3). Each section contains subsections that further elaborate on experiments performed within the step in the projects. Sequences of the final assembled product as well as primer oligo nucleotides can be found in the *Appendix* section.

3.1 Cell Lines

In the course of the project two cell lines were applied in protein expression: *BL21 (DE3) competent E.coli* (New England BioLabs, Catalog # C2527H) and *SHuffle T7 Express competent E.coli* (New England BioLabs, Catalog # C3029H). A summary of the two cell lines can be found in Table 3.1).

An intermediate cell line, *NEB 5 alpha competent E.coli* (New England Biolabs, Catalog # C2987), expressed the assembled construct in *pUC57* in one cloning cycle. This cell line was not used for protein expression but merely served to facilitate the transformation of the assembled cloning construct into the expression cell line *BL21 (DE3)*.

All cell lines were cultured in in-house produced LB medium with addition of kanamycin sulfate (Sigma Aldrich, Catalog # 25389-94-0) at a concentration of $50 \mu\text{g ml}^{-1}$ for *BL21(DE3)* and $100 \mu\text{g ml}^{-1}$ for *SHuffle T7* cells.

BL21 (DE3 *E.coli*)

The cell line features the promoter *T7*, which can be switched on to express genes downstream of the promoter by IPTG (Calbiochem, Catalog # 420322) addition to the

medium, and is classified as a B strain because it is deficient in Lon protease (cytoplasm) and OmpT protease (outer membrane). "DE3" specifies that λ DE3 lysogen is contained, which carries the gene for T7 RNA polymerase under control of the lacUV5 promoter. BL21 (DE3) is resistant to T1 Phage, an extremely virulent phage that requires a specific receptor for uptake and infection (denoted as *fhuA2*). Deletion of this gene protects the cell line from infection, but otherwise does not necessarily contribute to transformation or growth characteristics. BL21(DE3) is among the most common *E.coli* recombinant protein expression cell lines.

SHuffle T7 Express *E.coli*

The Shuffle T7 Express competent cell line is an enhanced BL21 derivative. This *E.coli* cell line is specifically engineered to form proteins containing disulfide bonds in the cytoplasm, which is normally a reducing environment. This is possible because the two reductases *glutaredoxin reductase* and *thioredoxin reductase* have been deleted in SHuffle T7 Express (denoted by Δ trxB and Δ gor) and a mutation in the peroxiredoxin enzyme protects the cells from the resulting lethality of the two deletion mutations.

In addition, SHuffle T7 Express expresses a version of the periplasmic disulfide bond isomerase DsbC, which is retained in the cytoplasm. The enzyme corrects mis-oxidized disulfide bonds and has also been shown to be an effective chaperone in the folding of target proteins, independent of the presence or absence of disulfide bonds (Ref. [33]).

Due to a deficiency in endonuclease I, a non-specific endonuclease in the *E.coli* periplasm, plasmid preparation from SHuffleT7 is greatly improved. A deficiency in two proteases assists the production of proteins from cloned genes: each *E.coli* B strain is inherently deficient in the lon protease that in other strains serves to degrade misfolded proteins. Additionally, SHuffle T7 Express is deficient in the OmpT protease, which is found in the surface of various *E.coli* strains. Like BL21, SHuffle T7 Express is resistant to T1 Phage.

For a summary of the two expression cell lines refer to Table 3.1.

3.2 Molecular Cloning

Molecular cloning was performed twice within the course of the project: once in the vector pUC57 and then again in pET30a. Plasmid identity was verified by restriction digestion. Two types of restriction enzymes were used: BAMH1 and EcoR1. Ape software was used to find restriction sites and resulting fragment lengths (Ref. [59]).

For BAMH1, about 300 ng of plasmid DNA were digested with 1 μ l enzyme (FastDigest BamHI, Thermo Fisher Scientific, Catalog #FD0054) in 2 μ l buffer (FastDigest Green reaction buffer, Thermo Fisher Scientific) and sterile water to 20 μ l at 37°C for 30 minutes.

Cell Line	Genotyp	Feature
BL21(DE3)	fhuA2 [lon] ompT gal (λ DE3) [dcm] Δ hsdS λ DE3 $=\lambda$ sBamHIo Δ EcoRI-B int::(lacI::PlacUV5::T7 gene1) i21 Δ nin5	Routine T7 expression
SHuffle T7 Express	fhuA2 lacZ::T7 gene1 [lon] ompT ahpC gal λ att::pNEB3-r1-cDsbC (SpecR, lacIq) Δ trxB sulA11 R(mcr-73::miniTn10-TetS)2 [dcm] R(zgb-210::Tn10-TetS) endA1 Δ gor Δ (mcrC-mrr)114::IS10	Disulfide bond isomerase DsbC, T7 RNAP, deficient in proteases Lon and OmpT

Table 3.1: Summary of expression cell lines

For EcoRI, two different enzymes were used, EcoRI (NEB, Catalog # R0101T or R0101S) and EcoRI HF (High-Fidelity EcoRI, Catalog # R3101T). For regular EcoRI self-made 3x EcoRI-buffer was used (300mM Tris HCl, 150mMNaCl, 30mM MgCl₂, 0.075% Triton-X100, ultra pure water, pH=7.5 at 25°C). For the high-fidelity version of the enzyme CutSmart buffer was used (CutSmart Buffer, NEB, Catalog # B7204S). EcoRI digestions were incubated at 37°C for one hour in volumes of 20 μ lor 50 μ l, and then heat-inactivated at 65°C for 20 minutes. If DNA-polymerase was present in the sample, the heat-inactivation step was skipped, or DNA polymerase was removed from the sample by PCR-purification.

20U of EcoRI (HF) enzyme were used for 1 μ g of plasmid DNA, and 50U were used for 10ng of hybridized DNA oligos (84bp). DNA hybridization was performed by incubating oligo nucleotides with 3x excess adapter sequences for 2 minutes at 95 °C in 1xTE buffer supplemented with 200mM MgCl₂, followed by cooling down to room temperature at 4°C for annealing.

The protocol followed the basic steps for Gibson Cloning described in the previous chapter.

Preparations

The fragments were amplified by two PCRs, one for the insert fragment and one for the vector, with primers that had overlaps equal to the adjacent fragment sequence on their 5' ends. Q5 Hot Start was used as a high fidelity polymerase with Q5 GC Enhancer and Q5 Reaction Buffer (all components by NEB, Catalog # 's: M0493S, B9028S, B9027S). Primers were designed to have overlapping regions: There are four different primers in use, a forward and reverse primer for the insert region and a forward and reverse primer for the vector region. Each primer consists of an approximately 25 bp region that anneals to the fragment and a region of approximately the same length that extends into

the adjacent fragment (refer to Figure 3.1a). The primers were tested for similar GC-contents and melting temperatures and that within the last five base pairs there are no more than three and no less than 1 G-C base pair on the 5' and 3' ends. Runs and repeats of base pairs were avoided. The primers were tested for hair pin formation, self- and cross dimerization, and sequence similarity by BLAST (NCBI) and the IDT online tool (Ref. [74]).

All primers that were used in the course of this thesis were ordered from IDT (Ref. [74]) and supplied as lyophilized powder. The tubes were briefly centrifuged and the powdered oligo nucleotides were diluted in sterile H₂O to a concentration of 100 μ M and stored in the freezer at -20 °C. Working stocks were stored in the fridge at 4 °C in sterile H₂O or 1xTE buffer (500mM Tris, 50mM EDTA in high purity RO H₂O, adjusted to pH 7.5 at 25°C, 0.2 μ m filtered, affymetrix, Catalog # 75834) at a concentration of 10 μ M.

Dpn1 was added directly to the reaction tubes at a concentration of 1000 units per reaction with 1x buffer (CutSmart Buffer, NEB, Catalog # B7204S) and incubated at warm room temperatures for one hour. After one hour the enzyme was heat inactivated for 20 minutes at 80°C. The reactions were treated with a commercially available PCR-purification-kit (QIAquick PCR Purification Kit, Qiagen), which removes primers, nucleotides, enzymes, mineral oil, salts, agarose, ethidium bromide, and other impurities from DNA samples by a silica membrane assembly for binding of DNA in high-salt buffer and elution with low-salt buffer. The kit uses a simple step-by-step guide to a bind-wash-elute procedure in a spin column. Samples of the crude, Dpn1 digested, and purified PCR products were run on a 1% agarose gel (unless mentioned otherwise) for control before commencing with Gibson Assembly.

Gibson Assembly

Gibson Assembly was performed using an in-house prepared master mix (1x Isothermal Amplification Buffer (ISO), 10 U/uL T5 exonuclease, 2U/uL Phusion polymerase, 40U/uL Taq ligase, all purchased from NEB, sterile filtered H₂O). The purified insert and vector PCR products were added at equimolar amounts, or at a ratio of insert : vector = 2:1, to a total of 300 fmol (estimating each bp of dsDNA as 650 g/mol). The mixture was incubated at 50 °C for 1 hour and then transformed into *BL21 (DE3)* (in the case of pET30a vector) or *NEB 5 alpha* (in the case of pUC57 vector) competent *E.coli* cells according to high efficiency transformation procedure (Ref. [8], refer to section 3.2.1). In addition, colonies were sent for sequencing by GENEWIZ (Ref. [30]) to confirm the correctness of the assembled construct and the absence of mutations. Colonies that passed all quality controls were prepared as 25% glycerol stocks and stored at -80°C.

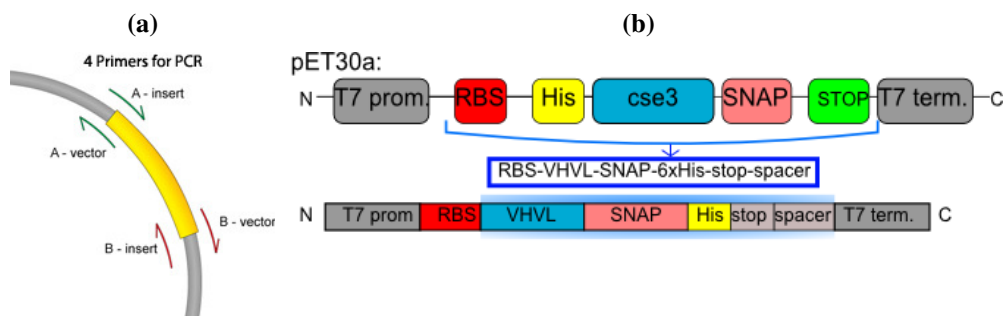


Figure 3.1: (a) For Gibson Assembly fragments need to be amplified with overlaps, which can be done by PCR. Primers are designed to anneal to the fragment and extend into the adjacent fragment by about 25 base pairs (termed "overhang"). (b) Outline of the final product to be assembled. The upper line provides a scheme of the vector pET30a, where the insert fragment will replace the region enclosed in blue brackets (ribosome binding site (RBS), His tag, cse3, SNAP tag, and Stop codon). The insert consists of a ribosome binding site (RBS), a VH and VL gene (variable antibody region), a SNAP tag for spacing, and a His tag for purification. The final product is shown in the lower line. Antibiotic resistance against Kanamycin is included in the vector in the case of pET30a.

The sequence for the entire construct of pET30a-VH-SNAP-His as well as primer sequences can be found in the *Appendix* section.

3.2.1 Transformation and Quality Controls

Standard high efficiency transformation (NEB, Ref. [8]) calls for thawing of competent cells on ice for ten minutes or until all ice crystals disappeared. Then, about 50ng of plasmid are added in a volume of 5 μ l to the competent cells. The tubes are flicked, but not vortexed, and incubated on ice for 30 minutes, followed by a heat shock treatment at exactly 42 $^{\circ}$ C for exactly 30 seconds. The cells were put back on ice for another five minutes and then rescued with 950 μ l Super Optimal Growth (SOC) medium, a very rich medium with added glucose for *E.coli*. After incubated at 37 $^{\circ}$ C (BL21 (DE3)) or 30 $^{\circ}$ C (SHuffle T7 Express) for one hour, the cells were diluted in SOC medium in multiple serial dilution steps and spread onto LB-Kanamycin selective plates (previously prepared according to standard recipe: 5g NaCl, 5g Tryptone, 2.5g Yeast Extract, 7.5g Agar, sterile H₂O to 500 ml, autoclaved, kanamycin-sulfate was added to a concentration of 100 μ g ml⁻¹ once the temperature cooled down to about 60 $^{\circ}$ C, poured under sterile conditions, and set to cool at room temperature overnight) using a commercially available sterile spreader loop (Sterile Colony Spreader, Thermo Fisher Scientific, Catalog # R4853000). Colony plates were incubated at 37 $^{\circ}$ C overnight. Freshly prepared plates were stored in the cold room at 4 $^{\circ}$ C for later use for up to one month.

Step	Temperature [°C]	Time
Initial Denaturation	94	30s
30 cycles	94	25s
-	55	35s
-	68	1 min. per kb = 5.5 min. (vector) or 1.66 min. (insert)
Final extension	68	5 min.
Hold	4	forever

Table 3.2: *Assembly and Transformation control PCR*

Colonies were subjected to a colony PCR (pUC57 and pET30a in BL21 (DE3)) or miniprep using a spin miniprep kit for purification of molecular biology grade plasmid DNA (QIAprep Spin Miniprep Kit, Qiagen, Catalog # 27104) and subjected to PCR (pET30a in SHuffle T7) to check successful fragment assembly or transformation. Colony PCRs were performed with Taq DNA polymerase (M0267L, NEB) and Standard Taq buffer (B9014S, NEB) applying an initial lysis step in the thermocycle protocol to lyse bacterial cell walls.

All miniprep plasmids prepared in the course of this thesis were checked for concentration and purity with a spectrophotometer (NanoDrop 200c, Thermo Scientific). Both the vector and the insert were checked with separate pairs of primers, and positive and negative controls were included. Taq polymerase and Taq polymerase Standard buffer were used with 1ng of control template (vector or insert respectively, with sterile H₂O as negative control) or a minimum amount of colony picked with a sterile pipet tip in a sterile environment and dissolved in sterile H₂O for 15 minutes. The reactions were subjected to a PCR cycle that can be found in Table 3.2).

In addition, a restriction digest with BAMH1 was performed (FastDigest enzyme and FastDigest Green Buffer, both purchased from Thermo Fisher Scientific, Catalog # FD0054). The restriction digest required 1µl of enzyme with 300ng of sample plasmid DNA in 2µl of buffer and sterile H₂O to 20µl .

Four cultures of pET30a in BL21 (DE3) were miniprep and transformed into the cell line SHuffle T7 (according to high efficiency transformation procedure (Ref. [8], refer to section 3.2.1).

For the SHuffle T7 Express cell line a colony PCR was performed but it was unsuccessful, so the cells were cultured, miniprep, and correctness was confirmed by PCR and restriction digest with BAMH1. For the PCR a new set of primers, which amplified the insert and part of the vector upstream and downstream, was designed. The PCR as run with Taq polymerase and Standard Taq buffer on 1ng of template or controls (vector, plasmid from previous experiments that was proven to contain insert in pET30a, and sterile H₂O). The thermocycle can be found in Table 3.3.

Step	Temperature [°C]	Time
Initial Denaturation	95	30s
30 cycles	95	25s
-	55	35s
-	68	1 min. per kb = 2 min. 3s
Final extension	68	5 min.
Hold	4	forever

Table 3.3: control PCR SHuffleT7 transformation

All DNA products were visualized on a 1% agarose gel (unless mentioned otherwise) (Lonza, Catalog # 50004) with 1.8mM MgCl₂ (dissolved in sterile H₂O and sterile filtered, Sigma Aldrich, Catalog # 7786-30-3) at a voltage between 80 and 95V. Purple loading dye (NEB, Catalog # B7024S) and sterile water were used for sample preparation. Agarose gels were visualized by SybrSafe dye (10µl per 150ml gel).

3.3 Protein Expression and Processing

Protein expression was pursued in BL21(DE3) and in SHuffleT7 Express. Both cell lines feature the IPTG-inducible T7 promoter and can, therefore, be induced by addition of IPTG to the medium.

3.3.1 Bacterial Cell Culture

Medium was prepared in-house (standard LB medium) and kanamycin-sulfate antibiotic (Sigma Aldrich, Catalog # 70560-51-9) was added from frozen aliquots at a concentration of 100 µg ml⁻¹ freshly.

Both cell lines were inoculated into 5-8ml LB-Kanamycin medium in glass tubes, or in 60ml in glass flasks for time course experiments, and left shaking at 37°C (BL21(DE3)) or 30°C (SHuffle T7 Express) at 200rpm until an OD of 0.4 - 0.6 (BL21) or 0.3 - 0.5 (SHuffle T7) was reached (continuous observation by sampling at regular intervals), at which point the cells were induced at concentrations between 0.25mM and 1mM. A control flask containing a sterile pipette tip in medium was always incubated alongside the samples to check for contamination. In some cases cells were inoculated overnight and then re-inoculated at a ratio of 1:100 the following morning. Overnight incubation times never exceeded 14 hours to ensure a healthy state at re-inoculation. BL21 (DE3) cells were transferred to either 37°C, 18°C, or 15°C whereas SHuffle T7 Express cells were transferred to either 30°C or 16°C and cultured for either 4 hours or overnight (18 to 22 hours). Samples were taken pre-induction and post induction. In time course experiments the cultures were sampled hourly for six hours. Initially, the sample volume

was normalized, taking a 2ml sample pre-induction and a sample volume corresponding to 1ml culture at OD 0.8 post-induction. Later on the samples were normalized by sampling the same volume and basing lysis buffer volumes on the measured OD pre- and post-induction. Pelleted cell culture samples were stored at -20°C.

3.3.2 Sample Lysis and Analysis

Lysis

For lysis, previously taken samples were thawed on ice. Lysis was performed both chemically and physically initially but was soon replaced by chemical lysis with addition of lysozyme from chicken egg white (1 mg ml^{-1} , Sigma Aldrich, Catalog # L6876) due to concerns of protein degradation.

For BL21 (DE3), xTractor lysis buffer (Clontech Laboratories, Catalog # 635623) was mainly used. Volumes of buffer were based on linear interpolation of suggested volumes per volume lysate and OD at the point of sampling. Cells were gently resuspended in buffer and incubated on ice for 15 minutes. In later experiments, lysozyme from chicken egg white (1 mg/mL) together with phenylmethylsulfonyl fluoride (PMSF) (Sigma Aldrich, Catalog # 329-98-6) in isopropanol (1 mM) as an Ethylenediaminetetraacetic acid (EDTA)-free protease inhibitor, and 2U DNase1 (NEB, Catalog # M0303S) per cell lysate replaced physical lysis by sonication. Lysozyme aids cell lysis by catalyzing hydrolysis of chemical bonds in the outer cell walls of bacteria. PMSF is a common serine protease inhibitor that protects the extracted protein from degradation, while DNase1 is an endonuclease that reduces the viscosity of the lysate by nonspecifically cleaving single stranded and double stranded DNA. Cells were incubated in an end-over-end rotary mixer at room temperature for 15 minutes. If the supernatant fraction was analyzed separately from the pellet fraction, the cells were spun at $16.9 \text{ k} \times \text{g}$ at 4°C for 20 minutes and the pellet was resuspended in 1x phosphate buffered saline (PBS).

Most of the samples collected from BL21 (DE3) cells transformed with pET30a as well as all samples from SHuffle T7 Express cells were lysed using CellLytic B buffer (Sigma Aldrich, standard strength, Catalog # B7435). Again, buffer volumes were based on linear interpolation of suggested amounts provided for the CellLytic B buffer. Pellets were resuspended in buffer and briefly vortexed. Then, lysozyme (1 mg ml^{-1} lysate), DNase1 (2U/lysate), and PMSF (1 mM) were added to the mixture at appropriate concentrations and the mixture was incubated in an end-over-end rotary mixer at room temperature for 15 minutes. If the supernatant fraction was analyzed separately from the pellet fraction, the cells were spun at $16.9 \text{ k} \times \text{g}$ at 4°C for 20 minutes and the pellet was resuspended in 1x PBS.

Sonication (Qsonica, Q125 Sonicator) was performed initially but soon abandoned. The equipment was set to 20% amplitude and two pulses of 30s each with 2s off time in

between. Samples were kept in a cold water bath in the cold room. Sonication was replaced by lysozyme addition in the chemical lysis due to concerns of damage to proteins by the procedure.

Refolding of Inclusion Bodies

Samples taken from the construct in the pET30a vector transformed into BL21 (DE3) underwent the process of refolding. The samples were freshly lysed using CelLytic B buffer with added lysozyme, PMSF, and DNase1 following the procedure explained in section 3.3.2. Then the lysates were centrifuged at 16.9 k x g at 4°C for 20 minutes and the supernatant fractions were removed and saved.

The pellet fractions were weighed to estimate the volume of inclusion body solubilization buffer (CelLytic IB Inclusion Body Solubilization Reagent, Sigma Aldrich, Catalog # C5236). To 1g wet IB weight a volume of 8ml buffer was added. The suspension was vortexed for 1 minute and then transferred into a shaker and incubated at room temperature for 30 minutes. After complete solubilization, cell debris was removed by centrifugation at 16,000 x g at room temperature for 15 minutes. Supernatant fractions containing the soluble protein were carefully saved and pellet fractions were re-suspended in 1x PBS.

The inclusion body solubilization buffer contains denaturing urea, which needs to be removed or vastly diluted before the protein can be analyzed by SDS PAGE. Part of the samples were subjected to trichloroacetic acid (TCA) precipitation (refer to section 3.3.2) to remove denaturants and achieve the natural confirmation, which in turn allows analysis by SDS PAGE. Another part was diluted to retain the denatured form and still allow analysis by SDS PAGE. These gels were stained using the Silver Stain technique because of its lower detection limit than Coomassie Blue (refer to section 3.3.2).

TCA Precipitation

TCA precipitation was performed on pellets from cell lysates that were suspected to contain the desired protein based on analysis by SDS PAGE. Solubilization of these pellets retained denaturants contained in the solubilization buffer in the sample. The denaturants can be removed by dialysis, or, as was done in this experiment, by TCA precipitation.

The supernatant collected at the end of the inclusion body solubilization procedure (refer to section 3.3.2) was subjected to TCA precipitation. The steps in the protocol published by A.J. Link and J. LaBaer (Ref. [50]) were followed, except that for final evaporation no heat and low pressure was used.

The protocol comprised addition of 0.11 volumes of ice cold 100% TCA (solubilized in sterile water) to the solubilized protein samples. The mixture was incubated on ice for 10 minutes. 0.5ml of 10% TCA was added to the samples and the mixture was placed on

ice for 20 minutes. Centrifugation at 20,000 x g for 30 minutes collected the precipitated protein on the bottom of the tube. The supernatant fractions were removed. 0.5ml of acetone (Sigma Aldrich, Catalog # 67-64-1) was added to carefully wash the pellet fractions and the samples were centrifuged at 20,000 x g for 10 minutes. Again, the supernatant fractions were removed carefully and disposed. Finally, the protein pellet was dried in a vacuum evaporator for 3 minutes at room temperature and low pressure. The pellets were then stored at -20°C for subsequent analysis of the proteins in their natural confirmation by SDS PAGE. Pellets were resuspended in their original volume of 1xPBS buffer.

His-Tag Chromatography

His tag chromatography was performed twice, once for a sample in pUC57 eluting with a higher imidazole concentration in the elution buffer in a native system, and once for a sample in pET30a, where elution was based on a change in pH in a denaturing system. For the sample in pUC57, the Binding Buffer, Wash Buffer, and Elution Buffer recipes as well as the procedure were based on the protocol by Thermo Fisher Scientific (batch method, HisPur Ni-NTA Superflow Agarose, Catalog # 25214 and associated protocol, see below for detailed description). All buffers contained 20mM sodium phosphate and 300mM sodium chloride at pH 7.4 but varied in imidazole concentration. Elution imidazole concentration was ten times greater than Wash imidazole concentration. For the sample in pET30a, the previously mentioned lysis and inclusion body solubilization protocols were performed. After complete inclusion body solubilization was shown by SDS PAGE, samples that did not undergo TCA precipitation were subjected to His-tag chromatography because proteins needed to be in their denaturated state to expose the His-tag. 30µl of sample in inclusion body solubilization buffer were analyzed in liquid form (see section 3.3.2).

The protocol that was followed was published by Thermo Fisher Scientific (batch method, HisPur Ni-NTA Superflow Agarose, Catalog # 25214 and associated protocol), but recipes for buffers were based on the protocol by McLab Molecular Cloning Laboratories (manual provided for Catalog # NINTA-200).

For elution by change in pH, three denaturing buffers were prepared from a 10x Stock Solution A (200 mM sodium phosphate, monobasic, 5 M NaCl) and 10x Stock Solution B (200 mM sodium phosphate, dibasic, 5 M NaCl). Refer to Table 3.4 for buffer recipes. All buffers were filtered using a 450nm filter before use.

His-tag chromatography was performed using Ni-NTA beads and agarose resins provided by Thermo Fisher Scientific. The procedure for purification of His-Tagged proteins by batch method for small resin beds was followed. All centrifugation steps were carried out at 700 x g. Re-suspension by pipetting up and down was avoided throughout the procedure due to possible loss of beads.

200µl of Ni-NTA beads were added to the resin and centrifuged at 700 x g for two

Reagent	mass or volume
Denaturing Binding Buffer	
10x Stock Solution A	0.58 ml
10x Stock Solution B	9.42 ml
Urea	48.1g
Adjust to pH 7.8 at 25°C	
Sterile water	to 100 ml
Denaturing Wash Buffer	
10x Stock Solution A	7.38ml
10x Stock Solution B	2.62ml
Urea	48.1g
Adjust to pH 6.0 at 25°C	
Sterile water	to 100 ml
Denaturing Elution Buffer	
10x Stock Solution A	10ml
Urea	48.1g
Adjust to pH 4 at 25°C	
Sterile water	to 100 ml

Table 3.4: Buffer recipes for His tag chromatography

minutes. Two resin bed volumes of Binding Buffer were added and mixed carefully by flicking the tube. The column was centrifuged twice and the supernatant fraction was carefully removed by pipette aspiration. 30 μ l of sample were mixed with 270 μ l of Binding Buffer and added to the tube to be slowly mixed by end-over-end rotation for 30 minutes at 4°C. The mixture was centrifuged for two minutes and the flow through was collected in a fresh Eppendorf tube for downstream analysis. The binding step was repeated another time to improve initial resin binding and the flow through was saved in the same tube. The resin was washed once with 400 μ l and then twice with 50 μ l Wash Buffer by centrifugation for two minutes, collecting the supernatant every time in a fresh Eppendorf tube. Finally, the bound protein was eluted by adding 50 μ l Elution buffer to the resin and mixing by end-over-end rotation for ten minutes. The mixture was centrifuged for 2 minutes and the elution was collected. The elution process was repeated and the second elution was saved as well. The column as well as the Ni-NTA beads were discarded without re-equilibration.

Samples were stored in the fridge at 4°C for later analysis by SDS PAGE.

Visualization by SDS PAGE

Lysed samples were analyzed using pre-cast Bis-Tris SDS PAGE gels (Thermo Fisher Scientific, Catalog # NP0322BOX) with MES SDS Running Buffer (20x) (Thermo Fisher Scientific, Catalog # NP0002).

10 μ l of cell lysate were mixed with 4 μ l LDS Sample Buffer (4x) (Thermo Fisher Scientific, Catalog # NP0008), or pellet fractions were resuspended in 1x PBS (DPBS, no calcium, no magnesium, Thermo Fisher Scientific, Catalog # 14190144), incubated at 70°C for 10 minutes, and then chilled at 4°C. In later experiments dithiothreitol (DTT) was added at a concentration of 50mM as a reducing agent before loading the samples to increase sharpness of the bands. A protein marker was included (SeeBlue plus2 Prestained Protein Marker, Thermo Fisher Scientific, Catalog # LC5925) and it was made sure that the gel is asymmetric to simplify interpretation after staining. Gels that were run under non-reducing conditions were run for 30 minutes at 200V and gels that were run under reducing conditions were run for 45 minutes on ice at 200V.

The completed gels were washed with plenty of sterile H₂O five times for one minute in the microwave (set to maximum power) and then covered with Coomassie Blue stain (Coomassie Brilliant Blue R-250 Staining Solution, Biorad, Catalog# 1610436), unless mentioned otherwise. The gels were put back into the microwave for 15 seconds, swirled, returned into the microwave for another 15 seconds, swirled, and then left overnight in sterile H₂O covered with foil and gently swirling to destain. Gels were imaged using a fluorescence imaging machine (FluorChem M FM0423, white conversion screen with Orange filter and Trans UV light, 490ms exposure) and adjusted for brightness and region of interest in the software ImageJ (Ref. [60]), as well as labeled in the software Inkscape (Ref. [36]).

Gels with sample concentrations below the detection limit of Coomassie Blue (100ng) were visualized by silver stain (Pierce Silver Stain Kit, Thermo Fisher Scientific, Catalog # 24612). The gel was incubated twice for 15 minutes in a solution of sterile H₂O, 100% ethanol (200 proof, Fisher Scientific, Catalog # 22032601) and acetic acid (Glacial acetic acid, Sigma Aldrich, Catalog # 64-19-7) were mixed at a ratio of 6:3:1. Gels were washed in 10% ethanol twice for 5 minutes and in sterile H₂O twice for 5 minutes. 50 μ l Sensitizer solution plus 25ml sterile H₂O were mixed and added to the gel for exactly one minute, followed by a quick wash with sterile H₂O for twice one minute. 500 μ l Enhancer solution plus 25ml Silver Stain solution were mixed and added to the gel for 30 minutes. Before development the gel was quickly washed with sterile H₂O. To develop the silver stained gel, 500 μ l Enhancer solution were mixed with 25ml Developer solution and the gel was incubated until bands appeared at the desired intensity. 5% acetic acid was used as a Stop solution. The gel was washed with sterile H₂O before imaging on a white conversion screen and stored in sterile H₂O.

Visualization by Denaturing PAGE

Denaturing PAGE gels were used for analysis of short DNA sequences that could not be observed on agarose gels. Typically 12-comb wells were used with 1.0mm gel chambers. 10% PAGE gels were mixed from 5ml 25% -urea-acrylamide mixture (Urea gel system concentrate, National Diagnostics, Catalog # EC-830), 1ml 10x urea-TBE mixture (UreaGel Buffer, National Diagnostics, Catalog # EC-835), and 4ml of urea in ultra pure water (UreaGel Diluent, National Diagnostics, Catalog # EC-840). 0.07% ammonium persulfate (APS) and 5µl TEMED were added and the mixture was briefly mixed before pipetting it into a commercially available gel box. The gel was left to polymerize for 30 minutes and stored at 4°C in wet paper towels.

Samples were mixed with 2x Xylene Cyande FF denaturing loading dye (10mM NaOH, 1mM EDTA, 90% formamide, 0.2% w/v Xylene Cyande FF dye), boiled at 70°C for ten minutes and left to cool. 10 bp DNA ladder (ThermoFisher Scientific, Catalog # 10821015) was diluted in ultra pure water to a concentration of 0.01 µg ml⁻¹(1:100), mixed with 2x FF loading dye, but not boiled. Gels were generally run at 300V for 30 minutes and stained with Sybr Gold (SYBR Gold Nucleic Acid Gel Stain (10,000X Concentrate in DMSO), ThermoFisher Scientific, Catalog # S11494) or 15-20 minutes for visualization.

CHAPTER 4

Results

The results given in the following chapter were obtained in accordance with the procedures described in the chapter 3. It was the goal to express the ScFv anti-DEC205 either in its VH-VL form or in its VL-VH form with a SNAP and a His-tag, and preferably as a soluble protein, rather than a protein aggregate.

In short, a SNAP tag was cloned into a pUC57-Kanamycin vector and transformed into the competent cell line BL21(DE3). Expression was unsuccessful. The entire VH-VL-SNAP-His-gene was inserted into the pET30a vector, where it replaced a His-Cse3-SNAP gene. Some evidence suggested that a protein at the predicted molecular weight was expressed as an inclusion body in samples taken from high temperature inductions. However, no protein of interest could be isolated by His-tag chromatography. Solubilization of protein aggregates resulted in no change of the apparent molecular weight visualized by SDS PAGE. The gene construct was transformed into a more potent competent cell line, which was still unable to produce the target fusion protein. Various quality controls showed that, in theory and given the correct expression conditions, the genetic code should permit expression of the target protein.

All results will be summarized concisely in section 4.7).

4.1 Molecular Cloning in pUC57

Gibson Cloning was the method of choice in both of the two cloning experiments performed.

4.1.1 Cloning pUC57 in BL21(DE3)

The ScFv is fusion protein of the variable regions of the heavy (VH) and light chains (VL) of the anti-DEC205 protein, connected with a short linker peptide. There are two

possible structures of the same ScFv read from N- to C-terminus: VH - (linker peptide) - VL, referred to as *VHVL* in this project; or VL - (linker peptide) - VH, referred to as *VLVH* in this project.

The plasmid "pUC57-Kanamycin" was verified by restriction digestion, transformed into NEB turbo competent cells for glycerol stocks, and again mini prepped. The plasmids were stored at -20°C for subsequent amplification as a vector backbone containing the *VHVL* and *VLVH* genes. The SNAP tag was cloned into the vector as an insert.

ScFv VHVL DEC205

pUC57-kanamycin *VHVL* (vector backbone) and pSNAP-tag (T7)-2 Vector (NEB) were amplified using Gibson primers FA003-006 (designed by *Frances Anastassacos*) with overhangs and using Q5 HotStart high fidelity polymerase. The PCR products were Dpn1 digested and purified using a PCR clean up kit (Qiagen). The two fragments were assembled in equimolar amounts (75ng each) in Gibson Assembly Mastermix (prepared by *Frances Anastassacos*) according to standard procedure (refer to previous chapter). 5µl of assembled plasmid were transformed into *NEB 5 alpha competent cells* according to standard protocol and plated onto LB-kanamycin plates.

The colonies were mini-prepped and a restriction digest with *NheI* and *SalI* was performed (refer to Figure 4.1). Additionally, colonies were sent for sequencing and the alignment was compared to the desired sequence (Ref. [30], by *F. Anastassacos*). The alignment was deemed satisfactory. Two plasmids were transformed into *BL21(DE3) competent cells*, double checked by restriction digestion with BamHI, and stored as glycerol stocks in 25% glycerol at -80°C.

ScFv VLVH DEC205

For *VLVH*-SNAP in pUC57 four longer primers with 30 bp homology regions on each overhang were designed (FA018-FA021). The fragments were amplified, Dpn1 digested, and purified. Gibson Assembly was performed in Gibson Assembly Mastermix in excess of the insert fragment at a ratios of 1:1, 1:6, 1:10, and 1:20 (vector : insert), where 1:20 proved to be the most successful. The assembled construct was transformed into *NEB 5 alpha competent cells* and plated onto LB-kanamycin plates. Three colonies from each dilution were picked and subjected to colony PCR and sequencing. One colony picked from the 1:20 assembly plate yielded the best results and was transformed into *BL21(DE3)*, double checked by restriction digestion with BamHI, and stored as a glycerol stock in 25% glycerol at -80°C.

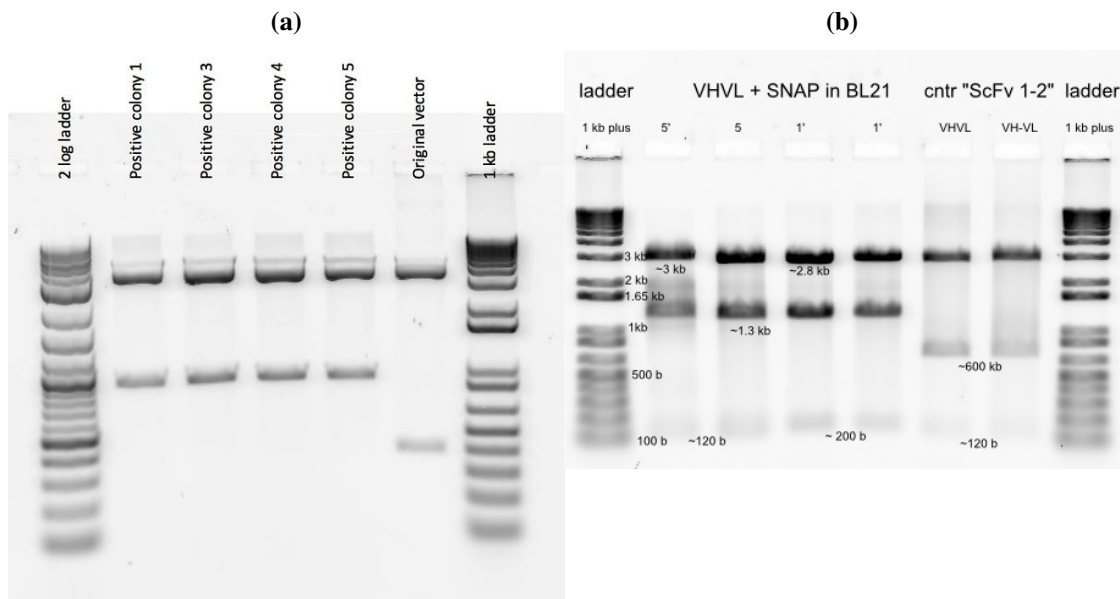


Figure 4.1: (a) Agarose gel demonstrating the successful restriction digest of assembled Gibson Construct pUC57-VHVL with SNAP in NEB 5 alpha competent cells. Correct assembly results in two bands at 896 bp and 3268 bp. By F. Anastassacos.; (b) BL21(DE3) competent cells were transformed with two plasmids and re-tested with BamHI. Expected bands are at 2820, 1235, 112 for the correctly assembled pUC57 vector with the SNAP tag insert. ScFv1-2 is the original vector pUC57-VHVL without the inserted SNAP tag.



Figure 4.2: After Gibson Assembly the desired product features a T7 promoter, a VHVL gene, a SNAP tag, and a His tag. Image by F. Anastassacos

4.2 Protein Expression in pUC57

Both VHVL and VLVH glycerol stocks were tested for protein expression. The desired protein was calculated to have a mass of 49kDa based on the amino acid sequence. Cultures were grown to an OD of 0.4-0.6, at which point a pre-induction sample was taken and the cultures were induced with IPTG to a final concentration of 0.4 mM or 0.86mM. The cultures were left at 18°, 23°, or 37°C overnight shaking at 200 rpm. Cells were lysed in xTractor buffer and by sonication, but without the addition of lysozyme. Protein expression was analyzed by denaturing PAGE. No temperature and or IPTG con-

centration setting could elicit a significantly higher expression of a protein at 49kDa. After cell lysis, one pellet sample with the VHVL-insert in pUC57-kanamycin was subjected to His-tag chromatography, because a band close to 49kDa could be seen and the identity of this band needed to be determined. A protein at 49kDa was washed off in the three washing steps, but none was eluted in the elution steps. Hence, even though a small amount of protein of about 49kDa was present in the pellet fraction of the BL21(DE3) culture induced at 37°C, it was not shown to feature a His-tag and was, therefore, not found to be the desired protein (refer to Figure 4.3 for SDS PAGE gels).

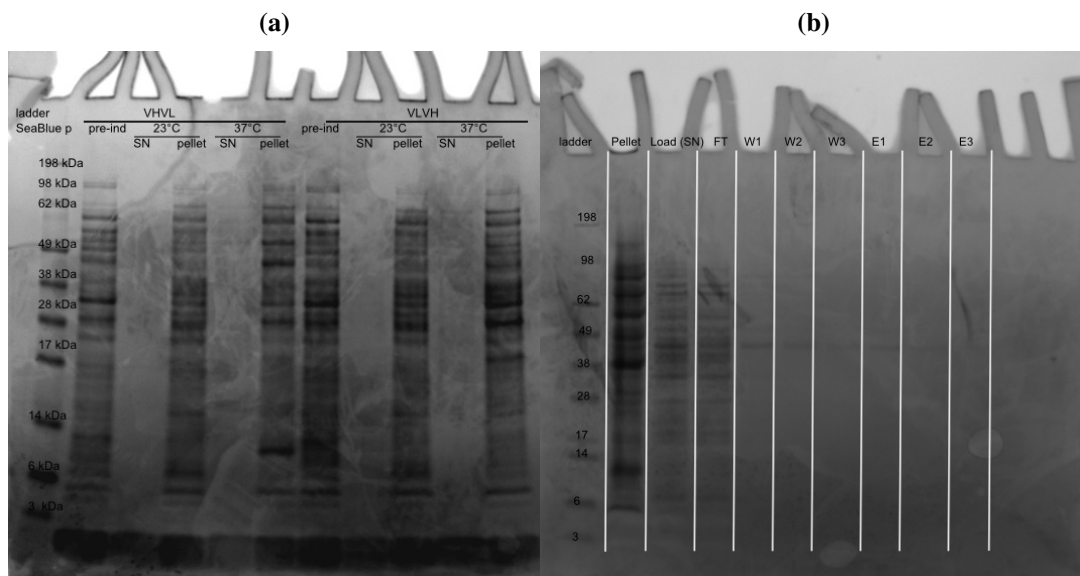


Figure 4.3: (a) SDS PAGE of VHVL and VLVH at 0.4mM IPTG induction overnight at 23°C and 37°C. Samples were lysed with xTractor buffer and sonication. (b) On one sample, VHVL pellet fraction at 37°C, a His chromatography run was performed to determine the identity of the band at about 49kDa. A protein at about 49kDa was washed off in the washing step, but none was eluted.

A final induction run was performed in BL21(DE3) comparing the two glycerol stocks transformed with the assembled VHVL and VLVH construct to untransformed competent BL21(DE3) cells. The cultures were induced at 18°C and at 37°C overnight. Additionally, 2ml culture samples were mini prepped and once again presence of the inserted SNAP-tag was checked by PCR using the Gibson primers that anneal to and amplify the SNAP tag-insert.

The two transformed cultures did show to have the insert. Yet, no expression was detected on an SDS PAGE gel (refer to Figure 4.4 for the final SDS PAGE gel of samples

with the pUC57 vector).

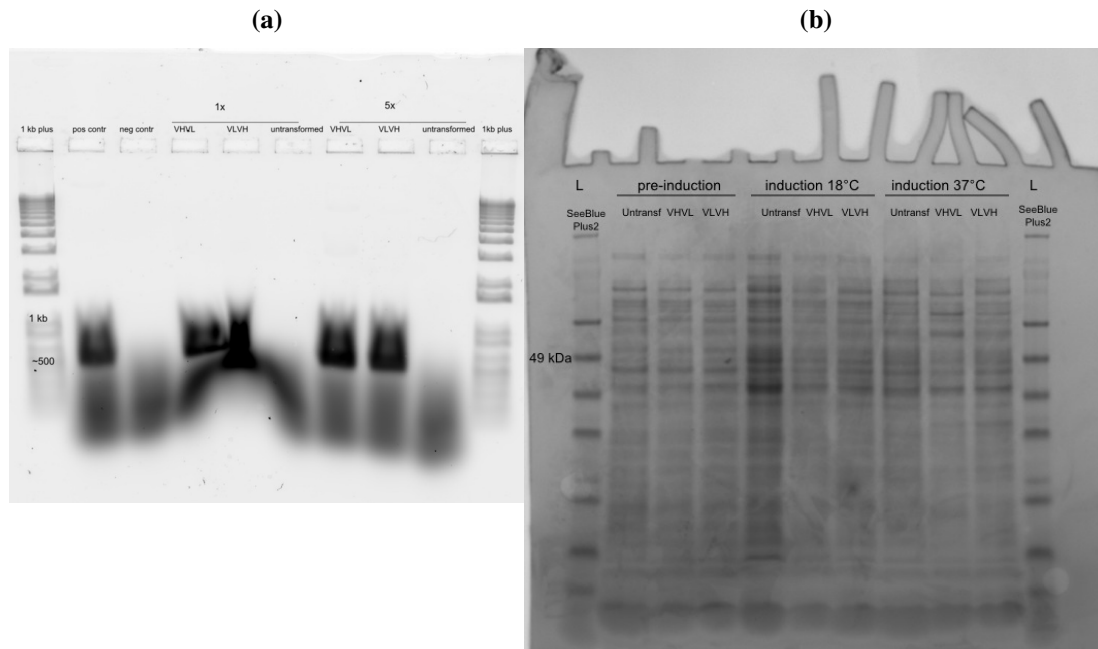


Figure 4.4: (a) PCR on mini prepped cultures of transformed and untransformed competent BL21(DE3) cells before induction. 1x and 5x denotes template concentration in ng per reaction. Primers amplified the SNAP tag region in the pUC57-vector, which comprises about 500bp. The experiment shows the presence of the insert in the pUC57 vector. (b) SDS PAGE of total cell lysates of VHL- and VLH transformed BL21(DE3) cultures at 0.4mM IPTG induction overnight at 18°C and 37°C. Samples were lysed with xTractor buffer and sonication. No significantly increased protein expression could be detected.

Various verifications showed that the insert has been successfully cloned into the pUC57 backbone and that the assembled construct is present in the transformed glycerol stocks of BL21(DE3). Yet, bacteria could not be prompted to express the desired ScFv protein under multiple temperature- and two IPTG concentration settings. The vector pUC57-kanamycin does not seem to encourage expression of this protein. Previous experiments in the lab confirmed the suggestion. As common theme, pET-based plasmids enabled expression of proteins that remained unexpressed in pUC. Hence, we were motivated to clone the insert into a different vector that was present in the lab and known to promote expression of a CRISPR associated endoribonuclease (*cse3*) protein: the pET30a vector.

4.3 Molecular Cloning in pET30a

The T7 promoter-gene, lac operon, and kanamycin resistance gene were included in the pET-vector-backbone. The insert present in pET30a at that point contained a His-tag at the N-terminus and a SNAP tag at the C-terminus, next to the protein *cse3*.

The entire insert, containing *His-Cse3-SNAP* genes, was replaced by the desired gene sequence *VHVL-SNAP-His* by Gibson Cloning. The replacement happened right after the T7 promoter region, instead of further downstream after the first start codon (compare Figure 4.5). This precaution decreases the likelihood of mutation in the ribosome binding site (RBS) and in the start codon. Primer annealing sites are known to be more prone to mutation, in which case the start codon would be lost. Likewise, after the His-tag there is a short sequence of less critical nucleotides: the stop codon triplet and BamHI restriction site. Spacers sequences are placed between VH- and VL-gene (1x, 4x, 1x GGTGGTGGCGGTAGT) and between Snap- and His-tag (refer to graphic in Figure 4.5).

The new insert was derived from the pUC57-kanamycin VHVL colony 1- plasmid, which was previously verified to contain the SNAP-tag insert in the pUC57-VHVL vector (refer to Figure 4.1 for verification).

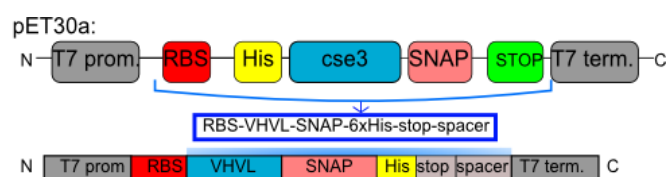


Figure 4.5: The original insert in the pET30aCse3 vector has been completely replaced (top row). After Gibson Assembly the desired product features a T7 promoter, a VHVL gene, a SNAP tag, and a His tag (bottom row). RBS= ribosome binding site. Top: original pET30aCse3 vector, middle: desired insert, bottom: desired product.

Primers were designed as previously: a set of two primers amplified the pET30a vector backbone with overhangs complementary to the insert sequence, and another set of two primers amplified the insert sequence present in the pUC57 vector with overhangs complementary to the pET30a insertion site. Both fragments were amplified using PCRs with a high fidelity polymerase enzyme. The PCR products were Dpn1 digested. Dpn1 destroys the plasmid template selectively: the plasmid is methylated while the PCR-product is not, so only the plasmid is cleaved and destroyed. The products were purified and verified on an agarose gel.

The insert fragment needed to be purified by gel extraction due to unwanted amplification products. The yield was too low for Gibson Assembly, so a completely new set of Gibson-primers with more closely matching G-C contents and melting temperatures

was designed, as well as another set of shorter primers that anneal to the overhangs on the insert region and thereby amplify the gel-purified PCR product. The PCR thermo cycle was optimized for the annealing temperature of the new primers (for agarose gels of amplified fragments and purified products, refer to Figure 4.6).

The two fragments were assembled at a 1:2 and 1:1 molar ratio (vector : insert) in Gibson Assembly master mix. The assembled constructs were transformed into BL21(DE3) right away, skipping the cell line NEB 5 alpha, which lead to a much lower yield of colonies on the LB-kanamycin transformation plates.

Two colony PCRs were performed on the all four colonies found on the 1:2 and 1:1 transformation plates: once with the Gibson vector-primers and once with the Gibson-insert primers (refer to Figure 4.7 for the two colony PCR results). The four colonies were sent for sequencing by GENEWIZ (Ref. [30], by *F. Anastassacos*) for a final verification.

All four colonies qualified, where colony 1 and colony 2 had the best alignments to the target sequence. All four colonies were kept as glycerol stocks at -80°C.

4.4 Protein Expression in pET30a

A test expression was performed by a co-worker (*L. Chou*). The four colonies were induced with 0.4mM IPTG at an OD between 0.4 and 0.6 and incubated overnight at 18°C. An SDS PAGE gel on the next day suggests that a protein at about 49kDa is over-expressed in the pellet fractions of all four culture samples, and especially in the pellet fractions of colonies STW-VH-1 and STW-VH-2. This result made sense, since the two colonies also achieved the best sequencing results.

Further experiments were performed to replicate the result and create circumstances that favor the expression in the soluble fraction. Proteins that are expressed in soluble form do not need to undergo solubilization and re-folding under native conditions.

A scanning experiment was performed, where STW-VH-1 was inoculated from the glycerol stock in two separate runs. Cultures were grown at 37°C until an OD of 0.4-0.6 was reached, and then induced with 0.25mM, 0.5mM, and 1mM IPTG at 37°C, 18°C, and 15°C each overnight. The exact OD was noted down at the time of induction so that post-induction sample volumes could be OD-normalized. Samples were lysed using xTractor buffer and sonication and were run on a denaturing PAGE gel (refer to Figure 4.8).

In samples incubated at 37°C an additional band could be found in the pellet fraction. The band was not exactly at 49 kDa, but slightly less than that (approximately 42kDa). It was noticed that this band is also present in the pre-induction sample, but in the soluble fraction. Since T7 is known to be a "leaky" promoter, which allows expression without induction to a small degree, this fact did not disqualify the band as a candidate

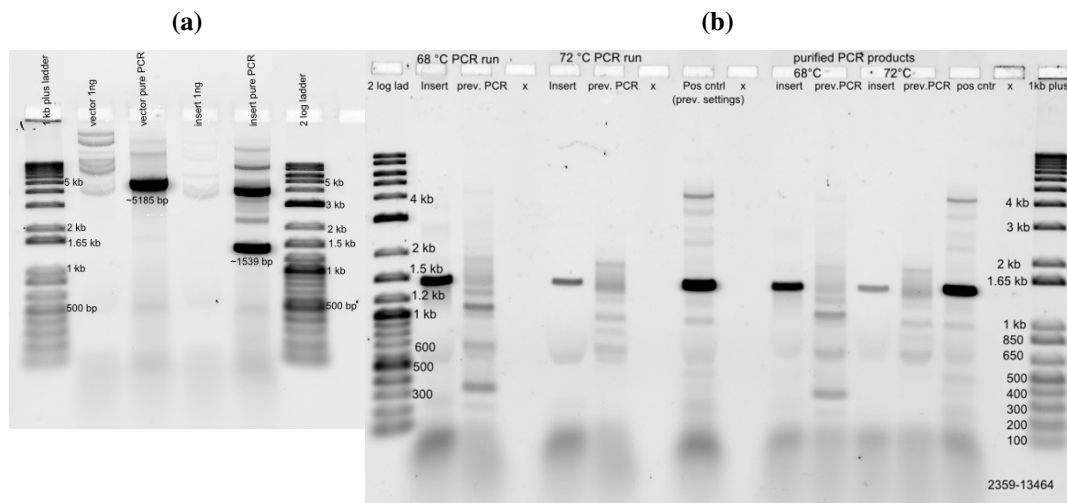


Figure 4.6: (a) The pET30a vector could be amplified from a plasmid of pET30a with a cse3-SNAP insert present in the laboratory using Q5 HotStart high fidelity polymerase with GC Enhancer. (b) The insert (= VHVL-SNAP-His) was derived from the pUC57Kan-VHVL-SNAP plasmid previously assembled by Gibson Cloning. The PCR amplification of the insert yielded unwanted additional bands next to the expected band at about 1.5kb (see central lane "pos cntr"). Primers with more closely matching melting temperatures were designed (lanes "Insert") and the annealing temperature in the cycle was modified (lanes "68°C PCR run" and "72°C PCR run"). Runs with the newly designed Gibson-primers are referred to as "insert". PCR-runs with primers that anneal to the overhangs of the insert-PCR product that was gel-purified are referred to as "prev. PCR". Eventually, the product of lane "pure PCR 68°C" was picked for Gibson Assembly.

for the desired ScFv.

Neither in samples incubated at 15°C nor in samples incubated at 18°C any additional bands around 49kDa could be detected, regardless of the IPTG concentration for induction.

In a further attempt to produce the protein in the soluble fraction rather than in the pellet fraction a time course experiment was performed. Information could be extracted from the time course experiment in two different ways: (1) the protein might be expressed at one point in time, but might be degraded due to instability, and (2) the protein is found in the samples incubated at 37°C might be soluble at one point but insoluble after overnight incubation.

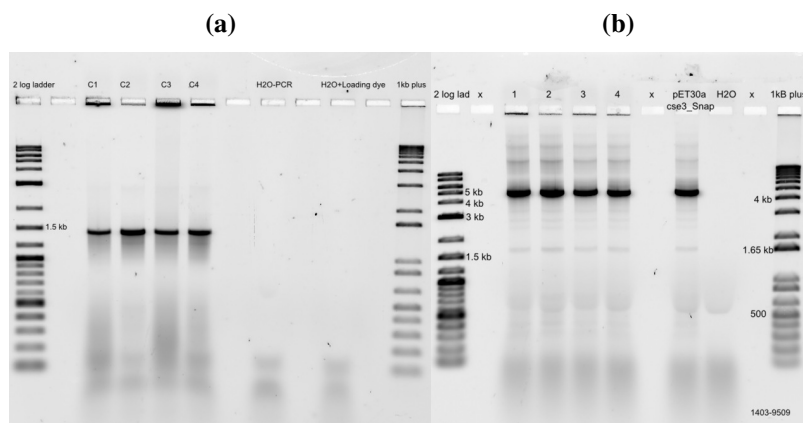


Figure 4.7: (a) The colony PCR with the Gibson primers amplifying the insert region proves the presence of the VHVL-SNAP-His insert in all four picked colonies. (b) The same PCR was performed using the vector-amplifying Gibson primers as a double-control. The vector sequence has not been compromised.

4.4.1 Time Course Experiments

Cells were incubated from the STW-VH-1 glycerol stock, left to grow, and then re-inoculated in 60ml LB with kanamycin the following morning. Cells were left to grow until on OD of 0.4-0.6 was reached. The cells were induced at the lowest tested IPTG concentration (0.25mM) and incubated at reduced temperature (18°C). Then, samples were taken pre-induction, hourly for six hours, and the next morning after overnight induction. All samples were lysed with xTraction buffer and by sonication. The supernatant and pellet fractions were run on a denaturing PAGE gel including a protein marker. All post-induction sample lanes look identical to the pre-induction lane (data not shown).

Another time course experiment was performed at 18°C and 37°C with four times the IPTG concentration for induction (1mM). Samples were taken bi-hourly for six hours and after overnight induction. Samples were normalized by basing the buffer volume on the measured OD and were additionally lysed by sonication.

The total cell lysates (TCLs) of the four hour, six hour, and overnight sampling points were analyzed on a denaturing PAGE gel. Samples of the TCL allowed no confident statement about enhanced expression (data not shown). The samples were separated into pellet (P) and supernatant (S) fractions and analysed by denaturing PAGE separately. Again, in the samples incubated at 18°C no significant difference in expression could be found, regardless of the time span of incubation. However, as previously found, samples incubated at 37°C for four hours, six hours, as well as overnight convincingly show an additional band in the pellet fraction, albeit slightly below the 49kDa mark (approximately 42kDa, refer to Figure 4.9).

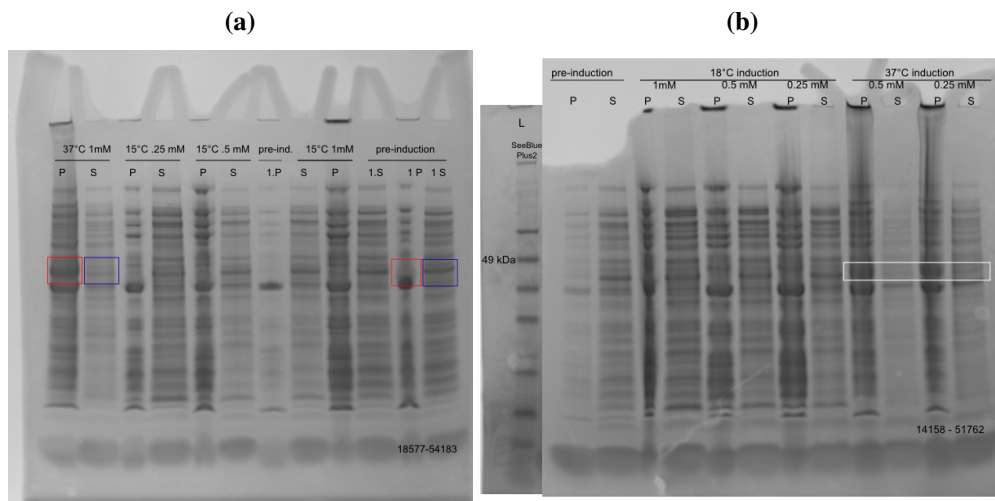


Figure 4.8: (a) *BL21(DE3)* protein expression at 15°C and 37°C with 0.25, 0.5, and 1.0mM IPTG induction. (b) *BL21(DE3)* protein expression at 18°C and 37°C with 0.25, 0.5, and 1.0mM IPTG induction. A ladder from a previous gel run under the same conditions was pasted next to gel to approximate molecular weights. There is no significant additional protein expression at 15°C or 18 °C at any IPTG concentration. However, at all three IPTG concentrations an additional band of around 49kDa size can be seen in the insoluble (P) fraction at 37°C induction.

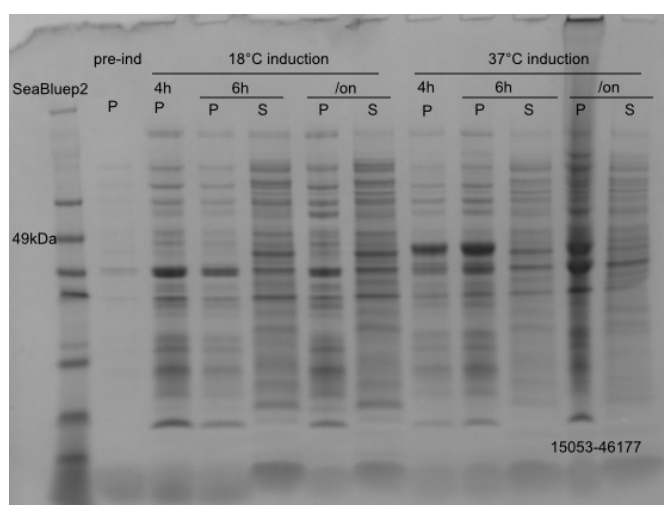


Figure 4.9: A time course experiment was performed at 18°C and 37°C sampling bi-hourly for six hours and overnight. The TCL was inconclusive, so the cell lysates were separated and analyzed on different gels. Supernatant fractions of the last three samples in either temperature setting do not show any additional band when compared to the pre-induction sample. Pellet fractions of the samples incubated at 37°C, however, show an additional band slightly below 49 kDa.

4.4.2 Selected Sample Analysis: Lysis

In two different time course experiments as well as in previous overnight inductions at 37°C an additional band slightly below 49kDa could be found in the insoluble fraction. Attempts to produce the same band in the soluble fraction failed.

Before assuming that the protein of interest is present in the samples as an *inclusion body*, an aggregate of the over-expressed or toxic protein, complete lysis must be guaranteed. Incomplete cell lysis could be falsely interpreted as protein aggregation and could prevent successful harvesting of the target protein.

To improve the lysis protocol, two commercially available buffers were compared (CellLytic B buffer by *Sigma Aldrich* and xTractor buffer by *Clontech*) with and without addition of lysozyme from chicken egg white. Sonication was intentionally omitted, because the heat created in the process might cause protein aggregation, even in a cold water bath in the cold room with adequate "off"-cycle times. Both buffers performed similarly well and the addition of lysozyme made a marginal difference compared to no addition (data not shown).

The subsequent inclusion body solubilization was planned to be performed using an inclusion body solubilization buffer produced in the same product line as the lysis buffer CellLytic B by *Sigma Aldrich*. Anticipating a better compatibility of the two buffers by *Sigma Aldrich*, CellLytic B buffer was selected as a lysis buffer for future experi-

ments. Henceforth, the addition of lysozyme together with DNase1 or Benzonase and PMSF as an EDTA-free protease inhibitor replaced sonication. This precaution reduced probability of protein aggregation during cell lysis. Also, it was found that the addition of DTT to the boiled samples prior analysis in a denaturing PAGE gel increased band sharpness. Addition of DTT will be denoted as "SDS PAGE under reducing conditions".

After lysis-optimization the band still resided in the pellet fraction, so it was concluded that the protein may likely be produced as an inclusion body. It is possible that the inclusion body formation slightly shifts the apparent molecular weight of a protein in an SDS PAGE gel, which could explain the extra band at 42kDa instead of 49kDa.

A culture sample obtained four hours post-induction at 37°C in a time course experiment was freshly lysed and the pellet fraction was solubilized using inclusion body solubilization buffer. The four hour induction at 37°C -sample was chosen from the three samples (four-hour, six-hour, overnight, refer to Figure 4.9).

The denaturants contained in the buffer needed to be removed before analysis by SDS PAGE could be performed. This was achieved by TCA precipitation of the solubilized protein. The two processing steps, solubilization and precipitation, greatly decreased the amount of protein. Only a faint, barely visible band could be detected on a gel stained with Coomassie Brilliant Blue. The re-folded protein had the same molecular weight as previously detected bands, which is about 42kDa (data not shown).

4.4.3 Trouble Shooting: Glycerol Stocks

An additional band could only be seen at 37°C induction and in the very first test expression run. The band was consistently slightly less than 49kDa. After inclusion body solubilization and precipitation of the re-folded protein the band still appeared at the same level, which lead the operator to doubt the genetic code of the cultures and consider the possibility of damage done to the glycerol between the test expression run and the consecutive expression runs. A number of tests were performed:

- A final expression run was performed with all four cultures that were transformed with the Gibson-Assembly construct (named STW-VH-1, STW-VH-2, STW-VH-3, and STW-VH-4). The four cultures were induced at a concentration of 0.4 mM IPTG at 18°C overnight, exactly replicating the very first test run. The samples were lysed in xTractor buffer and sonicated, as was done in the first test run. No additional bands could be observed post-induction. On the contrary, one band at about 58kDa was missing in VH-culture 2 in the pellet fraction.
- The glycerol stock cultures were incubated and grown to an OD of about 0.5. 1:100 or 1:1000 dilutions were plated onto LB-kanamycin plates, and left to grow

overnight. Two single colonies were picked from the crowded plates and inoculated to make fresh glycerol stocks. Plasmid mini-preps were prepared from these daughter colonies.

- One minipreped daughter colony-plasmid each from STW-VH-1, STW-VH-2, and STW-VH-3 underwent a restriction digest with BamHI (refer to Figure 4.10a) as well as a PCR using the insert and vector primers designed for Gibson Cloning (refer to Figure 4.10b). STW-VH-4 was omitted in the restriction digest due to low plasmid concentration, but was included in the two PCRs. In the restriction digest all expected fragments showed up at the predicted base pair lengths. In the PCR the vector was amplified correctly, but the insert was only amplified in the plasmid derived from VH- colony 1. This is the culture that had been consistently used for expression experiments because it was previously determined that it had the best sequencing results.

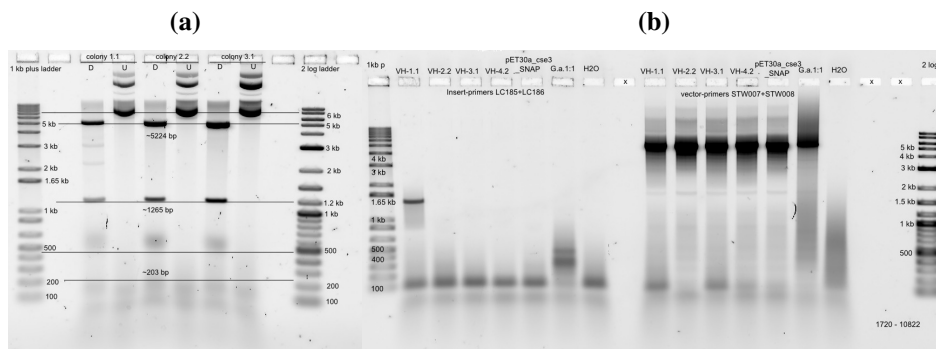


Figure 4.10: (a) The plasmids with the highest concentration underwent a restriction digest with BamHI, which has two restriction sites, cutting the circular plasmid into two fragments. The fragments were expected at 5224bp and 1265bp. Bands can be observed at about 5.2kb and 1.27kb, as well as faintly at about 600bp and 200bp.; (b) PCR with primers that were used for amplification of insert (LC185 and LC186) and vector (STW007 and STW008) with overhangs for Gibson Cloning. Vector sequences are amplified in all samples as well as the Gibson Assembly construct (labeled 'G.a.1:1' denoting a 1 to 1 vector to insert ratio). pET30aCse3 SNAP served as a template for vector amplification in Gibson Cloning. The insert region was amplified in the STW-VH-1.1 daughter colony, which stems from re-plating of culture VH-1. It was this culture that had been used for expression experiments. G.a. was intended as a positive control, but the sample was still in solution of Gibson Assembly master mix, which contains a T5 exonuclease that cannot be heat-inactivated. Hence, the exonuclease is expected to digest any open-ended DNA product.

4.4.4 Protein Expression and Solubilization

Based on the restriction digest and the PCRs it could be concluded that at least the daughter colony VH-1.1 and possibly also the other two daughter colonies (VH-2.2 and VH-3.1) tested in the restriction digest have the correct insert.

Using the fresh glycerol stock made from the daughter colonies another expression run was performed (0.4mM IPTG, 18°C and 37°C for 24 hours instead of the usual approximately 18 hours). Post-induction samples and one pre-induction samples were lysed with CellLytic B buffer and lysozyme addition. Pellet fractions (refer to Figure 4.11 for SDS PAGE) and supernatant fractions (not shown) were analyzed by SDS PAGE. No extra bands were found in the supernatant fraction, but in the pellet fraction a convincing band at around 49kDa appeared. It was suspected that the protein was over-expressed and possibly aggregated.

Complete protein solubilization needed to be verified before proceeding with analysis and identification of the particular band by His-tag affinity chromatography.

His tag Chromatography of Solubilized Protein

A fresh sample of VH-1.1 and VH-2.2 was lysed and separated into pellet and supernatant fraction. The pellet was solubilized in commercially available inclusion body solubilization buffer. Samples of the TCL, the supernatant- and pellet fractions after lysis, and the supernatant- and pellet fractions after inclusion body solubilization (solubilized protein and cell debris) were analyzed by SDS PAGE.

As previously seen, the prominent band at about 49kDa appeared in the TCL and the pellet lane. However, the band disappeared after inclusion body solubilization. It is likely that most of the sample was lost due to precipitation: The inclusion body solubilization buffer contained urea, and the SDS sample loading buffer contained SDS. After mixing of the two components a large amount of proteins precipitated.

The lysis and solubilization was repeated with samples from VH-3.1 and VH-4.2, vastly diluting the solubilized protein before mixing it with SDS loading buffer and thereby diluting the urea content. As a result, the solubilized protein concentration was below the detection limit of Coomassie Blue dye, while the lysis-samples were clearly visible. All sample concentrations in the gel needed to be normalized in order to proceed with a Silver Stain protocol.

Another gel analysis was performed, where all samples were equally diluted. Based on the silver-stained SDS PAGE gel it was shown that inclusion body solubilization indeed solubilizes a majority of the pelleted proteins. Close to all protein bands could be transferred to the soluble fraction leaving only a faint band at about 49kDa behind (refer to Figure 4.11b) for Silver-stained SDS PAGE). The solubilization was deemed effective enough for analytical purposes.

A His-tag affinity chromatography run under denaturing conditions was performed on

30µl of one of the samples that were demonstrated to be solubilized close to completeness. Sample 3.1 was picked for His-tag chromatography. Proteins were eluted by change in pH, where the washing buffer had a pH of 6.0 and the elution buffer had a pH of 4.0. Fractions were collected after equilibration, washing steps, and after elution steps and analyzed on an SDS PAGE. Protein bands were visualized by Silver Stain due to the low sample concentrations (refer to Figure 4.12).

Only one additional band could be observed in the second elution, rather than the first elution, presumably due to delayed buffer exchange. This protein band was not relatively more intense than other fractions of the sample. It has an estimated size of 58kDa, which disqualifies it as a candidate for the desired protein. The band at about 42kDa, which was observed many times in previous experiments, was washed off after the second washing step.

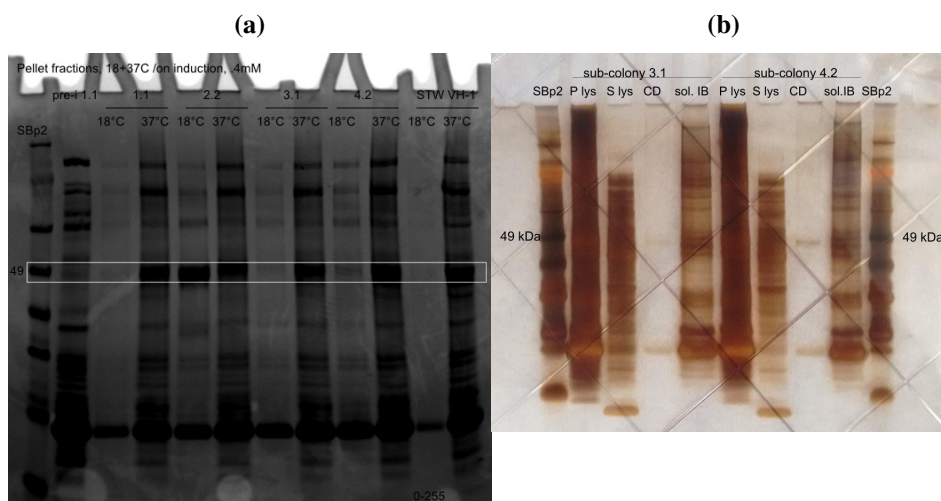


Figure 4.11: (a) Fresh glycerol stocks from daughter colonies of STW-VH-1, STW-VH-2, STW-VH-3 and STW-VH-4 were induced with 0.4mM IPTG and incubated for 24h at 18°C or 37°C. Lysed cells were pelleted and analyzed by SDS PAGE. At 37°C all four cultures show a band at around 49kDa and even at 18°C culture VH-2.2 seems to show a band slightly below 49kDa. STW-VH-1 is the original colony picked after Gibson Assembly in pET30a and the parent culture of VH-1.1. (b) Samples of VH-3.1 and VH-4.2 pellet fractions were solubilized in inclusion body solubilization buffer and analyzed on an SDS PAGE gel by the Silver Staining method. The fraction of proteins carried over to the soluble fraction at around 49kDa was deemed large enough for analytical purposes.

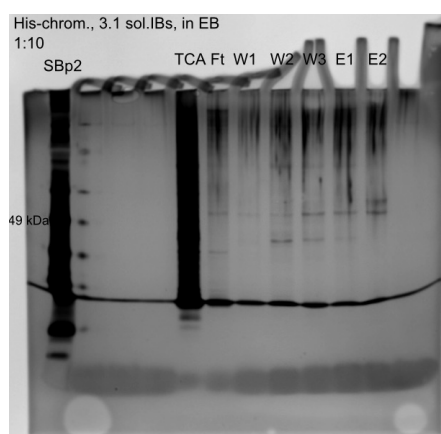


Figure 4.12: Samples from cultures 3.1 and 4.2 post-induction were lysed and solubilization of proteins in inclusion body solubilization buffer was verified. The denatured sample 3.1 was subjected to His-tag chromatography under denaturing conditions. Protein were eluted by change in pH, where the washing buffer had a pH of 6.0 and the elution buffer a pH of 4.0. An additional band after the second elution step (E2) can be seen, but it has an estimated molecular weight of about 58kDa instead of 49kDa, which disqualifies it as a candidate for the target protein.

4.5 SHuffleT7 Express Protein Expression

Previous protein expression was performed in the *E.coli* cell line BL21(DE3). At high induction temperatures an additional band at 49kDa, or slightly lower, was observed. Lysis experiments revealed that the protein may likely be expressed as an inclusion body. Inclusion body solubilization followed by His-tag affinity chromatography was performed on 30 μ l of sample VH-3.1 to check for its identity. A fraction of the sample of 42kDa was washed off in the washing steps. Another fraction was eluted in the elution steps in equal amounts as the other fractions, but it had a weight of about 58kDa. The band at about 49kDa could be found in the flow through, all washing steps, and the elution step. Hence, it can be concluded that this band shows no specific affinity to the Ni-NTA column. Only one of the fractions showed specific affinity to the column, but it was about 10kDa off the expected value (58kDa instead of 49kDa). The protein of interest was not identified in the sample.

The SHuffle T7 cell line is known to have a higher success rate with protein high in di-sulfide bonds and other difficult to express proteins, such as ScFvs. This cell line may be capable of expressing the desired protein and potentially even expressing it in the soluble fraction.

The daughter culture plasmids VH-2.2 and VH-3.1, as well as later on VH-1.1, were

chosen for transformation based on the restriction digest evaluation with BamHI (all three qualified) and the PCR with the Gibson-vector and insert primers (only 1.1 qualifies, but the available positive control is unreliable). The thick band at about 49kDa could be observed in all four VH daughter culture samples in the previous expression run in BL21(DE3), most promisingly in VH-2.2 and VH-3.1, even though analysis does not confidently confirm the band or any fraction of it as candidate for the desired protein.

4.5.1 VH-2.2 and VH-3.1

About 50ng of the plasmids VH-2.2 (second daughter colony picked from STW-VH-2 culture) and VH-3.1 (first daughter colony picked from re-plated STW-VH-3 culture) were transformed into the cell line. As a negative control, water was added to the cells. First, the transformation was performed for plasmids VH-2.2 and VH-3.1. From the 1:100 dilution-transformation plates two colonies each were picked under sterile conditions, grown as liquid cultures, mini-prepped and stored as glycerol stocks. The new stocks were named VH-2.2SH1, VH-2.2SH2 (both from VH-2.2 transformation), VH-3.1SH1, and VH-3.1SH2 (both from VH-3.1 transformation).

A PCR was performed on the four mini-prepped plasmids using the two sets of Gibson primers annealing to the insert and the vector (with annealing temperature of 55°C) and OneTaq polymerase (refer to Figure 4.13a for the PCR reactions on VH-2.2SH and VH-3.1SH daughter colony plasmids). When the insert-PCR was repeated with fresh primers both the positive control (=VH-1.1 plasmid) and the Gibson Assembly construct were amplified, but neither of the four tested SHuffleT7 Express plasmid samples 2.2SH1 and SH2 or 3.1SH1 and SH2 were amplified (data not shown).

However, when the four plasmids were digested with BamHI the expected fragments appeared for all plasmids as well as for the positive control (=parent STW-VH-1 plasmid, refer to Figure 4.13b for the restriction digest). Additionally, a fuzzy band appeared at about 600bp, whose origin is unknown, as can be seen.

One daughter culture each from VH-2.2 and VH-3.1 in SHuffleT7 Express were subjected to an experimental expression run. The cells were grown at 30°C to an OD of about 0.5, induced with 0.4mM IPTG for four hours at 30°C or overnight at 16°C. The collected samples were lysed using CelLytic buffer B and lysozyme, separated into soluble and insoluble fractions by centrifugation, and analyzed on a reducing SDS PAGE gel (data not shown).

There was no enrichment of bands around 49kDa, even though a relatively more intense band at about 42kDa appeared in all pellet fractions of the 30°C inductions; the expression was not further pursued. Instead, the plasmid VH-1.1 was transformed into the SHuffleT7 Express cell line in the same fashion.

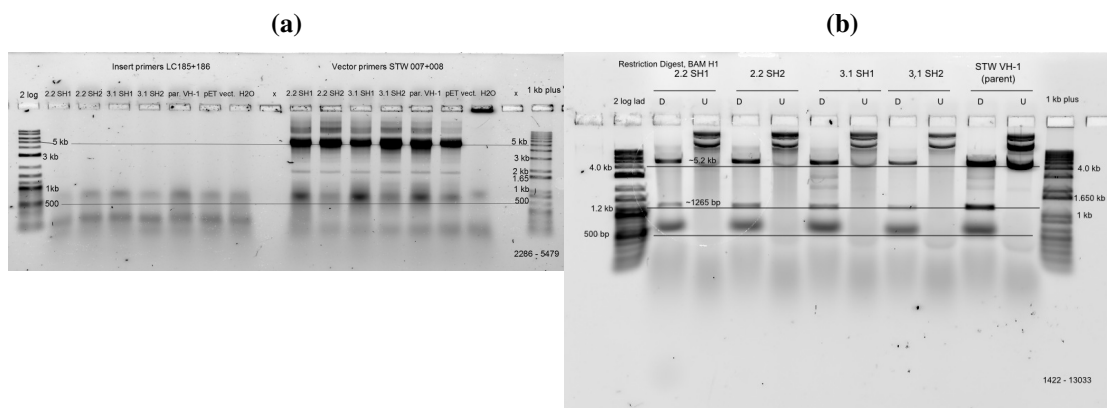


Figure 4.13: (a) A confirmatory PCR was performed on the mini-prepped plasmids of the transformed SHuffleT7 Express cells using the Gibson primers that anneal to the vector and the insert. The insert fragment was not amplified in either the samples or the positive control (=parent STW-VH-1). When the PCR was repeated with fresh primers only the positive controls showed a band at the expected base pair length. The vector fragment was amplified. Note that the vector reactions also have a band at about 1.8 kb. The overhangs of the primer binding to the insert would give about a fragment of about 1.5kb ; (b) The restriction digest with BamHI shows the expected result, two bands at about 5.2kb and 1.3 kb. Additionally, a fuzzy band at about 600 bp of unknown origin can be seen.

4.5.2 VH-1.1

About 50ng of the plasmid VH-1.1 (first daughter colony picked from re-plated STW-VH-1 culture) were transformed into the competent cell line SHuffleT7 Express. The transformed cells were diluted, plated and from the 1:10 dilution-plate five single colonies were picked. The cells were subjected to an identical quality control and test expression process, which will be described below.

A colony PCR was performed using the OneTaq polymerase and the two sets of Gibson primers that anneal to the vector and the insert. All vector-lanes were completely smeared and the insert lanes were empty, indicating either a too short initial lysis step before DNA denaturation in the PCR thermocycle, or too much colony sample (data not shown).

The cells were grown as liquid cultures, miniprepped and the PCR was repeated on the plasmids. Again, all lanes appeared evenly smeared. The conclusion drawn from this result was that one or more of three disturbances must be the reason:

1. A component of the PCR reaction must be contaminated.
2. The reaction tubes may not be tight: about 20-25% volume evaporation was measured after the reaction was completed.

3. The thermocycle program is not ideal.

Either of the three possibilities listed above or a combination of them can apply. *Number 3* is the least likely because previous PCR reactions were successful with the same program using OneTaq polymerase, the same primers, and a plasmid template. The PCR will be further investigated and troubleshooted in a later section (refer to section 4.6).

A restriction digest with BamHI was performed on all five plasmids, yielding the usual two expected bands at about 5.2kb and 1.63kb as well as a faint band at 600bp. The restriction digest, therefore, tested positively (refer to Figure 4.14 for image).

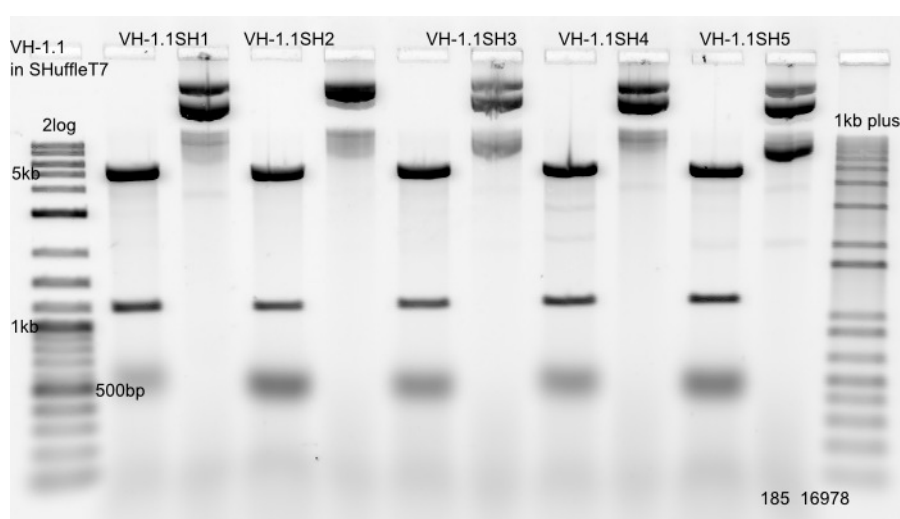


Figure 4.14: *VH1.1* was transformed into *SHuffleT7* competent cells. The plasmid restriction digestion with *BamHI* yielded the expected two bands (5.2kb, 1.3 kb) for all colonies picked after *VH-1.1* transformation into *SHuffleT7 Express*, alongside with an additional fuzzy band at about 600bp.

A test expression run at 30°C for four hours and at 16°C overnight at 0.4mM IPTG induction was run regardless of the PCR result. No significantly increased protein expression could be detected in any of the five cultures grown from *SHuffleT7* colonies transformed with *VH-1.1* on an SDS PAGE gel compared to a pre-induction sample.

4.6 Troubleshooting: Genomic Code

The PCR previously performed solidly with OneTaq polymerase and Taq DNA polymerase using an annealing temperature of 55°C and the four Gibson primers (LC185 + LC186, STW07 + STW008). However, the same enzyme and thermocycle did not

yield conclusive results on either the plasmids isolated from the SHuffleT7 Express cells transformed with VH-1.1, or the two positive controls (plasmid 1.1 isolated from BL21(DE3) after re-plating, pET30aCse3SNAP plasmid used for Gibson Cloning). Various troubleshoot runs were performed on only the control plasmids and sterile water to stabilize the experiment before continuing. For every PCR experiment from this point on, ultra pure water was acquired freshly from the Millipore purification system.

First, the thermocycler instrument was changed to rule out evaporation and fresh working stocks of the primers were prepared. The lanes were still smeared, but a desired band could be detected in the positive control of the insert-amplifying PCR.

Then, the buffer was tested by running OneTaq polymerase with OneTaq buffer and with Standard Taq buffer. Cycle numbers were decreased from 30 to 20 cycles for these experiments to speed up the process, but were later increased again. The result was that sample lanes with OneTaq buffer were smeared, and sample lanes with Standard Taq buffer were empty. None of the lanes showed any desired band. The OneTaq buffer was identified as a source of contamination and was replaced. Cycle numbers were re-adjusted to 30 cycles.

Against expectations, when fresh OneTaq buffer was used all lanes were still evenly smeared. However, the desired band re-appeared in the positive control of the insert-amplifying PCR.

Next, the thermocycle program was optimized. So far, for Gibson primer quality control PCRs with OneTaq polymerase a 94°C - 55°C - 68°C thermocycle ramp was used. The temperature was increased for each segment (95°C - 63°C - 68°C for denaturation - annealing - extension). The result was that all lanes were empty, except for fuzzy bands at about 100bp. These bands were interpreted as unused primers. The conclusion that was reached was that the primers could not successfully anneal and stabilize the polymerase reaction.

Next, OneTaq polymerase was replaced by Taq DNA polymerase. Finally, some bands were detected for the positive control of the insert-amplifying PCR, but not for the vector. Still, the outcome was considered as a preliminary success for PCR troubleshooting at the time.

The extension time was further increased for the vector-amplifying PCR (1min/kb to 1.15 min/kb), but the vector lanes were still smeared and lacked the desired bands.

After this final PCR troubleshooting experiment the adjustments and their outcomes were considered acceptable, even though until the end the vector could not be amplified. The grounds for premature termination of PCR-troubleshooting were based on expert opinion that found that neither OneTaq polymerase nor Taq DNA polymerase can reliably transcribe large fragment lengths (>2kb). While the insert comprised only 1.54kb, the vector comprised as much as about 5.25kb. This reasoning, however, does not explain why the enzyme was capable of amplifying the vector in the previous ex-

periments (refer to, e.g., Figure 4.10b).

With this information in mind, another test expression was set up. The cells were induced with double the IPTG concentration, 0.8mM, and incubated at 30°C for four hours as well as at 16°C overnight. However, no visibly increased protein expression could be detected compared to pre-induction after lysis and analysis on an SDS PAGE gel.

4.6.1 Alternative Approach to Genome Verification

As an alternative approach, new primers that anneal to a section 250bp upstream of the insert and 250bp downstream of the insert and allow amplification of a insert-vector hybrid fragment of about 2.0kb were designed.

The templates and primer working dilutions were kept in 1xTE buffer at 4°C instead of in ultrapure water at -20°C to avoid degradation of the working stocks. A PCR thermocycle that fits the annealing temperature of the primer pair and the extension time of a 2.1kb section being amplified by Taq DNA polymerase was designed.

Both the vector template pET30aCse3SNAP and the insert template STW-VH-1 yielded a band at approximately the same fragment length, because the primers anneal to the pET30a vector section that the two templates share in common, rather than annealing to the VH-VL insert itself like the previous Gibson primer pair did. Both the VH-VL and the Cse3SNAP region have approximately the same length with only 133 base pairs difference. Hence, the resulting fragments are virtually the same length.

It should be mentioned that the PCR reaction was found to be rather inefficient. The reaction produced unusually faint bands. A reason for this inefficiency could be the presence of EDTA in the TE buffer. EDTA is known to inhibit Taq polymerase by chelating essential divalent ions, such as magnesium. It may also be due to slightly lower, but roughly equal, molar concentrations of the primers. The expected molar concentrations in the working stocks were 10 μ M each, whereas the calculated concentrations were found to be about 8.7 μ M. Calculations were based on the *Beer-Lambert law*, which states that absorbance at 260nm wavelength is equal to the product of the extinction coefficient, the (molar) concentration of the sample, and the path length of the UV cell.

After the primer volumes were adjusted to the calculated molar concentration in the working stocks and the PCR was performed with dilutions in ultra pure water, rather than in TE-buffer, the reaction continued to yield the same inefficient, yet sufficient, results. Faint primer bands continued to be detectable in agarose gels, indicating that primers were incompletely transformed into product. Thermocycle adaptations may increase efficiency.

The resolution of the agarose gel electrophoresis analysis of PCR products was maximized: samples were run on a 2% agarose gel (instead of 1%) applying an inverse current for 30 minutes and a standard catode-to-anode current for 140 minutes. The voltage was kept low (80V). The PCR amplicon containing the VHVL-SNAP insert was expected to have a length of about 2048 base pairs, and the fragment featuring the cse3-SNAP insert was expected to have a length of about 1915 base pairs. The difference is only about 133 base pairs, which could not be reliably distinguished in the agarose gel even with maximized resolution (refer to Figure 4.15 for agarose gel).

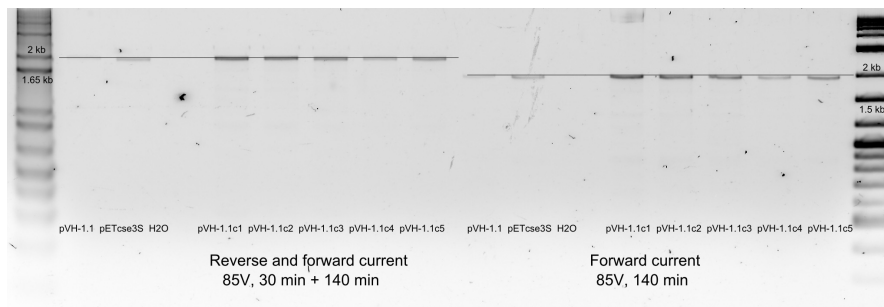


Figure 4.15: The primers *STW013* and *STW014* allow amplification of an about 2.0kb-segment consisting of 250bp upstream of the insert, the insert itself, and 250bp downstream of the insert. The vector insert *Cse3-SNAP* and the cloned insert *VHVL-SNAP* have similar lengths, hence the resulting fragments differ in an almost indistinguishable amount of base pairs (approximately 133bp). Inverting the field is an attempt to increase the resolution in a 2% agarose gel at low voltage (in the left lanes). Right: conventional catode-to-anode current only for comparison. The bands look sharper, but the fragment lengths cannot be confidently distinguished.

4.6.2 Verification by Restriction Digest

The PCR fragments were evaluated by restriction digestion with *EcoRI*, an enzyme that cuts the linear PCR amplicon of the *cse3-SNAP* fragment into two pieces (1.7kb + 300bp), while it cuts the PCR amplicon of *VHVL-SNAP* into three pieces (1154bp + 615bp + 279bp) because it has one additional restriction site in the *VH-VL* gene. An outline of the two plasmids *pET30aCse3-SNAP* and *pET30aVHVL-SNAP* with the restriction sites for *BamHI* as well as *EcoRI* can be appreciated in Figure 4.16.

The PCR products contained TE buffer, which needed to be removed by purification (Qiagen PCR purification kit) before a restriction digest could be set up. After purification the concentration of nucleic acid was vastly decreased, so for future restriction digests TE buffer was omitted in the PCR reactions and templates as well as primers were instead diluted in ultra pure water.

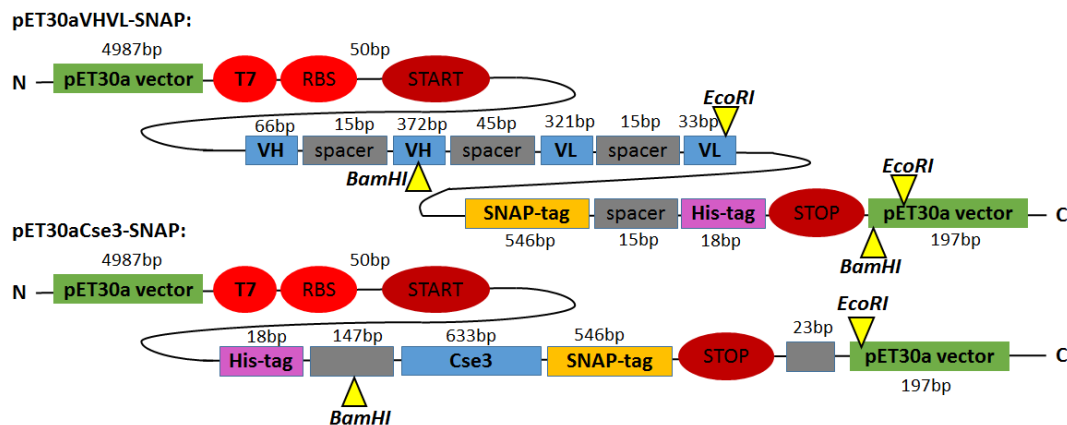


Figure 4.16: *pET30aVHVL-SNAP* and *pET30aCse3-SNAP* outlines with restriction sites marked for *BamHI* and *EcoRI*. The difference in restriction sites was taken advantage of in genome verification.

About 25ng of PCR amplicons of *pET30aCse3-SNAP*, *VH-1.1-SNAP*, and *SHuffleT7 Express VH-1.1* were digested in 1x *EcoRI* buffer using 1 μ l (20 units) of *EcoRI*. The concentration of the PCR amplicons was estimated by assuming 15 doublings in 30 amplification cycles. 1ng of template plasmid was used in the PCR reaction, where the amplicon was about one third of the entire sequence length. Hence, assuming a molecular weight of 650 daltons per base pair, about 5 μ l of PCR product contained 1 μ g of DNA of interest.

When analyzing the restriction digest it was found that both the *cse3-SNAP* and the *VHVL-SNAP* PCR amplicon (positive and negative controls respectively) as well as all samples (PCR amplicons of plasmids isolated from *SHuffleT7 Express* colonies 1 to 5) seemed to be cut into one fragment of about 1.7kb length, and another on the gel invisible fragment of 300bp, which was predicted and true for the negative control *pET30aCse3-SNAP* (refer to Figure 4.17a). An amplicon containing the *VH-VL SNAP*-insert should have been cut into three fragments of the lengths 1154+615+279bp.

A restriction digest under the same conditions was performed on **the original *pET30a-VHVL-SNAP* plasmid** isolated from *BL21(DE3)* after the Gibson Assembly, as well as on 300ng of the two fragments that were used to assemble the construct (**insert from *pUC57Kan-VHVL-SNAP* and vector backbone from *pET30aCse3-SNAP***):

- A plasmid containing the assembled *VHVL-SNAP* insert should be cut into two fragments by *EcoRI* (6kb + 600bp), while a plasmid containing the *Cse3-SNAP* insert instead should be cut into only one linear fragment. The original *STW-VH-1* plasmid was cut into only one linear fragment, as predicted for the *Cse3-SNAP* insert (refer to Figure 4.19b).

- The linear insert derived from pUC57 VHVL-SNAP should feature two EcoRI restriction sites, cutting it into three fragments (903bp + 615bp + 22bp). An insert that contains the Cse3-SNAP insert instead will be cut into two fragments of 1453bp + 22bp. The digested and undigested PCR samples yielded similar patterns in the gel, which is only one band at about 1.5kb. This result closely matches the result predicted for the Cse4-SNAP insert (refer to Figure 4.17c).
- The linear vector backbone fragment pET30a should not be cut as there is no additional cutting site. Only one linear fragment of about 5kb was detected, which appears at the same level as the undigested linear vector backbone fragment. (refer to Figure 4.17c). This digestion worked out as expected.

The evidence gathered from the EcoRI digestions of the about 2kb-PCR amplicons of pET30aCse3-SNAP and VH-1.1, as well as the digestions of the originally assembled STW-VH-1 plasmid and its components (VHVL-SNAP insert and pET30a vector backbone) strongly suggests that in fact the Cse3-SNAP insert is contained in the pET30a vector, rather than the VHVL-SNAP insert.

Since previous restriction digests with BamHI, PCR's using the Gibson primer pairs that anneal to the VHVL-SNAP insert, as well as the initial sequencing results of the four colonies picked after Gibson Cloning speak against the presence of the Cse3-SNAP insert, the restriction enzyme EcoRI was subjected to further analysis.

EcoRI Troubleshoot

The troubleshooting was performed on hybridized oligo nucleotides whose sequences were well-defined. The sequences were analyzed on a denaturing SDS PAGE gel. A sequence of 84 bases featured two restriction sites cutting it into two fragments of 65 + 19 bases. An adapter sequence of 15 bases hybridizes the oligo nucleotide sequence of 84 bases, yielding a 100bp-sequence, and can be cut into two fragments of 10 + 5 bases. Adapter sequences were added at 3x excess, so at most six fragments can be expected in a denaturing DNA PAGE gel:

- An uncut oligo nucleotide fragment of 100 bp
- Excess adapter sequences of 15 bases
- Digested oligo-fragments of 65bp and 19bp
- Adapter fragments of 10 and 5bp

20 pmoles of oligo sequences were hybridized with 60 pmoles of adapter sequences in 50µl 1xTE buffer supplemented with 200mM MgCl₂.

10ng of hybridized DNA were digested with 50U of EcoRI in self-made EcoRI buffer or commercially available CutSmart buffer, and with 50U of EcoRI HF in commercially available CutSmart buffer as a positive control. Reactions were heat-inactivated after restriction digestion. Digested and undigested DNA samples were loaded next to each other in equal amounts based on mass.

The undigested, hybridized sequence of about 100 base pairs was fully assembled, leaving no 80 base oligo sequences and a low amount of 20 base adapter sequences, left over. In all lanes featuring the digested samples (EcoRI in self-made buffer, EcoRI in commercially available buffer, and EcoRI HF in commercially available buffer) the digested fragments at roughly 70bp and 20bp can be clearly seen, alongside the two digested adapter fragments at 10bp and 5bp (refer to Figure 4.18).

These results provides evidence that EcoRI in fact digests reliably under all conditions. Hence, the previously collected results can be treated as reliable. It is very likely that the cutting site close to the C-terminal of the VH-VL insert is in fact inaccessible.

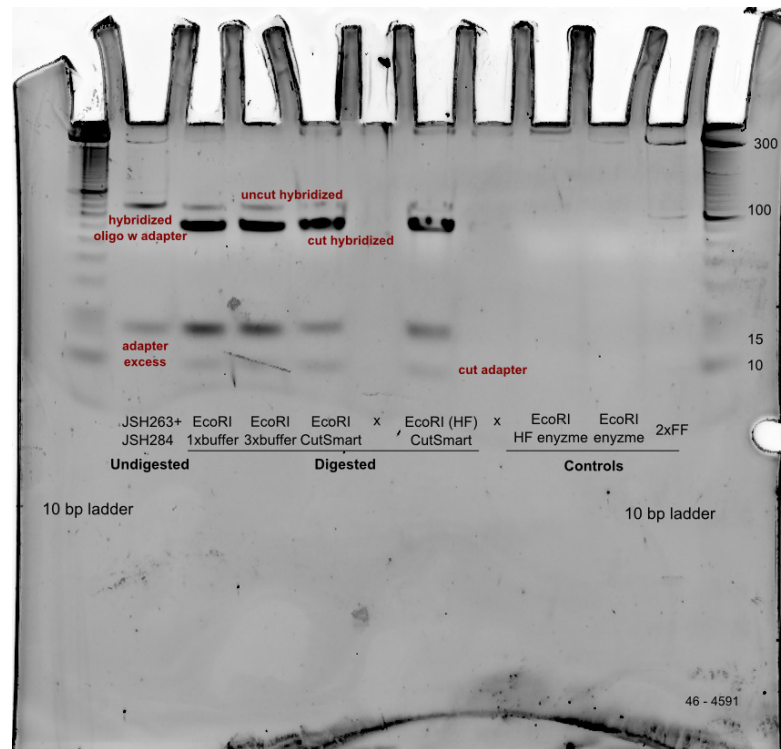


Figure 4.18: The *EcoRI* restriction enzyme was tested and compared to a high-fidelity version of it in commercially available buffer (*CutSmart*, *NEB*). The oligo nucleotides were correctly assembled (undigested, 100bp) and digested as expected under all experimental conditions (roughly 70bp and 20bp for the hybridized oligos, 10bp and 5bp for the adapter fragments). The results show that the enzyme digests reliably under all conditions and previous results can be fully trusted.

EcoRI and BamHI Cross-Control

Previous results obtained with the restriction enzyme *BamHI* were double checked in parallel to *EcoRI* restriction digestion. This step was necessary because results obtained in *EcoRI* restriction digestions supported the idea that Gibson Assembly of the *VHVL-SNAP* insert and the vector had been incomplete or corrupted.

The two plasmids *STW-VH-1* (*VHVL-SNAP* cloned into the *pET30a* vector), *VH-1.1* (daughter colony), as well as the PCR amplicon of *pET30aCse3-SNAP* generated with the two primers *STW013* and *STW014* (anneal to regions 250bp upstream and downstream of the insert) were subjected to restriction digestion with *BamHI* and in another batch with *EcoRI* (in *EcoRI* buffer) and *EcoRI HF* (in *CutSmart* buffer).

Equal amounts of undigested and digested DNA were analyzed on an agarose gel.

The parent plasmid *STW-VH-1* as well as its daughter plasmid *VH-1.1* were expected to be cut into two fragments each by each restriction enzyme given that both restriction

sites are accessible. Both restriction sites are accessible if the insert VHVL-SNAP is present and the site within accessible. The plasmids are cut into only one linear fragment if only one restriction site is present. The pET30aCse3-SNAP PCR product is expected to yield two fragments with both restriction enzymes as well.

In the BamHI restriction digestion both VH-1 plasmids and the pET30a PCR product performed as expected yielding all fragments at the expected base pair lengths (see Figure 4.19a). Hence, BamHI restriction digestion was not further investigated.

In the EcoRI digestion, pET30aCse3-SNAP was cut, but only the larger fragment at about 1.7kb could be detected. The two plasmids STW-VH-1 and VH-1.1 were each cut only once into a linear fragment at about 6.6kb. No other fragments could be seen (refer to Figure 4.19a and for better contrast of the STW-VH-1 plasmid-EcoRI digestion refer to Figure 4.19b). It was noted that EcoRI HF cut the plasmids more efficiently than EcoRI because less residual undigested plasmid was detected in the gel.

EcoRI restriction digestion was repeated with larger amounts of DNA as to increase the likelihood of detecting shorter digestion fragments that previously remained undetected. The shorter 300bp-fragment could not be detected, even though there was a definite shift and a convincing band at 1.7kb after digestion with EcoRI. Several controls were included in the gel analysis. Note that primer bands are clearly visible, emphasizing the low efficiency of the PCR amplification (refer to Figure 4.19c).

4.6.3 Sequencing of VH-1.1

The BamHI restriction digest yielded the expected results, while restriction digestion with EcoRI continued to read only one of two restriction sites. After it was shown that the EcoRI enzyme performed as expected on nucleotide oligos of known sequence, only two possibilities remained: either there is a point mutation in the specific restriction site in the original parent STW-VH-1, possibly even in the previously assembled VH-VL-SNAP insert in pUC57 and in VH-1.1; or the Gibson Cloning did not perform as expected and the insert VHVL-SNAP was never correctly assembled in the pET30a vector. In the latter case more point mutations must be present at convenient sites to justify correct BamHI restriction results.

Various indirect tests, such as restriction digestion with BamHI or PCR using the insert-Gibson primers, confirmed the presence of VHVL-SNAP in pET30a. Sequencing of the original STW-VH-1 plasmid after Gibson Cloning aligned the sequence to the desired outcome as well. To double check the exact sequence VH-1.1 was sent for sequencing. First, the region of interest was amplified by PCR, using the two primer that bind 250bp upstream and downstream of the insert (STW013 and STW014). A high fidelity polymerase (Q5 HotStart) transcribed the sequence in a standard Q5 thermocycle (no specific activation step, 98°C - 55°C - 72°C thermo ramp for denaturation, primer annealing, and extension). The PCR product was purified using a commercially available purification kit (Qiagen) and samples of the crude and purified PCR products were an-

alyzed on an agarose gel for verification of correct sequence length in the absence of byproducts (data not shown).

PCR product concentration and purity was measured in a spectrophotometer and aliquots of 10 μ l x 6ng/ μ l were prepared. Six sequencing primers that are snippets of about 20bp in about 280bp intervals spanning the region of interest were re-used from previous STW-VH-1, STW-VH-2, STW-VH-3, and STW-VH-4 sequencing, with the last primer covering 380bp. As an additional primer, the available amplification primer *STW013* (forward primer annealing to 250bp upstream of the insert) was used. Primer concentrations were calculated based on the *Beer-Lambert Law*. Dilutions of 5 μ M were made and 5 μ l were mixed with 10 μ l of template DNA, as is generally recommended by the vendor *GENEWIZ* (refer to Ref. [30]).

Sequencing results were inconclusive due to low template quality. Time did not permit re-submission of freshly prepared template DNA of higher concentration and purity.

The previous sequencing results for the initially Gibson-assembled VH-VL-SNAP-His insert in pET30a ("STW-VH-1") were double checked.

One cutting site right at the vector-insert intersection at the C-terminus of the sequence, which is also present in *His-cse3-SNAP* in pET30a, was found to be fine, whereas the second cutting side in the middle of the VH-gene was found to be mutated:

Instead of the EcoRI-specific G-AATTC sequence a gap was observed, spanning a site from 5870bp to 5905bp. These 35bp are the last part of the VH-gene, between a GGGS-spacer and the SNAP-tag (refer to Figure 4.16 for an outline).

The equivalent ten amino acids plus a stop codon make up a mass of only about 1kDa, which does not significantly change the expected protein mass; but it does remove the EcoRI recognition site and interfere with the restriction digest.

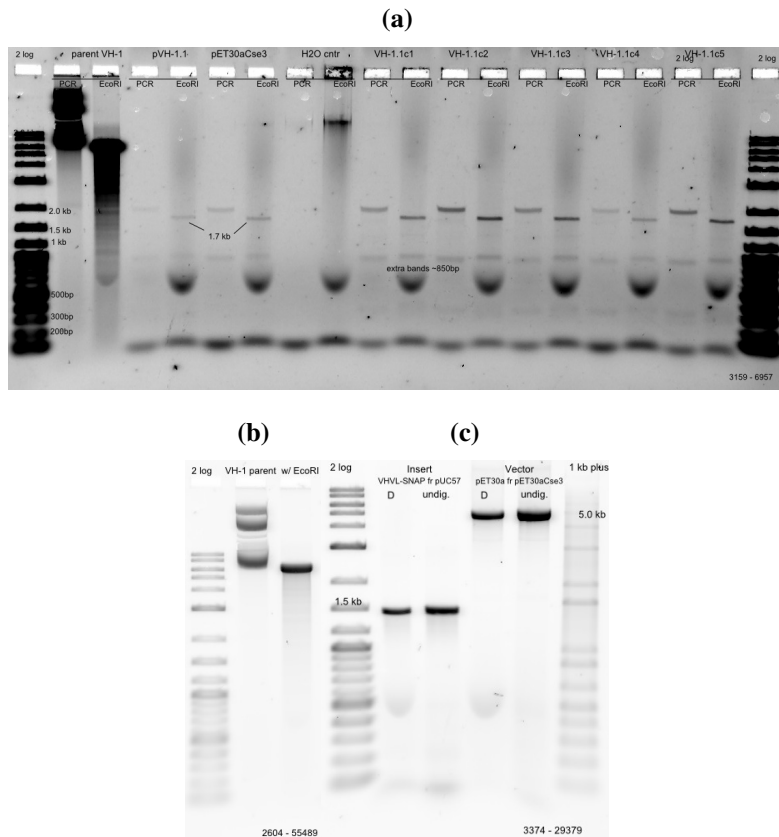


Figure 4.17: (a) A restriction digest with *EcoRI* in *1xEcoRI* buffer was performed. The negative control (PCR on the plasmid *pET30aCse3-SNAP*) contains the *Cse3-SNAP* insert +250bp upstream and downstream and should be cut into two fragments of 1.7kb and 300bp. The positive control (PCR on the plasmid *VH-1.1*) presumably contains the *VHVL-SNAP* insert +250bp upstream and downstream and should be cut into three fragments of roughly 1.1kb, 600bp, and 300bp (not observed). Both the positive and the negative control have the same restriction pattern as the samples, which is expected for a PCR-amplicon containing *Cse3-SNAP*. Note the extra band at about 800bp in the PCR product as well as, presumably, unused primers at about 100bp. (b) The original *STW-VH-1 pET30a*-plasmid isolated from *BL21(DE3)* colonies that were transformed with the Gibson construct is expected to be cut into two fragments of roughly 6kb and 600bp, but in fact on the gel only one linear fragment at 6.5kb can be observed. One of the two restriction sites is missing. (c) The two fragments that were assembled into the Gibson construct (*VHVL-SNAP* from *pUC57Kan-VHVL-SNAP* as "insert" and the vector backbone of *pET30aCse3-SNAP* as "vector") were double checked by *EcoRI* digestion. The insert should be cut into two detectable fragments and one tiny fragment (819bp + 615bp + 21bp) and the vector should remain uncut. While the vector fragment behaves as expected, the insert fragment remains uncut, meaning that the expected restriction site must be inaccessible.

4.7 Summary

Both the VH-VL and the VL-VH construct were cloned into the pUC57 vector by Gibson Cloning and transformed into NEB 5 alpha and BL21(DE3). NEB 5 alpha as well as BL21(DE3) derived plasmids were checked by restriction digestion and NEB 5 alpha derived plasmids were checked by sequencing. BL21(DE3) derived plasmids were later checked by PCR. All tests showed that the desired insert is present and protein expression should be possible. A list of expression experiments in the pET30a vector, the parameters and the outcomes is given in Figure 4.1.

Protein expression in BL21(DE3) was unsuccessful for both VH-VL and VL-VH. A pellet sample was subjected to His tag chromatography because a band near 49kDa was detected on an SDS PAGE gel. In the elution step, which was based on competitive binding by imidazole, no band was specifically eluted.

The insert cloned into pUC57 was amplified from a plasmid that was shown to contain the assembled insert-vector construct of VHVLSNAP in pUC57. The insert was cloned into the pET30a vector by Gibson Cloning, where it replaced another insert present in the vector (*His-Cse3-SNAP*). The assembled construct was transformed into BL21(DE3) and checked by colony PCR as well as by Sanger sequencing.

One expression run yielded a band at 49kDa in the insoluble fraction. The run could be replicated later on when the cultures were induced for 24 hours. However, the goal was to produce the protein in the soluble fraction rather than the insoluble fraction, because pelleted proteins require solubilization and refolding steps that greatly decrease the yield.

Various IPTG concentrations and induction temperatures were tested. 37°C induction repeatedly yielded a band slightly below 49kDa in the insoluble fraction 4 hour, 6 hours, and overnight post induction. Lower temperature settings were unsuccessful in producing any additional bands in either fraction. Expression in the soluble fraction was attempted in time course experiments, sampling at earlier time points than overnight. The band approximately 49kDa continued to be present in the pellet fraction of the samples. After lysis optimization the band was still found in the pellet fraction, which supported the conclusion that it was expressed as an inclusion body. The pellet was solubilized in inclusion body solubilization buffer and the denaturants were removed by TCA-precipitation. Analysis by SDS PAGE showed that the yield was vastly decreased and the band of the re-folded protein was detected at about 42kDa.

Fresh glycerol stocks were prepared by re-plating. Each daughter culture was mini prepped and the plasmids were double checked by restriction digestion (BamHI) and PCR. The restriction digest verified the presence of the insert in all tested plasmids. PCR results were unreliable due to a lack of a consistent positive control. A band for the insert was only detected for VH-1.1 and a band for the vector was detected for all four plasmids.

Protein expression was tested on the four daughter cultures. After 24 hour induction

bands at about 49kDa were found in all pellet fractions at 37°C, and one sample collected at 18°C. Inclusion body solubilization buffer was shown to solubilize the majority of the pelleted proteins. One of the solubilized samples (VH-3.1) was subjected to His-tag chromatography. One band at about 58kDa was specifically eluted by a change in pH in the elution steps. A band at about 42kDa eluted non-specifically in the washing steps. Bands at 49kDa were detected in all collected fractions comprising the flow-through, washing, and elution.

Expecting the SHuffleT7 Express cell line to be capable of producing the disulfide bond-rich protein in the soluble fraction, the plasmids VH-2.2, VH-3.1 and VH-1.1 were transformed into competent cells based on the thick band at around 49kDa after 24 hour induction, restriction digestion with BamHI, and a PCR that suggested the presence of the insert in VH-1.1.

The VH-2.2SH and VH-3.1SH plasmids were double checked for the presence of the insert and the vector by a PCR. After repetition of the PCR with fresh primers the positive controls worked out as expected, but no insert-bands were detected for the sample plasmids. A restriction digest with BamHI, however, suggested that the insert is present in the plasmid. An experimental protein expression run was performed. No extra bands were found.

The plasmid VH-1.1 was transformed into SHuffleT7 Express. Five colonies were picked, mini prepped, and tested for the presence of the insert and vector by a PCR and a restriction digest. The restriction digest with BamHI confirmed the presence of an insert for the plasmid VH-1.1, as expected. The PCR continued to turn out smeared and inconclusive and had to run through a series of troubleshooting experiments. The troubleshooting eventually led to a number of conclusions: the OneTaq buffer was likely contaminated, the thermocycle machines let part of the reaction volume evaporate, the OneTaq polymerase enzyme needed to be exchanged for Taq polymerase, and lastly, the thermocycle temperature ramp needed to be slightly adapted. Even though the insert-fragment region could be successfully amplified after all adaptations to the PCR had been made, the vector could still not be amplified. Taq DNA polymerase was assumed to be incapable of reliably transcribing 5kb fragments.

Yet, when an experimental expression run with the plasmid VH-1.1 in SHuffleT7 Express was performed, no extra bands could be detected. An alternative approach to double check the genome needed to be devised.

New primers that anneal to regions of the vector 250bp upstream and downstream of the insert were designed. The PCR reaction successfully amplified the regions for all samples, the positive control (VH-1.1) and the negative control (pET30aCse3 SNAP vector). However, there was only a 133bp difference between the positive and negative control, which was hard to judge based on an agarose gel.

The PCR products were digested with EcoRI, which should cut the positive and negative control into fragments of different lengths. However, all sequences were cut into

fragments of about the same length.

Furthermore, the original plasmid isolated after Gibson Assembly as well as the insert fragment that was assembled with the pET30a vector-backbone was cut into unexpected fragment lengths. The observed fragment lengths were predicted for the same constructs containing the Cse3SNAP insert, rather than the VHVL-SNAP insert. The plasmid yielded only one linear fragment instead of two fragments. The insert was cut into one fragment the length of which was predicted for Cse3SNAP and, presumably, another very short 22bp-fragment that is not detected in the gel. The vector performed as expected in the restriction digestion with EcoRI.

The EcoRI enzyme was subjected to trouble shooting experiments using oligo nucleotides of precisely known sequences. It was shown that the enzyme in fact performs as expected under all experimental conditions, indicating that previous results are reliable.

EcoRI and BamHI restriction digestion was double checked in the original STW-VH-1 plasmid, the VH-1.1 plasmid, as well as the PCR amplicon of pET30aCse3SNAP generated with the two primers that bind 250bp upstream and downstream of the insert. BamHI yielded the expected results, indicating that in fact the VH-VL SNAP insert is present in STW-VH-1 and VH-1.1.

EcoRI continued to cut the PCR amplicon of pET30aCse3SNAP into two fragments, only one of which was detectable (1.7kb + 300bp). The two plasmids that should contain the VH-VL SNAP insert were only cut into one linear fragment, instead of two fragments.

The conflicting results could only be resolved by repeated Sanger sequencing. Sequencing results of VH-1.1 were inconclusive, but re-investigation of original sequencing results of STW-VH-1 (VH-VL SNAP-His in pET30a isolated from BL21(DE3)) revealed that the distinguishing EcoRI cutting side is missing. In its stead a gap was found in the alignment. Only one EcoRI cutting side was left, which was shared by both the *cse3-SNAP-His* and the *VH-VL SNAP-His* insert in pET30a. The EcoRI restriction digestion consequently does not qualify as a valid method of differentiation between the two fragments. BamHI digestion, however, can be used as all cutting sides were shown to be intact.

Even though protein expression remained unsuccessful, a variety of control experiments approaching the issue from different angles provide evidence that, in theory and given the right expression circumstances, protein expression should be possible.

Cell line	c(IPTG) [mM]	Temperature [C]	Time	Treatment	Outcome
STW-VH-1 (BL21 DE3)	0.25, 0.5, 1	37, 18, 15	overnight	chem. lysis (xTractor), sonification	37C: band at 42kDa (insoluble) no extra bands
STW-VH-1 (BL21 DE3)	0.25	18	time course (hourly for 6h + on)	chem. lysis (xTractor), sonification	18C: no bands, 37C: band at 42kDa (insoluble)
STW-VH-1 (BL21 DE3)	1	37, 18	time course (bi-hourly for 6h + on)	chem. lysis (CellLytic + lysozyme)	no extra bands
STW-VH-1,2,3,4 (BL21 DE3)	0.4	18	overnight	chem. lysis (CellLytic + lysozyme)	no extra bands
STW-VH-1,2,3,4 (BL21 DE3)	0.4	37, 18	24h	chem. lysis (CellLytic + lysozyme)	37C: bands at 49kDa (insoluble), 18C: band in VH-2.2 at 49kDa (insoluble)
STW-VH-2.2, -3.1 (SHuffleT7 Express)	0.4	30, 16	4h, overnight	chem. lysis (CellLytic + lysozyme)	30C: bands at 42kDa (insoluble)
STW-VH-1.1 (SHuffleT7 Express)	0.8	30, 16	4h, overnight	chem. lysis (CellLytic + lysozyme)	no extra bands

Table 4.1: Expression experiments in the pET30a vector. All cultures were grown in LB-Kanamycin medium and induced at an OD of 0.4-0.6 with various concentrations of IPTG. The goal was to express a single-chain variable antibody fragment of 49kDa by IPTG induction, while avoiding protein aggregate formation. Bands at the target molecular weight, 49kDa, were observed at high temperature inductions with various molar IPTG concentrations. A sample that featured a more intensified band at 42kDa was refolded in inclusion body solubilization buffer and subsequently TCA-precipitated (37°C, 1mM IPTG induction, 4 hours post induction). The band remained at 42kDa. A sample that featured a more intensified band at 49kDa was refolded in inclusion body solubilization buffer and analyzed by His-tag chromatography (37°C, 0.4mM IPTG induction, 24h). In the chromatography, a band at 42kDa was washed off in the washing steps and a band at 58kDa was eluted in the second elution step. Bands at 49kDa were detected in all steps including the flow-through, washing steps, and elution steps. None of the bands qualified as the protein of interest. Expression in the BL21-derived cell line SHuffle T7 was not successful either, even though the transformed plasmid was shown to contain the correct, yet narrowly incomplete, genetic code for the protein of interest.

CHAPTER 5

Discussion

A series of sequential experiments and the appropriate quality control experiments have been presented in the previous chapter. Even though strong evidence exists that the correct genetic code is present and various attempts to protein expression have been made in two different expression cell lines, the target protein could not be expressed convincingly.

In the following chapter the end points of the experiments will be discussed. Alternative approaches are suggested in section 5.3 and further applications are discussed in section 5.4. Finally, a concise conclusion will be drawn and an outlook presented in sections 5.5 and 5.6.

5.1 Expression in pUC57 in BL21(DE3)

In this thesis, the ScFv anti-DEC205, for which expression in the supernatant fraction in the pET3a vector in BL21(DE3) had been demonstrated previously, was to be expressed as a fusion protein with a SNAP-tag. Since the pET3a vector was not available at the time, the ScFv gene in a pUC57 vector was used instead and a SNAP-tag sequence was cloned into the vector by Gibson Cloning.

Both versions of the ScFv, VH-VL-SNAP and VL-VH-SNAP, were transformed into BL21(DE3), but neither version of the fusion protein could be detected by SDS PAGE as a strongly intensified protein band post-induction at around 49kDa. His-tag chromatography was performed on one sample, but no protein was specifically eluted.

Previous experiments in the lab confirmed that the pUC57 vector does not readily support expression of certain proteins (e.g., a *CRISPR associated endoribonuclease Cse3* or the ScFv anti-DEC205 with a His tag but without a SNAP tag). However, it has been shown that the pET3a vector (in the case of anti-DEC205-SNAP) and the pET30a vec-

tor (in the case of Cse3-SNAP) enable expression of precisely these proteins. In fact, sources confirm that pET-based expression of ScFv's and Fab's is generally more successful (e.g., Ref. [31], [68]).

Restriction digestions (BAMH1), PCRs, and Sanger sequencing results confirmed the presence of the correctly inserted genetic code in pUC57. Therefore, the plasmid presented itself as a suitable template for Gibson Cloning into the pET vector present in the lab: *pET30a-cse3*.

Even though cloning in pUC57 did not yield expression of the protein of interest, it did provide a basis for Gibson Cloning in pET30a.

5.2 Expression in pET30a in BL21(DE3)

The entire gene sequence *His-Cse3-SNAP* which was present in the pET30a vector was replaced by the gene sequence *VH-VL-SNAP-His* transcribed from the pUC57 plasmid. Although the inserted region was extended beyond the actual target protein sequence to decrease the likelihood of mutations in the sequence, a gap formed at the C-terminus of the VH-VL sequence, skipping the final 35 base pairs between a GGTGGTGGTGGCTCC-spacer and the onset of the SNAP tag sequence. It could be possible that this discrepancy from the desired sequence was already carried over from the sequence present pUC57 vector.

Alternatively, the mistake may also have happened when the VH-VL-SNAP insert was cloned into pET30a. Either way, the absence of 35 base pairs corresponds to a lack of ten amino acids in the ScFv protein sequence, which lowers the expected molecular weight by only about 1kDa. This discrepancy in molecular weight does not justify the absence of an intensified protein band at around 49kDa post-induction.

Whether the function of the desired protein is compromised by the lack of ten amino acids at the end of the VH-VL protein where the VH-VL sequence attaches to the SNAP tag sequence remains debatable. It is strongly recommended to predict the protein structure and evaluate the criticality of the loss by use of structure prediction software tools before continuing with expression. Furthermore, it is recommendable to re-evaluate sequencing results of VH-VL in the original pUC57 plasmid and see if the transcription error was carried over from the original template. If the VH-VL gene was present in its entirety in pUC57, meaning that cloning into pET30a introduced the error, additional cloning experiments should be considered. However, if the gap was already present in pUC57, two conclusions can be drawn:

- The gap could explain why the protein anti-DEC205 without a SNAP-tag could not be expressed in pUC57 previously. This assumption only holds true if the

pET3a vector, which enabled expression in the supernatant fraction, does feature the entire protein sequence.

- As an extension of point 1, the gap may also be present in pET3a-VH-VL. If this is the case, it is unlikely that the loss of ten amino acids have anything to do with successful protein expression. Still, a compromise in protein function is not yet out of the picture.
- Lastly, the gap should be evaluated with regard to possible changes in protein structure and resulting changes in function. If the amino acid gap in the protein sequence is present in pUC57, it would be ill-advised to use the plasmid in any subsequent cloning and expression experiments of VH-VL-SNAP.

Independent of the presence or absence of the ten amino acid gap in the original pUC57 or pET3a plasmids, the error poses a threat to the protein function in the project and it is highly recommended to consider circumvention of the issue. Even though structure prediction tools may provide evidence that, in fact, the gap is most likely inconsequential, a minimal uncertainty will always remain.

5.2.1 Expression Parameters

Laboratory-scale protein expression is mainly influenced by parameters such as induction temperature, induction time, and IPTG-concentration, all of which depend on the expression strain in use and the protein to be produced. Each parameter was varied separately in order to determine a favorable expression environment. Parameters such as medium composition, agitation, or OD at induction were kept constant at a value recommended by the vendor (*NEB*).

Parameters that enabled anti-DEC205 expression in pET3a without a SNAP-tag did not apply to the expression of anti-DEC-205-SNAP in pET30a. Variation of the parameters did not significantly change the outcome of the experiments. Even though a protein at about 42kDa was repeatedly over-expressed at high induction temperatures, the band could not be identified as the protein of interest.

When the induction time was extended to an abnormally long time span of 24 hours, a band at higher molecular weight (about 49kDa - the predicted molecular weight of the target protein) could be detected in the samples, albeit in the insoluble fraction. However, analysis of the solubilized protein sample by His-tag chromatography showed that the band at 49kDa did not elute specifically, as should be the case for the protein of interest.

5.2.2 SHuffle T7 Express Cell Line

Addition of a SNAP tag to form a fusion protein is known to radically enhance the complexity of protein expression in many cases. Therefore, it was logical to move to a cell line that is perfected to express proteins that are high in disulfide bonds or generally difficult to express.

The cell line ShuffleT7 Express is an enhanced BL21 derivative. This *E.coli* cell line is specifically engineered to form proteins containing disulfide bonds in the cytoplasm, which is normally a reducing environment. This is possible because the two reductases *glutaredoxin reductase* and *thioredoxin reductase* have been deleted in SHuffle T7 Express and a mutation in the peroxiredoxin enzyme protects the cells from the resulting lethality of the two deletion mutations. In addition, SHuffle T7 Express expresses a version of the periplasmic disulfide bond isomerase DsbC, which is retained in the cytoplasm. The enzyme corrects mis-oxidized disulfide bonds and has also been shown to be an effective chaperone in the folding of target proteins, independent of the presence or absence of disulfide bonds (refer to Ref. [33]). A deficiency in two proteases assists the production of proteins from cloned genes. Additionally, SHuffle T7 Express is deficient in the OmpT protease, which is found in the surface of various *E.coli* strains.

The genetic code in pET30a has been extensively characterized by (colony-) PCRs, restriction digestions (first BAMH1, later on EcoRI in trouble shooting experiments), and Sanger sequencing. Therefore, the plasmids served as suitable candidates for transformation into SHuffle T7 Express.

However, the cell line did not prove capable of expressing the fusion protein. After having verified the genetic code in multiple troubleshooting experiments, further scanning experiments that apply a range of induction temperatures, IPTG concentrations, and induction times may solve the problem. Time constraints did not allow the pursuit of this theory.

As mentioned above, before continuing with any expression experiments it should be investigated whether the missing 35 nucleotides in the VH-VL gene could affect the function of the protein or its expression. Only once these two questions are answered, further expression experiments in SHuffleT7 Express make sense.

Having said that, it should be stressed once again that it would be much more sensible to circumvent the challenge of structure-function investigations and focus on the pursuit of alternative approaches.

5.3 Suggestions for Alternative Approaches

Expression of the fusion protein consisting of the ScFv anti-DEC205 and the SNAP tag proved to be more difficult than originally anticipated. Given that the full protein sequence of the ScFv anti-DEC205 in its VH-VL or VL-VH form is available, or that the

gap in the sequence was shown to be completely insignificant, separate expression of the protein without a SNAP-tag presents itself as an option. In this section, two alternative approaches for the production of anti-DEC205-SNAP and the use of a substitute affinity ligand are suggested.

5.3.1 Expressed Protein Ligation

Expression of anti-DEC205 without the SNAP tag may very likely be less complex than expression of a fusion protein. Several strategies for post-expression protein ligation exist. Some examples are listed below:

- *Native chemical ligation*, which assembles two or more unprotected peptide segments. A thiol group of an N-terminal cysteine residue reacts with a thioester group on the C-terminal of a second peptide.
- Ligations that rely on specific and unusual residues (e.g., Ref. [5])
- Intein- and enzyme-based ligation strategies that apply, for example, the bacterial transpeptidase *Sortase A*. This enzyme cleaves at a recognition motif to produce an acyl-enzyme intermediate and then form a native amide bond (e.g., Ref. [48]).

Hence, given that additional motives are engineered, fusion of a SNAP tag to the separately expressed ScFv can be achieved in various ways.

The advantage of this approach is that expression parameters for anti-DEC205 in pET3a have already been devised and may very well hold true for expression of anti-DEC205 in pET30a. Separate expression of a SNAP tag should not prove too difficult either, as the sequence is very well characterized and merely about 500bp long, which amounts to a protein mass of about 19.4kDa. Alternatively, purchase of a purified SNAP-tag protein is an option, as the protein is commercially available. Of course, the protein sequence may have to undergo additional engineering depending on the ligation method.

Nevertheless, the disadvantages of post-expression ligation clearly outweigh its advantages in this particular case. Due to the need to engineer additional motifs and recognition sites, which may or may not ultimately change the target protein's behavior, the approach can be regarded as rather roundabout and crude. Furthermore, the project presented in this thesis itself showcases the unpredictable nature of protein expression studies on one single protein, let alone two to three separate proteins, possibly including one completely unexplored enzyme. The chances of losing oneself in expression experiments only to discover that fusion of the SNAP tag and the ScFv does not work out as planned, or that the lack of amino acids in the VH-VL protein does make a considerable difference, are too high to justify the investment of valuable time, effort, and money.

5.3.2 RNA-Aptamer

A different approach is to completely replace the anti-DEC205-SNAP protein with a nucleic acid-based targeting approach.

Levy *et. al.* have recently proposed a DC targeting strategy for antigen cross presentation and subsequent CD8+TC activation in the scope of an improved TC-mediated cancer vaccine (refer to Ref. [77]). This was the first time that aptamers were proposed as a targeting agent that delivers antigen.

The lab specializes in the production and study of nucleic acid aptamers. A minimized aptamer was conjugated to the model antigen *ovalbumin* and the construct was presented to purified DCs for uptake and facilitated cross-presentation. Significantly increased cytokine production (IFN- γ , IL-2) by and proliferation of primary murine CD8+ TCs featuring a TCR specific for the ovalbumin-peptide was measured. The resulting immune responses were able to inhibit the growth of established ovalbumin-expressing tumor cells. In the absence of additionally supplied adjuvants (pIC or anti-CD40) the primed CD8+ TCs underwent deletion followed by tolerance. (Ref. [77]).

In this system, a nucleic acid aptamer replaces the protein-antibody that normally directs antigen to a readily endocytosed cell surface receptor, such as DEC-205. Aptamers can be made from peptides, DNA, or RNA *in vitro* by an iterative selection process referred to as *systematic evolution of ligands by exponential enrichment* (SELEX). In the SELEX process a large library of oligonucleotides of equal lengths but random sequences is exposed to a specific target, such as DEC205. Those sequences that bind the target are subjected to further runs of selection under more stringent conditions. Aptamers bind specific targets with high affinity, which makes them ideal for application in the project presented in this thesis.

It is clear that development of a process to make an aptamer identical to anti-DEC205 is beyond the scope of the project. Rather, it would be advantageous for both the Levy-Lab and the Shih-Lab to collaborate on a DEC-205-based immunotherapy that combines DNA-origami delivery and aptamer-based targeting. Hence, if the application of the aptamer technique is considered, collaborative work is highly recommended.

5.4 Further Applications

Besides an improved Th1-activation by manipulation of the cytokine environment for tumor immunotherapy, the concept of precise affinity ligand positioning on DNA origami has many more possible applications. Two possible ideas are briefly introduced below.

5.4.1 Th1-Bias

Within the scope of biasing the immune system for a Th1-response, other receptor ligands could be supplied together with the targeting ligand anti-DEC205. These ligands

may amplify the the immune response or prevent elimination of activated APCs. One example is the co-receptor CD40. Cross-linkage of CD40 by binding of trimeric CD40-L or anti-CD40 can further activate DCs and stimulate the production of pro-inflammatory cytokines (Ref. [47]). If a DNA origami structure is decorated with a sufficiently high density of CD40-L, receptor cross-linking may be achieved. In addition to targeting the receptor DEC205, which may be endocytosed to allow anti-gen presentation, cross-linking of co-receptors such as CD40 could further amplify the Th1-response and thereby improve the cancer vaccine.

5.4.2 Logic-Gated Cell Signaling

Another application of the idea is closely related to work in the field of programmable nanomaterials, which was briefly mentioned in the chapter 2 (refer to Ref. [22]). Logic gates on a nano robotic device open when both aptamers fixed on the sides of the lid pair with their complementary affinity ligands, essentially encoding an *AND*-function for the opening of the lid.

The same idea can be applied to cell-cell communication models. Signals may only be transmitted if the correct affinity ligands are arranged in a precise dimensional layout. DNA origami is a powerful tool to mimic such receptor-ligand layouts, thereby amplifying desired signals or gaining entry to a selective barrier, where cargo previously fitted into the structure may be deposited.

5.5 Conclusion

The fusion protein anti-DEC205-SNAP could not be expressed either in its soluble or in its insoluble form. Based on the genomic code, evidence exists that expression of the fusion protein is possible, even though a fraction of the sequence is missing.

In pursuit of the current project, one possibility is the variation of expression conditions in SHuffleT7 Express. This option, however, is not recommendable due to a gap at the C-terminus of the VH-VL sequence that may or may not change the protein's function and behavior.

Instead, if presence of this ten amino acid sequence can be proven in the original pUC57-plasmid, the plasmid may be used for additional expression studies of the ScFv alone without the SNAP-tag followed by post-expression ligation. However, this option is considered highly risky, time consuming, and roundabout.

A much smarter option would be to collaborate with another laboratory and use an aptamer affinity ligand to target DEC-205 instead of using a protein affinity ligand. The method is well-established especially for the targeting of DEC-205, as was shown in Ref. [47], and can guarantee a swift progression with cellular uptake as well as cytokine assays.

5.6 Outlook

The origami barrel structure needs to be designed with well-spaced protruding handles that are sufficiently far apart to discourage cross-linking of DEC-205 affinity ligands. Further, the origami structure needs to be purified and subsequently coated with polyethylene glycol (PEG) to protect it from degradation before the anti-DEC205-aptamer can be attached by *handle-anti handle* design. Once attachment is verified by gel electrophoresis and transmission electron microscopy (TEM), cellular uptake experiments with Chinese hamster ovary (CHO)/mDEC205 (a CHO cell line engineered to overexpress mDEC205) or CHO-cells can be started. Alternatively or in addition, primary mDEC205+ bone marrow derived dendritic cells (BMDCs) can be used. Evaluation of uptake can be performed by fluorescence activated cell sorting (FACS) or flow cytometry. Sufficient controls should always be in place.

List of Figures

2.1	Basic illustration of generation and regulation of antitumor immunity	4
2.2	Example <i>Ipilimumab</i> as CTLA-4 blocking antibody	8
2.3	Vaccine vehicles	11
2.4	nanoparticle anti-DEC-205	14
2.5	Immunization by DEC-205 decorated nanoparticles	16
2.6	Secondary immunization by DEC-205 decorated nanoparticles	17
2.7	DNA Origami design	19
2.8	DNA Origami design and examples	20
2.9	DNA Origami Robot	22
2.10	Gibson Assembly visualization	24
3.1	Gibson Cloning Molecular Outline	29
4.1	Restriction digest with Sall and NheII and with BamHI on VHVL-SNAP in pUC57-Kan derived from NEB 5 alpha and BL21(DE3) cells	41
4.2	Final assembly outline of SNAP tag and VLVH in pUC57-Kan	41
4.3	SDS PAGE in pUC57-VHVL and VLVH	42
4.4	final SDS PAGE and PCR in pUC57-VHVL and VLVH	43
4.5	Final assembly outline of VHVL - SNAP - His in pET30a	44
4.6	PCR amplifications of fragments in preparation for Gibson Assembly	46
4.7	cPCR on pET30a VHVL-SNAP-His transformations in BL21(DE3)	47
4.8	Scanning experiments Protein Expression BL21(DE3)	48
4.9	Time course: Pellet fractions of 37C at 18C	49
4.10	PCR and BamHI on original VH-colonies after Gibson Assembly	51
4.11	VH-daughter culture expression	53
4.12	His tag chromatography VH-3.1 sol. IB	54
4.13	PCR and RD on plasmids 2.2SH1+2 and 3.1SH1+2	56
4.14	VH-1.1 in SHuffleT7 Express, BamHI	57
4.15	Inverse Field Agarose gel Analysis of PCR	60
4.16	Plasmid outline pET30aCse3-SNAP and pET30aVHVL-SNAP with restriction sites	61
		81

4.18	Troubleshooting EcoRI	64
4.17	EcoRI restriction digestion	67
4.19	BamHI and EcoRI HF with controls	68

List of Tables

2.1	Summary of relevant cytokines	15
3.1	Summary of expression cell lines	27
3.2	Assembly and Transformation control PCR	30
3.3	control PCR SHuffleT7 transformation	31
3.4	Buffer recipes for His tag chromatography	35
4.1	Summary Expression in pET30a	72

Acronyms

- APC** antigen presenting cell
- APS** ammonium persulfate
- mAb** monoclonal antibody
- BMDC** bone marrow derived dendritic cell
- CHO** Chinese hamster ovary
- CLR** C-type lectin receptor
- CTL** cytotoxic T-lymphocyte
- CTLA-4** cytotoxic T-lymphocyte-associated antigen 4
- DC** dendritic cell
- DTT** dithiothreitol
- EDTA** Ethylenediaminetetraacetic acid
- ELISA** enzymatic immuno absorbent assay
- FACS** fluorescence activated cell sorting
- FDA** U.S. Food and Drug Administration
- FRET** Förster resonance energy transfer
- IFN- γ** interferon gamma

IL-10 interleukin-10

IPTG Isopropyl B-D-1-thiogalactopyranoside

ISO Isothermal Amplification Buffer

MHC major histocompatibility complex

NK natural killer

PAINT points accumulation imaging in nanoscale topography

PALM photo-activated localization microscopy

PBS phosphate buffered saline

PCR polymerase chain reaction

PEG polyethylene glycol

PD-L1 programmed death-ligand 1

PLGA poly lactide-co-glycolic acid

RBS ribosome binding site

PMSF phenylmethylsulfonyl fluoride

ScFv single chain variable fragment

SOC Super Optimal Growth

STORM stochastic optical reconstruction microscopy

TC T-lymphocyte

TCA trichloroacetic acid

TCL total cell lysate

TCR T-cell receptor

TEM transmission electron microscopy

TGF- β tumor growth factor beta

TLR toll-like receptor

TNF- α tumor necrosis factor alpha

VEGF vascular endothelial growth factor

WHO World Health Organization

Bibliography

- [1] Omar A. Ali and David J. Mooney. Immunologically active biomaterials for cancer therapy. pages 279–297, 2010.
- [2] Asim Amin, David H. Lawson, April K.S. Salama, Henry B. Koon, Troy Guthrie, Sajeve S. Thomas, Steven J. O’Day, Montaser F. Shaheen, Bin Zhang, Stephen Francis, et al. Phase ii study of vemurafenib followed by ipilimumab in patients with previously untreated braf-mutated metastatic melanoma. *Journal for ImmunoTherapy of Cancer*, 4(1):44, 2016.
- [3] Yaniv Amir, Eldad Ben-Ishay, Daniel Levner, Shmulik Ittah, Almogit Abu-Horowitz, and Ido Bachelet. Universal computing by dna origami robots in a living animal. *Nature nanotechnology*, 9(5):353–357, 2014.
- [4] Ebbe S. Andersen, Mingdong Dong, Morten M. Nielsen, Kasper Jahn, Ramesh Subramani, Wael Mamdouh, Monika M Golas, Bjoern Sander, Holger Stark, Cristiano L.P. Oliveira, et al. Self-assembly of a nanoscale dna box with a controllable lid. *Nature*, 459(7243):73–76, 2009.
- [5] Brenda Ayers, Ulrich K. Blaschke, Julio A. Camarero, Graham J. Cotton, Mande Holford, and Tom W. Muir. Introduction of unnatural amino acids into proteins using expressed protein ligation. *Peptide Science*, 51(5):343–354, 1999.
- [6] Annabell Bachem, Steffen Güttler, Evelyn Hartung, Frédéric Ebstein, Michael Schaefer, Astrid Tannert, Abdulgabar Salama, Kamran Movassaghi, Corinna Opitz, Hans W. Mages, et al. Superior antigen cross-presentation and xcr1 expression define human cd11c+ cd141+ cells as homologues of mouse cd8+ dendritic cells. *The Journal of experimental medicine*, 207(6):1273–1281, 2010.
- [7] Arunima Bandyopadhyay, Rebecca L. Fine, Stacey Demento, Linda K. Bockenstedt, and Tarek M. Fahmy. The impact of nanoparticle ligand density on dendritic-cell targeted vaccines. *Biomaterials*, 32(11):3094–3105, 2011.
- [8] New England Biolabs.

- [9] Christian Bode, Gan Zhao, Folkert Steinhagen, Takeshi Kinjo, and Dennis M. Klinman. Cpg dna as a vaccine adjuvant. *Expert review of vaccines*, 10(4):499–511, 2011.
- [10] Laura Bonifaz, David Bonnyay, Karsten Mahnke, Miguel Rivera, Michel C. Nussenzweig, and Ralph M. Steinman. Efficient targeting of protein antigen to the dendritic cell receptor dec-205 in the steady state leads to antigen presentation on major histocompatibility complex class i products and peripheral cd8+ t cell tolerance. *The Journal of experimental medicine*, 196(12):1627–1638, 2002.
- [11] Laura C. Bonifaz, David P. Bonnyay, Anna Charalambous, Dara I. Darguste, Shin-Ichiro Fujii, Helena Soares, Marie K. Brimnes, Bruno Moltedo, Thomas M. Moran, and Ralph M. Steinman. In vivo targeting of antigens to maturing dendritic cells via the dec-205 receptor improves t cell vaccination. *The Journal of experimental medicine*, 199(6):815–824, 2004.
- [12] Julie R. Brahmer, Charles G. Drake, Ira Wollner, John D. Powderly, Joel Picus, William H. Sharfman, Elizabeth Stankevich, Alice Pons, Theresa M. Salay, Tracee L. McMiller, Marta M. Gilson, Changyu Wang, Mark Selby, Janis M. Taube, Robert Anders, Lieping Chen, Alan J. Korman, Drew M. Pardoll, Israel Lowy, and Suzanne L. Topalian. Phase i study of single-agent anti-programmed death-1 (mdx-1106) in refractory solid tumors: Safety, clinical activity, pharmacodynamics, and immunologic correlates. *Journal of Clinical Oncology*, 28(19):3167–3175, 2010. PMID: 20516446.
- [13] Julie R. Brahmer and Drew M. Pardoll. Immune checkpoint inhibitors: making immunotherapy a reality for the treatment of lung cancer. 1(2):85–91, 2013.
- [14] Paul B. Chapman, Axel Hauschild, Caroline Robert, John B. Haanen, Paolo Ascierto, James Larkin, Reinhard Dummer, Claus Garbe, Alessandro Testori, Michele Maio, et al. Improved survival with vemurafenib in melanoma with braf v600e mutation. *New England Journal of Medicine*, 364(26):2507–2516, 2011.
- [15] Marcello Chieppa, Giancarlo Bianchi, Andrea Doni, Annalisa Del Prete, Marina Sironi, Gordana Laskarin, Paolo Monti, Lorenzo Piemonti, Andrea Biondi, Alberto Mantovani, et al. Cross-linking of the mannose receptor on monocyte-derived dendritic cells activates an anti-inflammatory immunosuppressive program. *The Journal of Immunology*, 171(9):4552–4560, 2003.
- [16] Chung-Ching Chu, Niwa Ali, Panagiotis Karagiannis, Paola Di Meglio, Ania Skowera, Luca Napolitano, Guillermo Barinaga, Katarzyna Grys, Ehsan Sharif-Paghaleh, Sophia N. Karagiannis, et al. Resident cd141 (bdca3)+ dendritic cells in human skin produce il-10 and induce regulatory t cells that suppress skin inflammation. *The Journal of experimental medicine*, 209(5):935–945, 2012.

- [17] Karine Crozat, Rachel Guiton, Vanessa Contreras, Vincent Feuillet, Charles-Antoine Dutertre, Erwan Ventre, Thien-Phong Vu Manh, Thomas Baranek, Anne K. Storset, Jacqueline Marvel, et al. The xc chemokine receptor 1 is a conserved selective marker of mammalian cells homologous to mouse $cd8\alpha+$ dendritic cells. *The Journal of experimental medicine*, 207(6):1283–1292, 2010.
- [18] Luis J. Cruz, Paul J. Tacken, Remco Fokkink, Ben Joosten, Martien Cohen Stuart, Fernando Albericio, Ruurd Torensma, and Carl G. Figdor. Targeted plga nano-but not microparticles specifically deliver antigen to human dendritic cells via dc-sign in vitro. *Journal of Controlled Release*, 144(2):118–126, 2010.
- [19] Tyler J. Curiel, George Coukos, Linhua Zou, Xavier Alvarez, Pui Cheng, Peter Mottram, Melina Evdemon-Hogan, Jose R. Conejo-Garcia, Lin Zhang, Matthew Burow, et al. Specific recruitment of regulatory t cells in ovarian carcinoma fosters immune privilege and predicts reduced survival. *Nature medicine*, 10(9):942–949, 2004.
- [20] Nathan D. Derr, Brian S. Goodman, Ralf Jungmann, Andres E. Leschziner, William M. Shih, and Samara L. Reck-Peterson. Tug-of-war in motor protein ensembles revealed with a programmable dna origami scaffold. *Science*, 338(6107):662–665, 2012.
- [21] Hendrik Dietz, Shawn M. Douglas, and William M. Shih. Folding dna into twisted and curved nanoscale shapes. *Science*, 325(5941):725–730, 2009.
- [22] Shawn M. Douglas, Ido Bachelet, and George M. Church. A logic-gated nanorobot for targeted transport of molecular payloads. *Science*, 335(6070):831–834, 2012.
- [23] Shawn M. Douglas, Hendrik Dietz, Tim Liedl, Björn Högberg, Franziska Graf, and William M. Shih. Self-assembly of dna into nanoscale three-dimensional shapes. *Nature*, 459(7245):414–418, 2009.
- [24] Mark E. Dudley, John R. Wunderlich, Paul F. Robbins, James C. Yang, Patrick Hwu, Douglas J. Schwartzentruber, Suzanne L. Topalian, Richard Sherry, Nicholas P. Restifo, Amy M. Hubicki, et al. Cancer regression and autoimmunity in patients after clonal repopulation with antitumor lymphocytes. *Science*, 298(5594):850–854, 2002.
- [25] Tarek M. Fahmy, Robert M. Samstein, Casey C. Harness, and W. Mark Saltzman. Surface modification of biodegradable polyesters with fatty acid conjugates for improved drug targeting. *Biomaterials*, 26(28):5727–5736, 2005.
- [26] Jessica Fioravanti, José Medina-Echeverz, and Pedro Berraondo. Scavenger receptor class b, type i: a promising immunotherapy target. 2011.

- [27] Camilla Foged, Birger Brodin, Sven Frokjaer, and Anne Sundblad. Particle size and surface charge affect particle uptake by human dendritic cells in an in vitro model. *International journal of pharmaceutics*, 298(2):315–322, 2005.
- [28] Jinglin Fu, Minghui Liu, Yan Liu, Neal W. Woodbury, and Hao Yan. Interenzyme substrate diffusion for an enzyme cascade organized on spatially addressable dna nanostructures. *Journal of the American Chemical Society*, 134(12):5516–5519, 2012.
- [29] Laurent Galibert, Geoffrey S. Diemer, Zhi Liu, Richard S. Johnson, Jeffrey L. Smith, Thierry Walzer, Michael R. Comeau, Charles T. Rauch, Martin F. Wolfson, Rick A. Sorensen, et al. Nectin-like protein 2 defines a subset of t-cell zone dendritic cells and is a ligand for class-i-restricted t-cell-associated molecule. *Journal of Biological Chemistry*, 280(23):21955–21964, 2005.
- [30] Genewiz.
- [31] Laurence Guglielmi and Pierre Martineau. Expression of single-chain fv fragments in e. coli cytoplasm. *Antibody Phage Display: Methods and Protocols*, pages 215–224, 2009.
- [32] Daniel Hawiger, Kayo Inaba, Yair Dorsett, Ming Guo, Karsten Mahnke, Miguel Rivera, Jeffrey V. Ravetch, Ralph M. Steinman, and Michel C. Nussenzweig. Dendritic cells induce peripheral t cell unresponsiveness under steady state conditions in vivo. *The Journal of experimental medicine*, 194(6):769–780, 2001.
- [33] Makoto Hirayama, Hiromi Shibata, Koji Imamura, Takemasa Sakaguchi, and Kanji Hori. High-mannose specific lectin and its recombinants from a carrageenophyta *kappaphycus alvarezii* represent a potent anti-hiv activity through high-affinity binding to the viral envelope glycoprotein gp120. *Marine Biotechnology*, 18(1):144–160, 2016.
- [34] Sachiko Hirose, Iraklis C. Kourtis, André J van der Vlies, Jeffrey A Hubbell, and Melody A. Swartz. Antigen delivery to dendritic cells by poly (propylene sulfide) nanoparticles with disulfide conjugated peptides: Cross-presentation and t cell activation. *Vaccine*, 28(50):7897–7906, 2010.
- [35] F. Stephen Hodi, Steven J. O’Day, David F. McDermott, Robert W. Weber, Jeffrey A. Sosman, John B. Haanen, Rene Gonzalez, Caroline Robert, Dirk Schadendorf, Jessica C. Hassel, et al. Improved survival with ipilimumab in patients with metastatic melanoma. *New England Journal of Medicine*, 363(8):711–723, 2010.
- [36] Nathan Hurst.

- [37] National Cancer Institute, 12 2016.
- [38] Darrell J. Irvine, Melody A. Swartz, and Gregory L. Szeto. Engineering synthetic vaccines using cues from natural immunity. *Nature materials*, 12(11):978–990, 2013.
- [39] Wanping Jiang, William J. Swiggard, Christine Heufler, Michael Peng, Asra Mirza, Ralph M. Steinman, and Michel C. Nussenzweig. The receptor dec-205 expressed by dendritic cells and thymic epithelial cells is involved in antigen processing. 1995.
- [40] Sarah L. Jongbloed, Andrew J. Kassianos, Kylie J. McDonald, Georgina J. Clark, Xincheng Ju, Catherine E. Angel, Chun-Jen J. Chen, P. Rod Dunbar, Robert B. Wadley, Varinder Jeet, et al. Human cd141+ (bdca-3)+ dendritic cells (dcs) represent a unique myeloid dc subset that cross-presents necrotic cell antigens. *The Journal of experimental medicine*, 207(6):1247–1260, 2010.
- [41] Sudhir Pai Kasturi, Ioanna Skountzou, Randy A. Albrecht, Dimitrios Koutsoumanos, Tang Hua, Helder I Nakaya, Rajesh Ravindran, Shelley Stewart, Munir Alam, Marcin Kwissa, et al. Programming the magnitude and persistence of antibody responses with innate immunity. *Nature*, 470(7335):543–547, 2011.
- [42] Yonggang Ke, Shawn M. Douglas, Minghui Liu, Jaswinder Sharma, Anchi Cheng, Albert Leung, Yan Liu, William M. Shih, and Hao Yan. Multilayer dna origami packed on a square lattice. *Journal of the American Chemical Society*, 131(43):15903–15908, 2009.
- [43] Keith L. Knutson and M.L. Disis. Tumor antigen-specific t helper cells in cancer immunity and immunotherapy. *Cancer Immunology, Immunotherapy*, 54(8):721–728, 2005.
- [44] Martin Kreutz, Paul J. Tacken, and Carl G. Figdor. Targeting dendritic cells—why bother? *Blood*, 121(15):2836–2844, 2013.
- [45] Arthur M. Krieg. Therapeutic potential of toll-like receptor 9 activation. *Nature reviews Drug discovery*, 5(6):471–484, 2006.
- [46] Himanshu Kumar, Taro Kawai, and Shizuo Akira. Pathogen recognition by the innate immune system. *International reviews of immunology*, 30(1):16–34, 2011.
- [47] Natalia Lapteva, Mamatha R. Seethammagari, Brent A. Hanks, Jianghong Jiang, Jonathan M. Levitt, Kevin M. Slawin, and David M. Spencer. Enhanced activation of human dendritic cells by inducible cd40 and toll-like receptor-4 ligation. *Cancer research*, 67(21):10528–10537, 2007.

- [48] David A. Levary, Ranganath Parthasarathy, Eric T. Boder, and Margaret E. Ackerman. Protein-protein fusion catalyzed by sortase a. *PloS one*, 6(4):e18342, 2011.
- [49] Tim Liedl, Björn Högberg, Jessica Tytell, Donald E. Ingber, and William M. Shih. Self-assembly of three-dimensional prestressed tensegrity structures from dna. *Nature nanotechnology*, 5(7):520–524, 2010.
- [50] Andrew J. Link and Joshua LaBaer. Trichloroacetic acid (tca) precipitation of proteins. *Cold Spring Harbor Protocols*, 2011(8):pdb-prot5651, 2011.
- [51] Steven R. Little. Reorienting our view of particle-based adjuvants for subunit vaccines. *Proceedings of the National Academy of Sciences*, 109(4):999–1000, 2012.
- [52] Karsten Mahnke, Ming Guo, Sena Lee, Homero Sepulveda, Suzy L. Swain, Michel Nussenzweig, and Ralph M. Steinman. The dendritic cell receptor for endocytosis, dec-205, can recycle and enhance antigen presentation via major histocompatibility complex class ii-positive lysosomal compartments. *The Journal of cell biology*, 151(3):673–684, 2000.
- [53] Ira Mellman, George Coukos, and Glenn Dranoff. Cancer immunotherapy comes of age. *Nature*, 480(7378):480–489, 2011.
- [54] Kingston H.G. Mills. Tlr-dependent t cell activation in autoimmunity. *Nature Reviews Immunology*, 11(12):807–822, 2011.
- [55] Rob Noad and Polly Roy. Virus-like particles as immunogens. *Trends in microbiology*, 11(9):438–444, 2003.
- [56] Michel Obeid, Antoine Tesniere, François Ghiringhelli, Gian Maria Fimia, Lionel Apetoh, Jean-Luc Perfettini, Maria Castedo, Grégoire Mignot, Theoharis Panaretakis, Noelia Casares, et al. Calreticulin exposure dictates the immunogenicity of cancer cell death. *Nature medicine*, 13(1):54–61, 2007.
- [57] Jason Z. Oh, Jonathan S. Kurche, Matthew A. Burchill, and Ross M. Kedl. Tlr7 enables cross-presentation by multiple dendritic cell subsets through a type i ifn-dependent pathway. *Blood*, 118(11):3028–3038, 2011.
- [58] Drew M. Pardoll. The blockade of immune checkpoints in cancer immunotherapy. *Nature Reviews Cancer*, 12(4):252–264, 2012.
- [59] A plasmid Editor.
- [60] Wayne Rasband.

- [61] Steven A. Rosenberg, Nicholas P. Restifo, James C. Yang, Richard A. Morgan, and Mark E. Dudley. Adoptive cell transfer: a clinical path to effective cancer immunotherapy. *Nature Reviews Cancer*, 8(4):299–308, 2008.
- [62] Paul W.K. Rothemund. Folding dna to create nanoscale shapes and patterns. *Nature*, 440(7082):297–302, 2006.
- [63] Kaori Sakuishi, Lionel Apetoh, Jenna M Sullivan, Bruce R. Blazar, Vijay K. Kuchroo, and Ana C. Anderson. Targeting tim-3 and pd-1 pathways to reverse t cell exhaustion and restore anti-tumor immunity. *The Journal of experimental medicine*, 208(6):1331, 2011.
- [64] David Sancho, Olivier P. Joffre, Anna M. Keller, Neil C. Rogers, Dolores Martinez, Patricia Hernanz-Falcón, Ian Rosewell, and Caetano Reis e Sousa. Identification of a dendritic cell receptor that couples sensing of necrosis to immunity. *Nature*, 458(7240):899–903, 2009.
- [65] David Sancho, Diego Mourão-Sá, Olivier P. Joffre, Oliver Schulz, Neil C. Rogers, Daniel J. Pennington, James R. Carlyle, and Caetano Reis e Sousa. Tumor therapy in mice via antigen targeting to a novel, dc-restricted c-type lectin. *The Journal of clinical investigation*, 118(6):2098–2110, 2008.
- [66] Nadrian C. Seeman. Nucleic acid junctions and lattices. *Journal of theoretical biology*, 99(2):237–247, 1982.
- [67] Arjun Seth, Fiona K. Ritchie, Nani Wibowo, Linda H.L. Lua, and Anton P.J. Middelberg. Non-carrier nanoparticles adjuvant modular protein vaccine in a particle-dependent manner. *PloS one*, 10(3):e0117203, 2015.
- [68] Sai Kiran Sharma, Mavanur R. Suresh, and Frank R. Wuest. Improved soluble expression of a single-chain antibody fragment in e. coli for targeting ca125 in epithelial ovarian cancer. *Protein expression and purification*, 102:27–37, 2014.
- [69] Alan Shaw, Vanessa Lundin, Ekaterina Petrova, Ferenc Fördős, Erik Benson, Abdullah Al-Amin, Anna Herland, Andries Blokzijl, Björn Högberg, and Ana I. Teixeira. Spatial control of membrane receptor function using ligand nanocalipers. *Nature methods*, 11(8):841–846, 2014.
- [70] William M. Shih, Joel D. Quispe, and Gerald F. Joyce. A 1.7-kilobase single-stranded dna that folds into a nanoscale octahedron. *Nature*, 427(6975):618–621, 2004.
- [71] Jin-Young Shin, Il-Hee Yoon, Jung-Sik Kim, Bonggi Kim, and Chung-Gyu Park. Vascular endothelial growth factor-induced chemotaxis and il-10 from t cells. *Cellular immunology*, 256(1):72–78, 2009.

- [72] Ken Shortman and William R. Heath. The cd8+ dendritic cell subset. *Immunological reviews*, 234(1):18–31, 2010.
- [73] Ingo H. Stein, Verena Schüller, Philip Böhm, Philip Tinnefeld, and Tim Liedl. Single-molecule fret ruler based on rigid dna origami blocks. *ChemPhysChem*, 12(3):689–695, 2011.
- [74] Integrated DNA Technologies.
- [75] Elizabeth A. Tivol, Frank Borriello, A. Nicola Schweitzer, William P. Lynch, Jeffrey A. Bluestone, and Arlene H. Sharpe. Loss of ctla-4 leads to massive lymphoproliferation and fatal multiorgan tissue destruction, revealing a critical negative regulatory role of ctla-4. *Immunity*, 3(5):541–547, 1995.
- [76] Vladimir P. Torchilin. Recent advances with liposomes as pharmaceutical carriers. *Nature reviews Drug discovery*, 4(2):145–160, 2005.
- [77] Brian C. Wengerter, Joseph A. Katakowski, Jacob M. Rosenberg, Chae Gyu Park, Steven C. Almo, Deborah Palliser, and Matthew Levy. Aptamer-targeted antigen delivery. *Molecular Therapy*, 22(7):1375–1387, 2014.
- [78] Hao Yan, Thomas H. LaBean, Liping Feng, and John H. Reif. Directed nucleation assembly of dna tile complexes for barcode-patterned lattices. *Proceedings of the National Academy of Sciences*, 100(14):8103–8108, 2003.
- [79] Eiji Yuba, Chie Kojima, Atsushi Harada, Shinobu Watarai, Kenji Kono, et al. ph-sensitive fusogenic polymer-modified liposomes as a carrier of antigenic proteins for activation of cellular immunity. *Biomaterials*, 31(5):943–951, 2010.
- [80] Zhiping Zhang, Songsak Tongchusak, Yo Mizukami, Yoon Joong Kang, Tetsuya Ioji, Maki Touma, Bruce Reinhold, Derin B Keskin, Ellis L. Reinherz, and Tetsuro Sasada. Induction of anti-tumor cytotoxic t cell responses through plga-nanoparticle mediated antigen delivery. *Biomaterials*, 32(14):3666–3678, 2011.

Sequences

B.1 Sequences of Insert Templates for Gibson Cloning

pSNAP-tag (T7):

ATG GAC AAA GAT TGC GAA ATG AAA CGT ACC ACC CTG GAT AGC CCG
CTG GGC AAA CTG GAA CTG AGC GGC TGC GAA CAG GGC CTG CAT GAA
ATT AAA CTG CTG GGT AAA GGC ACC AGC GCG GCC GAT GCG GTT GAA
GTT CCG GCC CCG GCC GCC GTG CTG GGT GGT CCG GAA CCG CTG ATG
CAG GCG ACC GCG TGG CTG AAC GCG TAT TTT CAT CAG CCG GAA GCG
ATT GAA GAA TTT CCG GTT CCG GCG CTG CAT CAT CCG GTG TTT CAG
CAG GAG AGC TTT ACC CGT CAG GTG CTG TGG AAA CTG CTG AAA GTG
GTT AAA TTT GGC GAA GTG ATT AGC TAT CAG CAG CTG GCG GCC CTG
GCG GGT AAT CCG GCG GCC ACC GCC GCC GTT AAA ACC GCG CTG AGC
GGT AAC CCG GTG CCG ATT CTG ATT CCG TGC CAT CGT GTG GTT AGC
TCT AGC GGT GCG GTT GGC GGT TAT GAA GGT GGT CTG GCG GTG AAA
GAG TGG CTG CTG GCC CAT GAA GGT CAT CGT CTG GGT AAA CCG GGT
CTG GGA

VH-VL-SNAP-His insert from pUC57-Kanamycin:

ccc gcg aaa tta ata cga ctc act ata ggG GAG ATA CTA GAG AAA GAG GAG AAA
CAT ATG AAA TAT CTG CTG CCG ACC GCA GCA GCT GGT CTG CTG TTG
CTG GCG GCC CAG CCG GCT ATG GCG ATG GGT GGC GGT GGT AGC GAA
GTG AAA CTG GTT GAA AGT GGT GGC GGT CTG GTT CAG CCA GGC GGT
TCT CTC CGA CTG AGC TGC GCA GCG TCT GGT TTT ACA TTT AAC GAC
TTC TAT ATG AAC TGG ATC CGT CAG CCG CCG GGT CAG GCG CCG GAA
TGG CTG GGT GTG ATT CGT AAC AAG GGT AAC GGT TAT ACC ACC GAA
GTT AAT ACC TCG GTA AAA GGC CGC TTC ACT ATT TCT CGC GAC AAC
ACT CAG AAC ATC CTG TAC CTG CAA ATG AAT AGC CTG CGT GCT GAA

GAC ACC GCT ATC TAT TAC TGC GCG CGC GGT GGC CCG TAT TAC TAC AGC
GGT GAC GAT GCG CCG TAC TGG GGC CAG GGT GTT ATG GTT ACC GTG
TCT TCT GGT GGC GGT GGC TCC GGT GGC GGC GGC TCC GGG GGT GGT
GGC AGC GAT ATT CAG ATG ACA CAG TCT CCA AGC TTC CTT TCT ACT
TCT CTG GGT AAT AGC ATC ACG ATT ACC TGC CAC GCA TCT CAG AAC
ATC AAG GGC TGG CTG GCA TGG TAC CAG CAG AAG TCT GGT AAC GCT
CCG CAG CTG CTG ATT TAC AAA GCT AGC AGC CTG CAG TCT GGC GTG
CCA TCC CGT TTC TCT GGT TCC GGC TCT GGC ACT GAT TAC ATC TTC ACT
ATC AGC AAC CTG CAG CCA GAA GAT ATT GCT ACC TAC TAC TGC CAG
CAC TAC CAA TCC TTC CCG TGG ACC TTC GGC GGC GGC ACC AAA CTG
GAG CTG AAA GGT GGT GGT GGC TCC GAC TCG CTG GAA TTC ATT GCA
TCT AAA CTG GCT ATG GAC AAA GAT TGC GAA ATG AAA CGT ACC ACC
CTG GAT AGC CCG CTG GGC AAA CTG GAA CTG AGC GGC TGC GAA CAG
GGC CTG CAT GAA ATT AAA CTG CTG GGT AAA GGC ACC AGC GCG GCC
GAT GCG GTT GAA GTT CCG GCC CCG GCC GCC GTG CTG GGT GGT CCG
GAA CCG CTG ATG CAG GCG ACC GCG TGG CTG AAC GCG TAT TTT CAT
CAG CCG GAA GCG ATT GAA GAA TTT CCG GTT CCG GCG CTG CAT CAT
CCG GTG TTT CAG CAG GAG AGC TTT ACC CGT CAG GTG CTG TGG AAA
CTG CTG AAA GTG GTT AAA TTT GGC GAA GTG ATT AGC TAT CAG CAG
CTG GCG GCC CTG GCG GGT AAT CCG GCG GCC ACC GCC GCC GTT AAA
ACC GCG CTG AGC GGT AAC CCG GTG CCG ATT CTG ATT CCG TGC CAT
CGT GTG GTT AGC TCT AGC GGT GCG GTT GGC GGT TAT GAA GGT GGT
CTG GCG GTG AAA GAG TGG CTG CTG GCC CAT GAA GGT CAT CGT CTG
GGT AAA CCG GGT CTG GGA GGT GGT GGC GGT AGT CAT CAT CAC CAC
CAC CAC TAA TGA GGA TCC gaa ttc gag ctc cgt cga caa g

Cse3-SNAP insert in pET30a, sequenced:

NNN NNN NNN NNN NNN NNN NNC TNN NNN NAT TTT GTT TAA CTT TAA
GAA GGA GAT ATA CAT ATG CAC CAT CAT CAT CAT TCT TCT GGT CTG
GTG CCA CGC GGT TCT GGT ATG AAA GAA ACC GCT GCT GCT AAA TTC
GAA CGC CAG CAC ATG GAC AGC CCA GAT CTG GGT ACC GAC GAC GAC
GAC AAG GCC ATG GCT GAT ATC GGA TCC GAA AAT TTG TAT TTT CAA
ATG TGG CTC ACT AAG CTC GTG CTG AAC CCG GCA TCC CGG GCC GCC
CGC CGG GAT TTG GCG AAC CCC TAC GAG ATG CAC CGC ACC CTC TCC
AAG GCG GTC TCC CGG GCC CTG GAG GAG GGG CGG GAG CGG CTT CTT
TGG CGC TTG GAG CCC GCC CGG GGT CTG GAG CCT CCC GTG GTC CTG
GTG CAG ACC CTC ACC GAG CCC GAC TGG AGC GTG CTG GAC GAG GGC
TAC GCC CAG GTC TTT CCG CCC AAG CCC TTC CAC CCC GCC CTG AAG
CCC GGC CAG CGC CTC CGC TTC CGC CTC CGG GCC AAC CCG GCG AAG
CGC CTC GCC GCC ACG GGG AAG CGG GTG GCC CTG AAG ACC CCG GCG
GAG AAG GTC GCC TGG CTG GAG AGG CGC CTT GAG GAG GGG GGG TTC

CGC CTC CTG GAG GGG GAA AGG GGC CCC TGG GTG CAG ATC CTC CAA
GAC ACC TTC TTG GAG GTC CGG CGG AAG AAG GAC GGG GAG GAG GCG
GGG AAG CTC CTC CAG GTG CAG GCG GTG CTC TTT GAG GGG CGC CTC
GAG GTG GTG GAC CCC GAA AGG GCC CTC GCC ACG CTA AGG CGG GGC
GTG GGC CCC GGG AAG GCC CTG GGC CTC GGC CTC CTT TCC GTG GCC
CCC ATG GAC AAA GAC TGC GAA ATG AAG CGC ACC ACC CTG GAT AGC
CCT CTG GGC AAG CTG GAA CTG TCT GGG TGC GAA CAG GGC CTG CAC
CGT ATC ATC TTC CTG GGC AAA GGA ACA TCT GCC GCC GAC GCC GTG
GAA GTG CCT GCC CCA GCC GCC GTG CTG GGC GGA CCA GAG CCA CTG
ATG CAG GCC ACC GCC TGG CTC AAC GCC TAC TTT CAC CAG CCT GAG
GCC ATC GAG GAG TTC CCT GTG CCA GCC CTG CAC CAC CCA GTG TTC
CAG CAG GAG AGC TTT ACC CGC CAG GTG CTG TGG AAA CTG CTG AAA
GTG GTG AAG TTC GGA GAG GTC ATC AGC TAC AGC CAC CTG GCC GCC
CTG GCC GGC AAT CCC GCC GCC ACC GCC GCC GTG AAA ACC GCC CTG
AGC GGA AAT CCC GTG CCC ATT CTG ATC CCC TGC CAC CGG GTG GTG
CAG GGC GAC CTG GAC GTG GGG GGC TAC GAG GGC GGG CTC GCC GTG
AAA GAG TGG CTG CTG GCC CAC GAG GGC CAC AGA CTG GGC AAG CCT
GGG CTG GGT TAG TAA TGA GAA TTC GAG CTC CGT CGA CAA GCT TGC
GGC CGC ACT CGA GCA CCA CCA CCA CCA CCA CTG AGA TCC GGC TGC

B.2 Primers

All primers are given in 5' to 3' direction. Primer oligo properties were derived from the *IDT* webpage (refer to Ref. [74]).

B.2.1 Gibson Cloning

VHVL insert into pUC57: by F. Anastassacos

FA004: pUC57-Kan vector backbone forward (VHVL): GCAATCTTTGTCCATG-
GAGCCACCACCACCTTTCAGC

FA005: VHVL: pUC57-Kan vector backbone reverse (VHVL): GGTAACCGGGTCTGGGAG-
GCTGGTGGTGGCGGTAGTCATC

FA003: pSNAP tag insert forward (VHVL): GCTGAAAGGTGGTGGTGGCTC-
CATGGACAAAGATTGC

FA006: pSNAP tag insert reverse (VHVL): GATGACTACCGCCACCACCAGCCTC-
CCAGACCCGGTTTACC

VLVH insert into pUC57: by F. Anastassacos

FA018: pUC57-Kan vector backbone forward (VLVH): GGTCATCGTCTGGGTAAAC-CGGGTCTGGGAGGAGGTGGTGGTTCTCACCATCACCACC

FA019: pUC57-Kan vector backbone reverse (VLVH): GGTACGTTTCATTTTCG-CAATCTTTGTCCATGGAACCACCACCACCGCTGCTGACGG

FA020: pSNAP tag insert forward (VLVH): CCGTCAGCAGCGGTGGTGGTGGTTC-CATGGACAAAGATTGCGAAATGAAACGTACC

FA021: pSNAP tag insert reverse (VLVH): GGTGGTGATGGTGAGAACCACCAC-CTCCTCCCAGACCCGGTTTACCCAGACGATGACC

VHVL insert into pET30a

STW007: pET30aCse3SNAP (vector) forward: CACCACCACCACTAATGAGGATC-Cgaattcgagctccgctgacaagc

Gibson cloning of VHVL insert into pET30a STW008: pET30aCse3SNAP (vector) reverse: CTCCTCTTTCTCTAGTATCTCCcctatagtgagtcgtattaatttcgcggg

LC185: pUC57-Kan VHVL-SNAP colony 1 (insert) forward: cccgcgaaattaatac-gactcactataggGGAGATACTAGAGAAAGAGGAGAAAC

LC186: pUC57-Kan VHVL-SNAP colony 1 (insert) reverse: cttgtcgacggagctc-gaattcGGATCCTCATTAGTGGTGGT

B.2.2 PCR and colony PCR

STW011=LC183: overhangs on the Gibson-insert, forward: CCT ATA GTG AGT CGT ATT AAT TTC GCG G

STW012=LC184: overhangs on the Gibson-insert, reverse: CTT GTC GAC GGA GCT CGA ATT C

STW013: pET30a 250bp upstream of insert, forward: gtagtaggtgaggccgttg

STW014: pET30a 250bp downstream of insert, reverse: tggcaagtgtagcggtc

B.2.3 Sequencing

STW-VH1, STW-VH2, STW-VH3, STW-VH4 after Gibson Cloning:

- (a) CGAAGTGGCGAGCCCGATCT;
- (b) TCAGCCAGGCGGTTCTCTCC;
- (c) CGTACTGGGGCCAGGGTGTT;
- (d) CACTATCAGCAACCTGCAGCCA;
- (e) CGCCGTGCTGGGTGGTCC;

(f) GGTTAGCTCTAGCGGTGCGG;

(g) CCCTATAGTGAGTCGTATTAATTTC;

VH-1.1: for quality control purposes:

(a) to (f), plus:

STW013;

Gcctctaaacgggtcttgag